# Representation of dissolved organic carbon from land to river system in JULES model

Submitted by
Mahdi Nakhavali

To the University of Exeter as a thesis for the degree of Doctor of Philosophy in Mathematics
In May 2019



I certify that all material in this thesis which is not my own work has been identified and that no material has previously been submitted and approved for the award of a degree by this or any other University.

Signature: .....

# Abstract

The lateral transfer of organic carbon along the terrestrial-aquatic continuum is an important link in the global carbon (C) cycle and an important process which should not be ignored when assessing or modelling changes in terrestrial and aquatic C budgets. The amounts of C exported from terrestrial ecosystem into the inland water network have so far only coarsely been estimated by closing a budget based on observed fluvial C exports to the coast and the still poorly constrained estimates of inland water $CO_2$ evasion and C burial in aquatic sediments. The representation of lateral C transfers in Earth System models (ESMs) will arguably help to improve the representation of soil C cycling and its response to climate change and atmospheric $CO_2$ increase. A first and critical step in that direction is to include processes of production and export of dissolved organic carbon (DOC) in soils.

Hence, in the first part of my thesis I developed an extension of the Joint UK Land Environment Simulator (JULES-DOCM) that integrates a representation of DOC production in terrestrial ecosystems based on incomplete decomposition of organic matter, DOC decomposition within the soil column, and DOC export to the river network via leaching. Our results showed that the model is able to reproduce the DOC concentration and controlling processes including leaching to the riverine system which is fundamental for integrating terrestrial and aquatic ecosystems.

In the second part of my thesis, I optimized JULES-DOCM for global scale application by recalibrating two key processes controlling soil DOC concentrations: the rate of DOC production associated with soil organic carbon decomposition and the rate of DOC decomposition for the locations where observations were available. Then I used JULES-DOCM with these optimised parameters to simulate the global distribution of soil DOC concentrations and DOC leaching fluxes from soils to rivers.

For the third part of my thesis, I used JULES-DOCM to simulate spatial-temporal trends in DOC inputs from soil to the river system from 1860 to 2010 at global scale, quantifying the impacts of major environmental drivers such as $CO_2$ fertilization, climate and land use change. At the global scale, $CO_2$ fertilization was identified as the main controller, followed by climate and land use change. Contrary to general assumptions, we find land use changes to only play a minor role in driving the changes in DOC leaching.

In the last of my work I used JULES-DOCM and three representative concentration pathways (RCPs), RCP 2.6, RCP 4.5 and RCP 8.5 in order to estimate the future of terrestrial

transported DOC flux to the river system. We find the increase of the atmospheric $CO_2$ concentration as the main reason of the future increase of transported terrestrial DOC.

In this thesis, I focussed on the detailed representation of soil DOC cycling and leaching, and simulated the historical and future trend of it. However, future work should include the fate of exported DOC in the river system as well as the exports of dissolved inorganic C and particulate organic C from soils to complete the representation of lateral C exports through the terrestrial-aquatic continuum.

**Acknowledgements**

To Pierre for his continuous support, for his patience, motivation and immense knowledge. I owe it all to you. Thank you!

To my brother: I miss our long-lasting chats over phone, giving me hope to go through the rest of day, from miles away. My mother, father and sister: who were always keen to know what I was doing although they never grasped what it was all about !

The last four years were full of happy and sad moments. My world became a million shattered pieces put together, glued by my tears, where each piece was nothing but a reflection of memories. To Anamarija: Where you used to be, there is a hole in the world, which I find myself constantly walking around in the daytime, and falling in at night. I miss you.

Through this period of my life, I felt like a glowing cloud devouring my entire world. I could hardly imagine that there's a world out there that might have anything else going on. And then the I met my partner. To Milica: You proved to me that only when life is broken and shattered into tiny pieces, only love prevented you from falling apart. Thanks for making each day of my life filled with positive thought and love.

I am grateful to my dear colleagues and friends Ronny Lauerwald and Sarah Chadburn who provided me through emotional and scientific support. Thank you Ronny for all the coffee breaks and talks. Thank you Sarah for all great tea and milks. Thanks for finding every opportunity to make me smile, and to offer random acts of kindness in everyday life.

I am also grateful to my friends in the C-CASCADES project: Anna Canning, Asa Horgby, Jo Snoalv, Anna Nydhal, Audrey Marescaux, Marie-Sophie Maier, Domitille Louchard, Jens Terhaar, Matteo Puglini, Adam Hastie, Philip Pika, Simon Bowring and Fabrice Lacroix. Special thanks to Emily Mainetti-cloarec for all her help and support.

I want to thank Pierre Regnier, Anna Harper and Bertrand Guenet for their constant support and help.

And finally, last but by no means least, also to everyone at the University of Exeter, ULB and UPMC. It was a great experience, working with all of you during the last four years.

Logic will get you from A to B. Imagination will take you everywhere.

---A. Einstein

# CONTENTS

## List of publications

1. **Mahdi Nakhavali**, Pierre Friedlingstein, Ronny Lauerwald, Jing Tang, Sarah Chadburn, Marta Camino-Serrano, Bertrand Guenet, Anna Harper, David Walmsley, Matthias Peichl, and Bert Gielen. Representation of dissolved organic carbon in the JULES land surface model (vn4.4_JULES-DOCM). *Geosci. Model Dev.* **11,** 593–609 (2018).

2. **Mahdi Nakhavali**, Ronny Lauerwald, Pierre Regnier, Bertrand Guenet, Sarah Chadburn and Pierre Friedlingstein. Soil dissolved organic carbon leaching is a minor source to inland water carbon budget, Nature Geosciences, *submitted*

3. **Mahdi Nakhavali**, Pierre Friedlingstein, Ronny Lauerwald and Pierre Regnier. Historical trend of lateral export of dissolved organic carbon from soil to river system, Global Biogeochemical Cycles Journal, *soon to be submitted*

4. **Mahdi Nakhavali**, Pierre Friedlingstein, Ronny Lauerwald and Pierre Regnier. Future prediction of dissolved organic carbon terrestrial transported to the river system, Earth System Dynamics Journal, *soon to be submitted*

# *Introduction*

# Introduction

## 1. The Carbon Cycle

Since 1750 the atmospheric $CO_2$ concentration has increased from 227 parts per million (ppm) to 402.8±0.1 ppm in 2016. While its increase was primarily caused by land-use change, since 1920 the emission from fossil fuel consumption became the dominant source of emissions (Le Quéré *et al.*, 2018). The traditional carbon (C) cycle models, which were previously used in the Global Carbon Project (GCP) and by the IPCC to study the fate of the anthropogenic $CO_2$ emissions, consider merely the vertical gas exchanges between terrestrial or oceanic reservoirs and the atmosphere, hence ignoring lateral transport of C from the continent to the oceans (Regnier *et al.*, 2013). This means that these models implicitly consider that all the $CO_2$ which is not respired to the atmosphere is stored on land, leading to an overestimation of heterotrophic soil respiration and/or C accumulation in the soil (Jackson, Banner and Jobbágy, 2002; Janssens *et al.*, 2003).

Hence we need to move towards a boundless C cycle model which integrates the whole continuum from land to ocean to atmosphere in order to better understand Earth's C cycle and thus produce more accurate projections of atmospheric $CO_2$ concentrations (Battin *et al.*, 2009). So far the exported terrestrial C into the inland water network has been coarsely estimated based on fluvial C exports to the coast, $CO_2$ evasion from inland waters and aquatic C burial in sediments. The active role of inland waters in processing the C was first introduced by Cole et al. (2007). They estimated 0.75 Pg C $yr^{-1}$ $CO_2$ evasion from inland waters to the atmosphere and 0.23 Pg C $yr^{-1}$ net sink in sediments. In order to balance these fluxes with 0.9 Pg C $yr^{-1}$ exported flux to the ocean, they proposed a land to inland water flux of 1.9 Pg C $yr^{-1}$ (Figure 1).

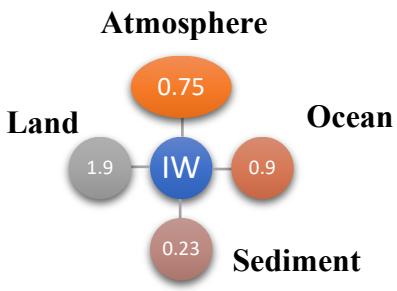


**Figure 1.** Cole et al (2007), C fluxes estimation

Tranvik et al. (2009), reviewed these fluxes and updated the evaded $CO_2$ from inland waters to the atmosphere to 1.4 Pg C $yr^{-1}$, and the net sink for C in sediments to 0.6 Pg C $yr^{-1}$. Hence in order to balance these fluxes with the 0.9 Pg C $yr^{-1}$ export to the ocean, land to inland water flux should be on the order of 2.9 Pg C $yr^{-1}$ (Figure 2).

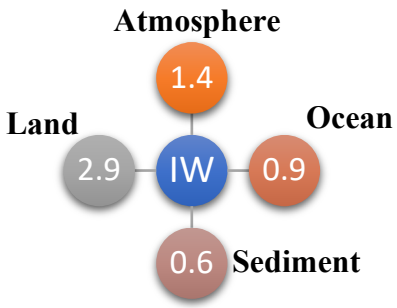


**Figure 2.** Tranvik et al (2009), C fluxes estimation

Battin et al. (2009) refers to Travnik's estimation but sets evaded $CO_2$ from inland waters to the atmosphere at 1.2 Pg C $yr^{-1}$. Hence they concluded that the land input of C to the inland waters should be 2.7 Pg C $yr^{-1}$ (Figure 3).

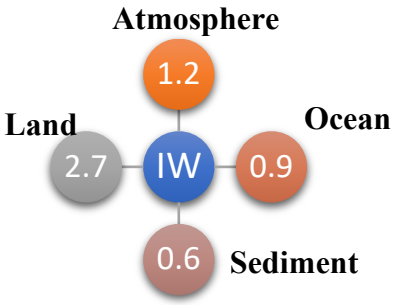


**Figure 3.** Battin et al (2009), C fluxes estimation

Finally, Regnier et al (2013) update the previous estimations by subtracting the chemical weathering (0.5 Pg C $yr^{-1}$), sewage (0.1 Pg C $yr^{-1}$) and net C fixation (0.3 Pg C $yr^{-1}$), resulting in estimated flux from the vegetation-soil system to inland waters of 1.9 Pg C $yr^{-1}$ (Figure 4).

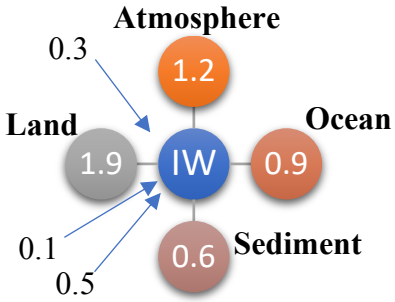


**Figure 4.** Regnier et al (2013), C fluxes estimation

Dissolved organic carbon (DOC) contributes about 37% of the global riverine carbon exports to the coast (Meybeck, 1993) and adds to the net-heterotrophy of inland waters and related $CO_2$ emission to the atmosphere. In addition, dissolved inorganic carbon (DIC) and particulate organic carbon (POC) contribute 45% and 18% of total riverine exports to the coast, respectively (Meybeck, 1993) (Figure 5). It has been shown that DOC is increased by anthropogenic perturbation such as land use change (i.e. deforestation) and increased atmospheric $CO_2$ concentrations (Regnier et al. 2013). It was hypothesized that the representation of DOC leaching from soil can explain the difference between land and atmospheric uptake in the European terrestrial ecosystem (Siemens, 2003). This flux can have a significant impact on chemical and biological properties of both aquatic and terrestrial ecosystems (Aitkenhead and Mcdowell, 2000; Kalbitz *et al.*, 2000).

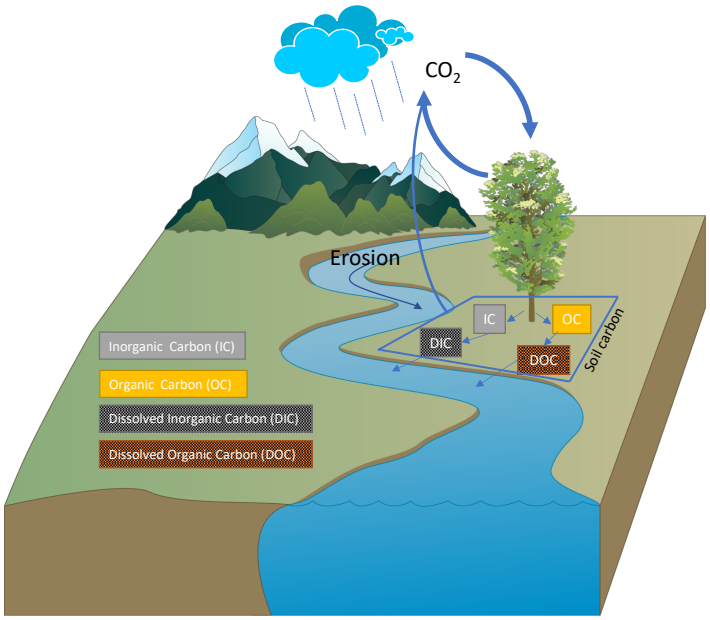


**Figure 5.** Conceptual schematic terrestrial C fluxes to inland waters ecosystem

The role of the DOC in terrestrial C cycle is so far estimated based on the riverine DOC flux which ranges from 0.17 to 0.36 (Table 1). However, it is difficult to estimate an accurate terrestrial flux based on this riverine flux as:

i) riverine fluxes are delivered from different land use systems with different DOC quality and leaching rate (Boyer and Groffman, 1996; Kindler *et al.*, 2011),

ii) due to the transformation in the streams it is difficult to diagnose the initial terrestrial DOC source, and

iii) it is difficult to separate the natural from anthropogenic fluxes (Schelker et al. 2013; Pierre Regnier et al. 2013).

**Table 1.** Global land to river and riverine C flux

| Reference | Flux (Pg C $yr^{-1}$) | Remark |
|---|---|---|
| | | **Land to river C flux** |
| Cole et al, 2007 | 1.9 | For all forms of C 0.9 Pg C $yr^{-1}$ (0.7 from soil + 0.2 direct ground water load which discharges to the sea without entering a river) is transferred from river to ocean. Cole estimated that 0.75 Pg C $yr^{-1}$ is evaded as $CO_2$ from inland waters to the atmosphere and there is a 0.23 Pg C $yr^{-1}$ net sink for C in sediments. In order to balance these fluxes with land he proposed that 1.9 Pg C $yr^{-1}$ is transferred from land to inland waters. |
| Tranvik et al, 2009 | 2.9 | Tranvik states that annual transported C to the ocean is 0.9 Pg C. He updated Cole's number of the evaded $CO_2$ from inland waters to atmosphere at 1.4 Pg C $yr^{-1}$ and the net sink for C in sediments to 0.6 Pg C $yr^{-1}$. Hence he concludes that the land flux must be on the order of 2.9 Pg C $yr^{-1}$. |
| Battin et al, 2009 | 2.7 | Battin refers to Travnik et al (in press) with 2.7 Pg C $yr^{-1}$ (he reports the evaded CO2 from inland waters to the atmosphere at 1.2 Pg C $yr^{-1}$, net sink for C in sediments at 0.6 Pg C $yr^{-1}$ and transported C to the ocean at 0.9 Pg C $yr^{-1}$. Hence the land input C to the inland waters should be 2.7 Pg C $yr^{-1}$). |
| Regnier et al, 2013 | 1.9 | Regnier studied the estimated C input to freshwater which was reported as 2.7 (from Battin) to 2.9 (from Travnik) Pg C $yr^{-1}$. Then he subtracted the chemical weathering (0.5 Pg C $yr^{-1}$), sewage (0.1 Pg C $yr^{-1}$) and net C fixation (0.3 Pg C $yr^{-1}$), resulting in 1.9 Pg C $yr^{-1}$. |

| | | Riverine DOC flux |
|---|---|---|
| Meybeck, 1982 | 0.21 | Based on averaged DOC content per climate zone |
| Smith & Hollibaugh, 1993 | 0.20 | Based on previous studies, assigned nominal value for fluvial DOC export to the ocean ($17\pm2 \times 10^{12}$ mol $yr^{-1}$) |
| Ludwig & Probst, 1996 | 0.21 | Based on measured OC fluxes and geomorphological and climatic patterns which have an impact on river basins |
| Aitkenhead & Mcdowell, 2000 | 0.36 | They calculated the riverine DOC flux to the oceans as 0.36 Pg C $yr^{-1}$ (with the highest flux for tropical climate zones (similar to our model)). Their calculation was based on an empirical model based on C:N ratio, using climate zone description from Meybeck 1981 and Schlesinger and Melack 1981 |
| Cauwet, 2002 | 0.25 | Based on major rivers' DOC flux measurements during 1990s |
| Harrison et al., 2005 | 0.17 | Based on NEWS model |
| Seitzinger et al., 2005 | 0.17 | Based on NEWS model |
| Cai, 2011 | 0.25 | Based on previous estimates |
| Dai et al., 2012 | 0.17 | Based on DOC concentration measurements from 118 rivers, and long term river discharge averages |

Therefore, a better understanding of soil DOC cycling processes, leaching, and SOC biogeochemistry in general is necessary. To that end, we need to i) identify the main controls of soil DOC stocks and fluxes, and ii) implement these processes in a land surface component of an ESM. These two steps are addressed in this thesis.

The following section deals with a review of soil DOC and its controls based on the Kalbitz et al. (2000) classification.

## 2. Soil dissolved organic carbon

Incomplete microbial decomposition of plant debris is known to be the origin of soil organic matter (Cotrufo *et al.*, 2013) and the dissolved forms of organic matter in soil solution are the source of substrate and nutrients that microbes use (Scheel *et al.*, 2008). Understanding the factors that control production and transport of these organic materials is important due to their role in nutrient cycling, tracking soil and groundwater gas fluxes and studying pollutants (Boyer and Groffman, 1996). Bioavailability of these organic materials is dependent on SOC chemical composition, which is controlled by plant type and age (more recalcitrant with greater age) and growth condition (Boyer and Groffman, 1996). Additionally, it also depends on land-use (Boyer and Groffman, 1996) as well as the soil depth, where in the deeper soil layers there is a shift from more fresh litter to more aged litter, which changes the SOM chemistry due to the slow reworking of organic materials by microorganisms (Moore and Dalva, 2001; Sanderman *et al.*, 2009)

The main sources of dissolved organic carbon (DOC) are the accumulated plant residues (Khomutova *et al.*, 2000), humus and root exudates (Kalbitz *et al.*, 2000; Van den berg, Shotbolt and Ashmore, 2012). Additionally, leaf litter carbon can also penetrate into the soil as DOC by means of either leaching or root exudates, after being physically and biologically mixed with roots (Sanderman and Amundson, 2008). There are several processes which immobilize soil organic carbon (SOC) such as mineralization and podzolization. The remaining SOC after these processes is subject to transport to the deeper soil layers (Boyer and Groffman, 1996). The DOC transfer to the lower layers and its retention by means of physio-chemical process are significant factors controlling C cycling in deep soil layers (Kalbitz *et al.*, 2000; Fröberg *et al.*, 2011).

However, the impact of all these processes, including production, sorption and consumption of DOC, can be estimated from the difference between the DOC concentration and flux in soil and the DOC export flux to the inland waters (Moore and Dalva, 2001). The following section reviews the main controls on these processes.

## 2.1. Soil DOC controlling factors

### 2.1.1 Temperature

Temperature is one of the main controls of soil organic matter decomposition (Davidson *et al.*, 2006), DOC production and mineralization (Gödde *et al.*, 1996; Neff and Hooper, 2002). A positive correlation between temperature and DOC production and transport (Raymond and Saiers, 2010) as well as DOC concentration and fluxes in terrestrial ecosystems has been observed (Liechty, Kuuseoks and Mroz, 1995; Michalzik *et al.*, 1999; Marschner and Bredow, 2002) which is possibly due to the impact of temperature on microbial processes and DOC solubility (Donnell et al. 2016). However, this effect can be altered by physical leaching and enzymatic activity of microbes (Moore and Dalva, 2001), as well as by soil type, where the impact of temperature is higher in organic than in mineral soils (Moore, Paré and Boutin, 2008).

There are environmental constraints that affect decomposition dependency on temperature directly and indirectly, such as physical protection, chemical protection, drought, flooding and freezing (Davidson *et al.*, 2006). Additionally, clay content might change decomposition dependency on temperature by adsorbing organic matter and retaining soil moisture (Davidson et al. 2006).

Finally, soil drainage might alter this dependency, since in well to moderate drained soil there is an inverse correlation between soil temperature and DOC concentration, where cooler environments have higher DOC concentration and poorly drained soils have the same DOC concentration in any temperature (Kalbitz *et al.*, 2000).

### 2.1.2 Precipitation and water fluxes

Soil hydrology has an important impact on DOC production, concentration and transport. DOC production increases during optimal moisture and high temperature (Michalzik *et al.*, 2001), DOC concentration decreases as precipitation increases (Van den berg, Shotbolt and Ashmore, 2012) and it increases during dry periods (Evans, Monteith and Cooper, 2005) as decomposition in dry soils is reduced and microbial products accumulate (Kalbitz *et al.*, 2000). These accumulated products can move by means of water flow within the soil layers, and be

advected to lower depth (Evans, Monteith and Cooper, 2005). However, the magnitude of this advective flux depends on soil texture, as the aggregated subsoil lets the soil solution with high DOM content transport more easily to lower layers than in a homogenized subsoil (Kalbitz *et al.*, 2000). This flow path can be altered by storms, as the dominant flow paths can be changed to macro pores and lateral flow (Kalbitz et al 2000).

Besides the loss of DOC by means of $CO_2$, DOC leaching plays an important role as a C input, transport and stabilization mechanism (Sanderman and Amundson, 2008). Lateral transfer of DOC can be identified as the release of DOM from soil at the beginning of large rainfall events (Kalbitz *et al.*, 2000) as higher leaching was observed during high precipitation (Michalzik *et al.*, 2001; Van den berg, Shotbolt and Ashmore, 2012). Hence total annual DOC flux is highly affected by large discharge events (Raymond and Saiers, 2010). This can be altered by land use change e.g. increased groundwater level after clear cutting, which enhances the DOC transport into streams (Schelker *et al.*, 2013).

Finally, precipitation and runoff can affect DOC production and transport through a process known as rewetting (Evans, Monteith and Cooper, 2005). DOC concentration in leaching is higher after the dry period (Kalbitz *et al.*, 2000) which is known as the rewetting effect. This effect is caused by: 1- Reduction of microbial DOC consumption because of dry conditions, 2- Enhanced concentration of microbial products by rewetting, and 3- Soil structure disruption which makes the stored carbon available in the form of DOC (Lundquist, Jackson and Scow, 1999).

### 2.1.3 Freeze/thaw cycle

Freeze/thaw cycles perturb soil biologically and physically (DeLuca, Keeney and McCarty, 1992), disrupt soil structure and make stored organic matter more available in the form of DOC. They have a similar effect to drying-rewetting cycles, as during snowmelt leaching of stored organic soil in upper soil layer increases (Kalbitz *et al.*, 2000).

### 2.1.4 Vegetation

DOC concentration is also controlled by the dominant vegetation (Currie et al. 1996) as this controls the quantity and quality of litter, processes inside the soil and water fluxes. Litter quality affects dissolved organic matter production (Kalbitz *et al.*, 2000) as well as DOC composition and leaching, e.g. leading to less accumulation of organic matter in grasslands compared to forests (Khomutova *et al.*, 2000).

As plant litter is the main C source for soil microorganism growth, its properties will affect microbial communities and consequently their by-products, of which DOC is one (Pregitzer *et al.*, 2004). Decomposability of litter defines its quality, with higher quality decomposing faster (labile) and recalcitrant litter decomposing more slowly. Litter quality is correlated positively with cellulose and negatively with lignin content in the organic matter (Moore et al. 2008). Therefore, fresh leaves contribute more to DOC release (Moore and Dalva, 2001) due to their higher quality of litter, which provides a higher rate of DOM production. On the contrary, lignin-encrusted celluloses, due their protected polymers, reduce substrate use efficiency (SUE) since microbes have to first depolymerize this protection (Cotrufo *et al.*, 2013). For instance, agricultural activities reduce the total soil organic carbon but at the same time crops provide higher litter quality than woody forest vegetation, hence they increase bioavailable DOC leading to higher DOC concentration in leaching (Boyer and Groffman, 1996).

Tree species control soil mineral weathering rate by affecting pH and decomposition of organic acids in soil. More acidic solution with higher DOC was found under Picea abies than under Fagus sylvatica, Quercus petraea or Quercus robur (Augustoa & , Jacques Rangera, 2002).

Finally, vegetation can also have an impact on water fluxes. For instance spruce stands have a large impact related to their leaf area and its impact on transpiration and interception loss (Fröberg *et al.*, 2011). Stika spruce, for example, shows a positive correlation with DOC concentration and soil water (Vanguelova *et al.*, 2010).

### 2.1.5 Clay

In the deeper soil layers where the decomposition rate is low, DOC transportation and adsorption controls C stabilization (Sanderman and Amundson, 2008). This processes is controlled by clay. Sorption depends on type and size of sorbent and age and type of microorganism as well as the environment of study (Filip 1971). Clay minerals and oxides adsorb DOC and reduce DOC concentration (Kalbitz *et al.*, 2000). This processes has been studied in the laboratory in detail and formulated by (Parton, W, Schimel and Ojima, 1987).

Clay also changes the rate and pathway of metabolism in microbial communities, modifies the solution environment and binds extracellular enzymes and modifies their activity (Stotzky, 1967; Sollins, Homann and Caldwell, 1996; Vogel *et al.*, 2015). In addition, clay content affects the competitive relationship between different kind of microorganism, and changes the physical conditions such as noncapillary pores, which can affect the microorganisms.
Finally, montmorillonite clay protects soil from overheating and dehydration, which also protects microorganisms against destructive radiation (Filip 1971)

### 2.1.6 Acid deposition and pH

Acid deposition affects DOC concentration and leaching by controlling soil acidity and ionic strength (IS) (Monteith et al. 2007). In the latest studies, IS was identified as the most important controlling factor for DOC concentration in soil, more important than pH and temperature (Mcdowell and Oulehle, 2009; Wu, Clarke and Mulder, 2010). Acid deposition controls IS: with higher acid deposition, higher IS occurs. The IS controls DOC mobilisation, where higher IS seems to reduce mobilization of DOC (Kalbitz *et al.*, 2000), and DOC leaching (Evans, Monteith and Cooper, 2005). On the contrary, lower IS, affected by multivalent ions, concentrations of sulphate and aluminium (Al), causes more DOC leaching (Haaland *et al.*, 2010)

Acid deposition directly affects organic matter decomposition when it reaches the forest floor in the form of throughfall (Waldner *et al.*, 2014) and indirectly affects microbial activity in the soil (Vanguelova *et al.*, 2010).

Also pH has an impact on the soil DOC concentration. Lower pH raises the Al level in soil. Al causes the precipitation of organic matter which makes it stabilised, less bioavailable and more resistant against microbial decay (Scheel *et al.*, 2008). Al binds with organic molecules and coagulates the soil organic matter, indirectly controlling the soil DOC concentration (Vanguelova *et al.*, 2010).

### 2.1.7 C:N ratio and N effect

C:N represents the quality of litter as a higher C:N is linked to lower quality of litter (Kindler *et al.*, 2011) and as discussed in Section 2.1.4, litter quality affects the microbial products such as DOC. It was hypothesized that due to the Nitrogen (N) need of microbial communities, higher C:N ratio forces them to process more organic matter to satisfy their N need, so they are producing more DOC during their soil organic matter degradation (Gödde *et al.*, 1996). Hence for the most part, high DOC concentration is associated with high C:N ratio and low alkyl ratio (Sanderman *et al.*, 2009; Van den berg, Shotbolt and Ashmore, 2012). However, this hypothesis was not supported by some other studies (Michalzik *et al.*, 2001; Moore, Paré and Boutin, 2008) leaving it still under question.
However, C:N is related to the refractory soil organic matter, which is an indicator for the resistance of organic matter against microbial uptake, consequently making more DOC available in the soil for leaching. So DOC concentration will increase with high C:N ratio since it limits mineralization of available DOC (Van den berg, Shotbolt and Ashmore, 2012).

Finally, It was argued that N deposition alters the substrates that form DOC, and alters the microbial activities that control the processing of organic matter (Pregitzer et al. 2004), enhancing enzymatic activity (like ß- glycosidase) which is involved in C release from organic matter and increases DOC release (Bragazza et al. 2006).

To sum up, understanding each controlling factor individually is a challenging task, as these factors interact with each other and vary on different temporal and spatial scales in different environments (Clark *et al.*, 2010). Although the role of some factors such as temperature, moisture and vegetation has been well studied, future work should be focused on more detailed study of these controls in different environments. Results from such studies will improve the representation of processes controlling soil DOC in models.

## 3 Modelling the terrestrial DOC transport

As highlighted in previous studies (Regnier *et al.*, 2013; Lauerwald *et al.*, 2017), due to the lack of observations and inadequate upscaling techniques, a data driven assessment of soil DOC stocks and fluxes is not feasible. Arguably a process-based Land Surface Model (LSM) can help overcome these difficulties.

LSMs, such as JULES (Figure 6), are a crucial component of Earth System Models (ESMs). These models account for energy, water and C cycling between atmosphere, vegetation and soil (see JULES model description in Best et al. (2011) and Clark et al. (2011) ). Generally, in an LSM, one of the two soil C models, Century (Parton 1987) or RothC (Coleman and Jenkinson, 2014), is implemented. In both models, the C is distributed into two pools, labile and recalcitrant, with the turnover time specified for each. However, these models are still missing some processes, including the lateral transport of C from the soil to the river system. Hence, the initial major step in simulating the boundless C cycle is a representation of soil DOC cycling and leaching.

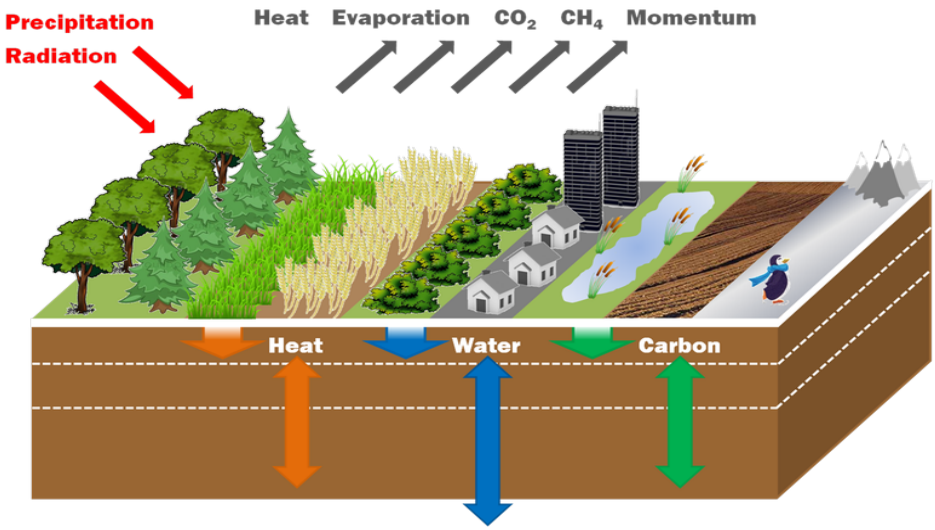


**Figure 6.** JULES land-surface model schematic diagram retrieved from: http://jules.jchmr.org/content/about

Several models have been developed to date to simulate soil DOC, with different temporal resolutions, from 15 minutes in SOLVEG-II (Ota, Nagai and Koarashi, 2013), hourly in TERRAFLUX (Neff and Asner, 2001), daily in INCA-C (Futter *et al.*, 2007), to monthly in

RivCM (Langerwisch *et al.*, 2015) and ECOSSE (Smith et al. 2010), as well as different spatial scales from site scale in DyDOC (Michalzik *et al.*, 2003) and Yurova (Yurova *et al.*, 2008) to global scale in TEM (Kicklighter *et al.*, 2013).

Most of these models consider the soil biogeochemistry as a single layer box and do not represent the discretized soil layers. Nevertheless, some of these models include the lateral transport of terrestrial DOC to the river system. Each model has its own definition of C and DOC pools and processes. For instance, the DOC production in DyDOC (Michalzik *et al.*, 2003) is based on chemical composition, while in Yurova (Yurova *et al.*, 2008) it is based on microbial production rate and in TERRAFLUX (Neff and Asner, 2001) it is based on turnover time (Table 2).

Each of these models were tested for specific study areas, with specific methods of calibration and validation (Table 3). However, with exception of TEM (Kicklighter *et al.*, 2013) which was tested for artic rivers, none of them is capable of global scale simulation of DOC.

**Table 2.** Soil dissolved organic carbon models

| MODEL | Target study area | Simulation time scale | Definition of pools | DOC production factors | Simulation process | Reference |
|---|---|---|---|---|---|---|
| **Coupled hydrology-DOC** | Permafrost-catchment | Daily | 2 pools (TOC and DOC) | DOC production coefficient and two additional terms using soil moisture, air temperature and a constant rate modifier | Decomposition of TOC to DOC; Transport of DOC with water flux | Lessels et al. |
| **DyDOC** | Forest – Site | Hourly daily | 3 HUM pools; HUM 1 and HUM 2 which are passed to DOC; HUM 3 is immobile | Temperature constant and rate constant for each pool | Decomposition of HUM1 and HUM2 to DOC; Leaching of DOC by drainage; Sorption of HUM1 and HUM2 to DOC | Michalzik et al. |
| **ECOSSE** | Peatland/ grassland – Field/ national (Scotland) | Monthly | 4 carbon pools; 1 DOC pool | Decomposition rate factor and rate modifiers (including moisture, temperature, crop and pH) | Decomposition of each carbon pool to DOC; Leaching of DOC by water flux to the lower layers; Sorption of DOC; Decomposition of DOC; | Smith et al. |
| **INCA-C** | Natural and semi natural forests/ peat-dominated forests-Catchments | Daily | 3 pools of SOC, DIC and DOC for upper and lower soil layer; 2 pools of DIC and DOC in stream | Decomposition rate factor (for upper and lower soil layer) | Decomposition of carbon pool to DOC and DIC; Leaching of DOC and DIC to streams; Sorption/Desorption of DOC to/from SOC; Mineralization of DOC to DIC; DIC evasion to atmosphere | Futter et al. |
| **LPJ-GUESS WHyMe** | Peatland - Catchment | Daily | 2 SOC pools; 2 DOC pools; 2 SPSOC pools | Soil temperature response, soil water content and basal production rate | Decomposition of C to DOC; Leaching of DOC to streams; ad/desorption DOC, DOC mineralization | Tang et al. |

| | | | | | | |
|---|---|---|---|---|---|---|
| **RivCM** | Amazon basin-Riverine | Monthly | POC, DOC and IC | Mobilization factor | Mobilization of Soil C and litter from soil to POC and DOC pools in river; Decomposition of POC to DOC; Mineralization of POC and DOC to IC; Transport of IC. POC and DOC from river to ocean | Langerwisch et al. |
| **SOLVEG-II** | Grassland – Site | 15 minutes | 3 carbon pools (active, slow and passive) and DOC pools | Distribution coefficient; proportionality factor | Decomposition of aboveground C to SOC; Leaching of DOC from aboveground to DOC; Sorption/desorption of DOC to/from SOC; Diffusion; DOC pool decomposition; vertical transport of DOC by means of water fluxes | Ota et al. |
| **TEM** | Forest/ peatland - Global | monthly | 1 carbon pool 1 DOC pool | Function of NPP, function of moisture and temperature | Decomposition of reactive carbon pool to DOC; Leaching of DOC by means of water yield | Kicklighter et al. |
| **TERRAFLUX** | United states, Europe | Hourly | Based on turnover time | Parameterized solubility factor | Microbial decomposition of surface litter, soil microbes and slow pool to soil soluble pool; Leaching of DOC by water flux; Sorption/Desorption of DOC | Neff and Asner |
| **Yurova** | Boreal Mires- Site | Daily – annual | Solid OC, SPSOC (Sorbed/potentially soluble OC) and DOC (dissolved OC) | Microbial DOC production rate | DOC production from solid OC pool; Desorption/sorption of DOC to/from SPSOC; Mineralization of DOC; Mineralization of SPSOC | Yurova et al. |

**Table 3.** DOC models, evaluation site, data and method

| MODEL | EVALUATION (LOCATION, SAMPLE PERIOD) | EVALUATION DATA/METHOD) | METHOD (VALIDATION/CALIBRATION) |
|---|---|---|---|
| **COUPLED HYDROLOGY-DOC** | Granger basin (sub-arctic alpine catchment within the Wolf Creek research basin) Yukon, Canada (2001-2008) | DOC in stream and shallow groundwater, Discharge | Their model was calibrated based on hydrological data from 2001 to 2003 and DOC observations collected during the summers of 2002 and 2003. 40 years spin-up. A Monte Carlo approach was used to evaluate a suitable range of model coefficients using $10^6$ model evaluations. The sensitivity analysis was undertaken using the Latin Hypercube one-factor-at-a- time method. |
| **DYDOC** | Birkenes (southern Norway), Waldstein (southern Germany) (1995-1997) | C, DOC export | DOC in HOR-1 in Birkenes and Waldstein for period 1995 to 1997 was compared with the measurements. The simulated values were 14-day averages to provide the similar resolution to the observation. Also comparison of DOC fluxes for both sites. |
| **ECOSSE** | 62 NSIS sites (2000-2009) | SOC | The degree of coincidence was determined by calculating the total error as the root mean squared error (RMSE) and the bias in the error as the relative error. The association between simulated and measured values was calculated as the correlation coefficient, and the significance of the correlation was determined using a t-test. Sources of model error were also examined using graphical plots. |
| **INCA-C** | Two forested headwaters streams near Dorset, Ontario, Canada (1984-2000) | DOC in headwater streams | All model runs at both sites were executed using data for the period 1 June 1984 to 31 May 2000. Model fit was assessed using the Nash-Sutcliffe (NS) R2 statistic [Nash and Sutcliffe, 1970]. First they estimated runoff and soil moisture with the HBV model. Then running INCA-C with simulated parameters. At the end the hydrological parameters were fixed at their best values. Comparison of modeled vs measured DOC for the studied period was performed. |
| **LPJ-GUESS WHYME** | Stordalen catchment (2007-2009) | DOC export | Sobol sensitivity analysis: Once at grid cell-level without DOC routing, once at catchment—level including DOC routing. Comparison of DOC export measurements and model simulation |
| **RIVCM** | Three sub-regions within Amazon subject to low to high land use intensity | CO2, TOC, POC, DOC (leaching/ concentration), IC | To identify the most important explaining variables (parameters) and the most sensitive response variables (carbon pools), a redundancy analysis (RDA) was performed. To evaluate the performance of RivCM, a comparison of observed |

| | | | |
|---|---|---|---|
| | | | with simulated data was conducted. TOC, POC, and DOC concentration were chosen, as well as exported carbon to the ocean (TOC, POC, and DOC per year) and exported carbon to the atmosphere (outgassed CO2 per year on different spatial domains). If possible, data from the same time period were compared. If the observation period was after the last simulation year 2003, the data were compared to simulated values from the reference period (1971–2000) |
| **SOLVEG-II** | Post Modesto (grassland ecosystem in eastern California) | SOC | Model performance was examined by the comparison of modelled active, slow and passive pools with observations. Differences in values were related to parameters controlling C and DOC. |
| **TEM** | Six major rivers in Eurasia and two major rivers in North America (~1970-~2008) | DOC export near the mouth of rivers, river discharge | Terrestrial DOC loading for each river watershed was estimated by summing the simulated DOC leaching flux estimates across the grid cells of the watershed. Similarly, river discharge for each river watershed was determined by summing the simulated water flux estimates across the grid cells of the watersheds. The watershed estimates of annual terrestrial DOC loading developed by TEM were then compared to the appropriate annual estimates of DOC export reported by various studies for stations near the mouth of an Arctic river. The estimates of annual river discharge developed by TEM were compared to the appropriate annual river discharge reported by various studies for stations near the mouth of an Arctic river. (they did not consider the processes in the river) |
| **TERRAFLUX** | United States and Europe (~1986, ~1999) | DOC flux data from temperate forests | Using the basic parameterizations for a temperate forest with 1500 mm of rain and a mean annual temperature of 9°C to study the sensitivity of dissolved carbon fluxes to variation in the DOC control parameters. Results were compared to the values from various DOC fluxes measurements from the US and Europe. |
| **YUROVA** | Kallkällsmyren mire site (1993–2001) | DOC export (concentration at the stream outlet) | Applying differential sensitivity analysis [monte carlo] to the key model parameters such as adsorption coefficient. Evaluating DOC concentration during the steady state and the rate of DOC release into the water by comparing simulations vs measurements. |

## Objectives

The objective of this thesis is first to develop an extension to the Joint UK Land Environmental Simulator (JULES) which is capable of representing the dissolved organic carbon (DOC) in soil and its transport out of the soil to the river system. The second step is to re-calibrate the model for simulation at the global scale and make a historical simulation and future projection with the calibrated model.

Specific objectives are as follows:

**Chapter 1:** explains the extension to the JULES model (JULES-DOCM) in order to represent DOC processes in soil and its transport out of the soil to the river system.

**Chapter 2:** explains the re-calibration of the main DOC controlling processes (production and decomposition) in JULES-DOCM, modifying these based on plant functional type. This modified version is capable of performing simulations at the global scale.

**Chapter 3:** represents the historical trend of DOC transported from the soil to the river system, studying $CO_2$ fertilization, climate and land use impacts on DOC stocks and leaching fluxes at the global scale.

**Chapter 4:** represents the future projection of terrestrial DOC exported to the global river system, studying its trend based on different future scenarios.

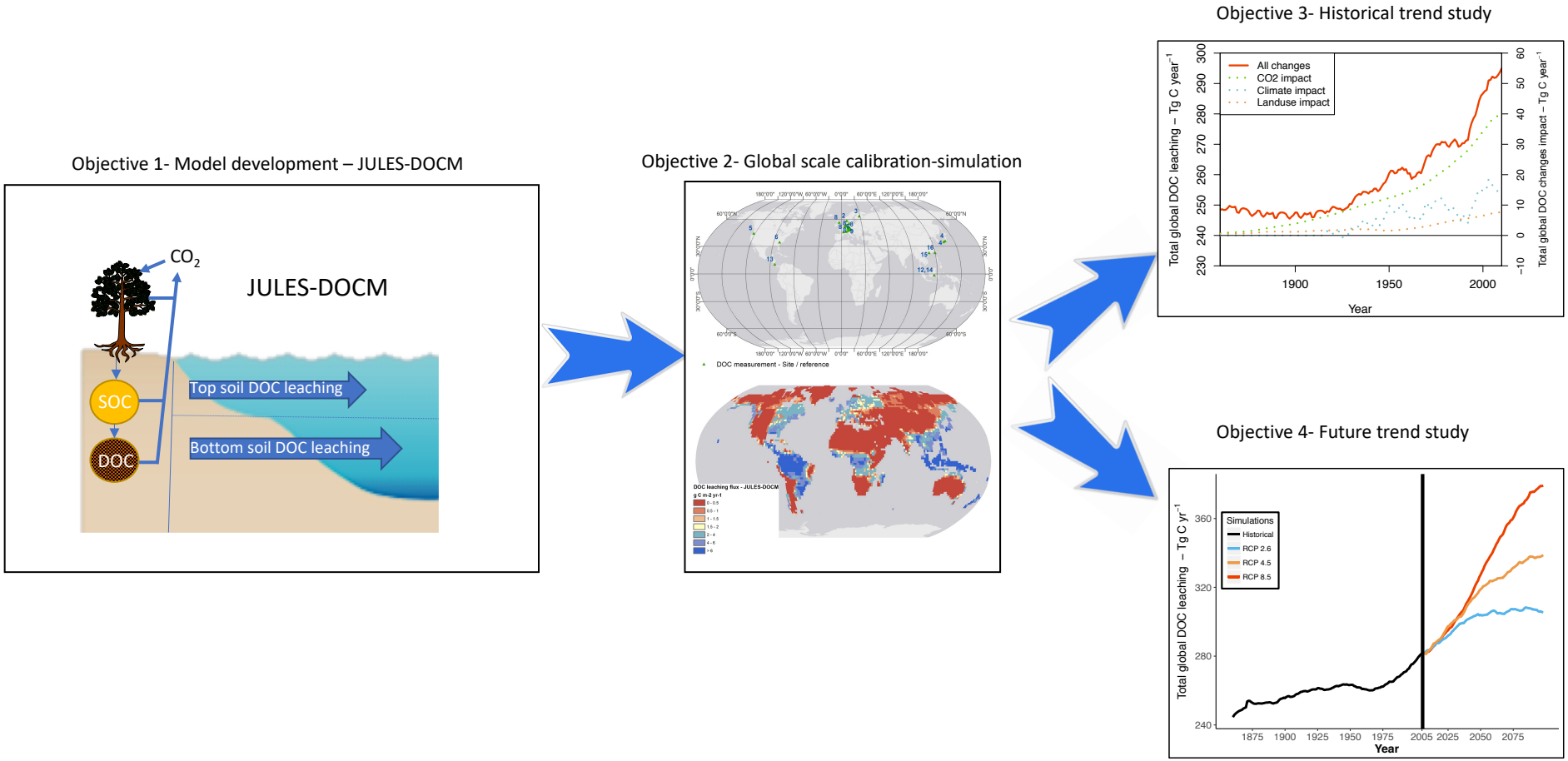


**Figure 7.** Conceptual schematic of this thesis

# Chapter 1

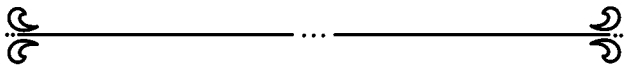

# Chapter 1 - Representation of dissolved organic carbon in the JULES land surface model (JULES-DOCM)

This chapter presents the developments I integrated in JULES in order to represent the cycling of DOC in soil and its transport out of the soil to the river system as described in the following publication:

Nakhavali,M., Friedlingstein,P., Lauerwald,R., Tang,J., Chadburn,S., Camino-Serrano,M., Guenet,B., Harper,A., Walmsley,D., Peichl,M., and Gielen,B.: Representation of dissolved organic carbon in the JULES land surface model (vn4.4_JULES-DOCM), Geoscientific Model Development, 11, 593-609,https://doi.org/10.5194/gmd-11-593-2018, 2018.

## Abstract

Current global models of the carbon (C) cycle consider only vertical gas exchanges between terrestrial or oceanic reservoirs and the atmosphere, thus not considering lateral transport of carbon from the continents to the oceans. Therefore, those models implicitly consider that all the C which is not respired to the atmosphere is stored on land, hence overestimating the land C sink capability. A model that represents the whole continuum from atmosphere to land and into the ocean would provide better understanding of the Earth's C cycle and hence more reliable historical or future projections. A first and critical step in that direction is to include processes representing production and export of dissolved organic carbon in soils. Here we present an original representation of Dissolved Organic C (DOC) processes in the Joint UK Land Environment Simulator (JULES-DOCM) that integrates a representation of DOC production in terrestrial ecosystems based on incomplete decomposition of organic matter, DOC decomposition within the soil column, and DOC export to the river network via leaching. The model performance is evaluated in five specific sites for which observations of soil DOC concentration are available. Results show that the model is able to reproduce the DOC concentration and controlling processes including leaching to the riverine system which is fundamental for integrating terrestrial and aquatic ecosystems. Future work should include the fate of exported DOC in the river system as well as DIC and POC export from soil.

# 1 Introduction

An estimated 1.9 Pg C $yr^{-1}$ is exported from soils through the river network to the oceans, which represents a significant flux in global carbon (C) cycle (Cole et al. 2007; Regnier et al. 2013) and can affect biological and chemical properties of both aquatic (Aitkenhead and Mcdowell, 2000) and terrestrial ecosystems (Kalbitz *et al.*, 2000). In land surface models that are part of Earth system models, only vertical fluxes of carbon between land and atmosphere are considered whilst lateral export fluxes are not included. This leads to an overestimation of soil organic C (SOC) sequestration and terrestrial C sinks (Jackson, Banner and Jobbágy, 2002; Janssens *et al.*, 2003). Hence we need to move towards a boundless C cycle model which accounts for lateral fluxes and thus produces more accurate projections of atmospheric $CO_2$ concentrations and C stocks (Battin *et al.*, 2009). One of the lateral fluxes that has been neglected is the transfer of carbon from terrestrial to aquatic ecosystems in the form of dissolved organic C (DOC), which has been shown to be increased by anthropogenic perturbation such as land use change such as deforestation and increased atmospheric $CO_2$ concentrations (Regnier *et al.*, 2013). DOC contributes about 37% of the global riverine carbon exports to the coast (Meybeck, 1993) and adds to the net-heterotrophy of inland waters and related $CO_2$ emission fluxes to the atmosphere.

The main sources of DOC in terrestrial ecosystems are plant residues (Khomutova *et al.*, 2000), humus and root exudates (Marschner, 1995; Kalbitz *et al.*, 2000; Van den berg, Shotbolt and Ashmore, 2012). DOC within the soil can be the product of in-situ production or be brought in by advective fluxes with soil water transport. It has been hypothesized that loss of the carbon from the soil by leaching has to be taken into account to reasonably re-assess the terrestrial C budget of Europe (Siemens, 2003). The fate of this DOC within inland water networks, i.e. the proportion transported to the coast or respired and emitted to the atmosphere, is the key to understanding the link to the other compartments of the Earth system (J. J. Cole *et al.*, 2007; Battin *et al.*, 2009). Nevertheless, it is a difficult task to link riverine and terrestrial fluxes by empirical methods, because 1) riverine fluxes are integrating fluxes from different land use systems (Boyer and Groffman, 1996; Kindler *et al.*, 2011) with different leaching rates and DOC quality, 2) in-stream transformation makes it difficult to trace back terrestrial DOC sources, and 3) the difficulty to separate natural and anthropogenic perturbation fluxes (Schelker et al. 2013; Pierre Regnier et al. 2013).

A physical-based modelling approach explicitly representing different terrestrial sources and processes involved in DOC cycling within the soil column and DOC leaching from the soil can help overcome these difficulties. Representation of DOC cycling within the soil column is also a major step toward simulating deep soil SOC formation (Rumpel and Kögel-Knabner, 2011). Physical-based models help to understand the processes involved in soil DOC cycling and leaching as well as biogeochemistry of SOC in general. So far several models have been developed that simulate DOC with different temporal and spatial resolution, from 15 minutes as in SOLVEG-II (Ota, Nagai and Koarashi, 2013) to monthly as in ECOSSE (Smith et al. 2010) or RivCM (Langerwisch *et al.*, 2015) and from site scale as in DyDOC (Michalzik *et al.*, 2003) to global scale as in TEM (Kicklighter *et al.*, 2013). Some of these models represent DOC leaching, whereas others do not. Each model has its own particular definition for carbon pools (including DOC) and DOC production processes which can be based on turnover time, as in TERRAFLUX (Neff and Asner, 2001), or based on chemical composition as in the DyDOC model (Michalzik *et al.*, 2003). Although all these models have been evaluated, with the exception of the TEM model which was tested for arctic rivers, none of them has demonstrated its ability of representing the DOC production, processing and transport at the global scale.

In general, most of the models containing decomposition are based on first-order kinetics (Olson, 1963). Frequently, models tend to represent the top soil layer as the major source for DOC production and export (Koven *et al.*, 2013), other studies (Rumpel and Kögel-Knabner, 2011; Braakhekke *et al.*, 2013) highlight the importance of DOC for SOC production in deeper soil layers.

Here we present an original representation of DOC processes in the Joint UK Land Environment Simulator (JULES-DOCM) that integrates a representation of DOC production in terrestrial ecosystems based on incomplete decomposition of organic matter, DOC decomposition within the soil column, and DOC export to the river network via leaching. JULES has been used to evaluate the global C cycle (e.g. LeQuéré, et al. 2015, Sitch et al. 2015) and its role in the Earth system, but to date lacks the critical processes of DOC production and export. The aim of this study is to include a representation of DOC produced in terrestrial soils down to 3 meters (as soil hydrology and Carbon are simulated over 3 meter soil profile in JULES), assuming an incomplete decomposition of organic matter and its subsequent fate as DOC including i) DOC decomposition and release as $CO_2$ to the atmosphere, and ii) DOC export to the riverine system via leaching; to test the new model in different ecosystems and to evaluate it against specific sites where soil DOC measurements were available. Other forms of

C need different processes to be represented to fully represent the land-to-ocean aquatic continuum of the global C cycle. Hence future work should include DIC and POC export from soils as well as the fate of all exported carbon in the river system.

# 2 Material and Methods

## 2.1 JULES model

JULES is a process-based model which represents energy, water and C cycling between vegetation, soil and atmosphere as described in Best et al. (2011) and Clark et al. (2011). Vegetation processes in JULES are represented in a dynamic vegetation model (TRIFFID), distinguishing 9 plant function types (PFTs) at the global scale: tropical and temperate broadleaf evergreen trees, broadleaf deciduous trees, needle-leaf evergreen trees and deciduous trees, C3 and C4 grasses, and evergreen and deciduous shrubs (Harper *et al.*, 2016).
The representation of SOC in JULES, follows the formulation of the RothC soil carbon scheme (Jenkinson *et al.*, 1990; Jenkinson and Coleman, 2008), distinguishing four carbon pools: decomposable plant material (DPM), resistant plant material (RPM), heterotrophic microbial biomass (BIO) and long-lived humified material (HUM). DPM and RPM pools receive litter inputs directly from the vegetation due to defoliation, mortality and disturbance, the allocation to DPM or RPM depending on the PFT characteristics with higher fraction of decomposable litter provided from grasses and higher fraction of resistant litter provided from trees (Clark *et al.*, 2011). HUM and BIO each receive inputs from the other two soil carbon pools, as a fraction of the decomposition that is not respired to the atmosphere.

## 2.2 JULES-DOCM model new features

JULES-DOCM is an extension of JULES based on version 4.4 (vn4.4 documentation in http://jules-lsm.github.io/vn4.4) , which explicitly represents DOC cycling in soils and considers DOC leaching from the soil profile. The following section deals with the representation of DOC fluxes and processes in more details.

### 2.2.1 Soil carbon profile

SOC is specified as the main source of DOC in JULES-DOCM. In JULES v4.4, each of the four SOC pools is treated as a single box down to 3 m, without any representation of its vertical distribution. This absence of vertical distribution has consequences in terms of simulating DOC fluxes, but also potential impacts on soil $CO_2$ fluxes, considering vertical variations of soil temperature and moisture. In JULES-DOCM, we introduce a vertical distribution of SOC for each soil carbon pool assuming an exponential decay with depth, with a weighting factor $\beta_0$ :

$$\beta_{0_i} = e^{-\frac{z_i}{z_0}} \times dz_i \qquad (eq.1)$$

Here, $z_0$ is the e-folding depth of C content within 1 meter of soil (i.e. depth at which SOC decreases by a factor of $e$ relative to the surface), $z_i$ is the soil depth of layer $i$, and $dz_i$ is the thickness of the soil layer. In order to estimate $z_0$, we used the soil data from Jobbágy & Jackson (2000) that provides the vertical distribution of SOC within a 3 m soil profile based on the observed soil carbon profiles across several biomes. Jobbágy & Jackson provides soil C content in the first meter [0-1m] and for the first 3 meters [0-3m], allowing us to estimate the fraction in the first meter and derive $z_0$ accordingly:

$$\int_0^1 e^{-\frac{z}{z_0}} d_z = x \int_0^3 e^{-\frac{z}{z_0}} d_z \qquad (eq.2)$$

where $x$ is the ration of SOC content within the first 1 meter of soil relative to the 3-meter profile for different biomes as given by Jobbágy & Jackson (in their Table. 3) (Jobbágy and Jackson, 2000). Jobbágy & Jackson provide data for 11 PFTs. Here we first estimate $z_0$ for each of those PFTs, then regrouped them into the 9 JULES PFTs (see tables S1 and S2).
In order to calculate the fraction of SOC that is used as input for DOC production in each layer of the DOC model, (see equation 4 below) the weighting factors are normalised ($ß_{zi}$):

$$\beta_{z_i} = \frac{\beta_{0_i}}{\sum_{i=1}^{i=4} \beta_{0_i}} \qquad (eq.3)$$

## 2.2.2 DOC fluxes and processes

In JULES-DOCM, four new DOC carbon pools have been added. First the model accounts for a labile and a recalcitrant DOC pool based on their decomposition rate (Aguilar and Thibodeaux, 2005; Thibodeaux and Aguilar, 2005). The labile pool is readily available for decomposition in soil solution at all times and the recalcitrant pool is subject to slower decomposition rate (Smith et al. 2010). DOC produced from plant material pools (DPM and RPM) and microbial biomass (BIO) is directed to the labile pool, while DOC from humus (HUM) is directed to the recalcitrant pool. Second, both the labile and the recalcitrant DOC pools have a dissolved and an adsorbed form, with only the dissolved pool being subjected to decomposition and leaching.

DOC production ($F_P$) follows first-order kinetics (Olson, 1963) and the flux of carbon from SOC to DOC pools ($k$ for labile or recalcitrant) in each soil layer (i) in kg C m$^{-2}$ day$^{-1}$($F_P$; arrows a-d Fig. 1) is calculated as:

$$F_{P_{k,i}} = \beta_{z_i} \times S_{C_k} \times \left(1 - e^{\left(-K_P \times F_S(S)_i \times F_T(T_{soil})_i \times F_v(v) \times D_f\right)}\right) \times e^{-\tau_{z_i}} \qquad (eq.4)$$

where $S_{Ck}$ is amount of carbon in the soil organic pool (DPM/RPM/BIO for DOC labile pool and HUM for recalcitrant pool) in kg C m$^{-2}$ in whole soil, $K_P$ is DOC production rate in day$^{-1}$, $F_S(s)_i$ and $F_T(T_{soil})_i$ are respectively the rate modifiers due to moisture and temperature, which are controlling decomposition in each soil layer (i), $F_v(v)$ is the fraction of the vegetation. All units are given in Table 2. The moisture and temperature rate modifiers are based on the RothC formulations (Coleman and Jenkinson, 2014). $\tau_z$ is the empirical factor for decrease of C decomposition rates with soil depth, as recently introduced in JULES (Burke et al. 2016).

The DOC production rate is further modified by $D_f$, which considers the decrease of SOC decomposition rate as increase of silt plus clay content given in fraction (Parton et al. 1987):

$$D_f = 1 - (0.75 \times (clay + silt)) \qquad (eq.5)$$

After decomposition, carbon pools ($S_C$) are updated by the changes in each time step (daily) as follow:

$$\frac{\Delta S_{C_{DPM}}}{\Delta t} = f_{DPM}\Lambda_c - R_{DPM} - \sum_{i=1}^{i=4} F_{P_{DPM_i}} \quad \textit{(eq.6)}$$

$$\frac{\Delta S_{C_{RPM}}}{\Delta t} = (1 - f_{DPM})\Lambda_c - R_{RPM} - \sum_{i=1}^{i=4} F_{P_{RPM_i}} \quad \textit{(eq.7)}$$

$$\frac{\Delta S_{C_{BIO}}}{\Delta t} = 0.46\,(1 - B_R)\,R_S - R_{BIO} - \sum_{i=1}^{i=4} F_{P_{BIO_i}} + \sum_{i=1}^{i=4} F_{BIO_{IN\,i}} \quad \textit{(eq.8)}$$

$$\frac{\Delta S_{C_{HUM}}}{\Delta t} = 0.54\,(1 - B_R)\,R_S - R_{HUM} - \sum_{i=1}^{i=4} F_{P_{HUM_i}} \quad \textit{(eq.9)}$$

where in RothC model fraction ($f_{DPM}$) of litter fall ($\Lambda_c$) is directed to DPM and RPM depending on vegetation type. C pools are subjected to decomposition. Part of decomposed C as a fraction (1-$B_R$) of total respiration ($R_s = R_{DPM} + R_{RPM} + R_{BIO} + R_{HUM} + R_{DOC}$) is partially feeding microorganisms in soil (BIO) and partially stored as recalcitrant C in soil (HUM) depending on soil texture and the rest ($B_R$) is released to the atmosphere. These parameters were already present in JULES (Clark *et al.*, 2011). In JULES-DOCM the update of carbon pools after DOC production was added (last term of each equation, $F_P$…, defined in equation 4 above) as well as $F_{BIO_{IN}}$ the input flux from DOC to BIO pool, described below.

We assume that the decomposition of DOC pools ($F_D$) (kg C m$^{-2}$ day$^{-1}$) also follows first-order kinetics depending on temperature and labile and recalcitrant DOC pool size as follow (arrows e-f Fig. 1):

$$F_{D_{k,i}} = S_{DOC_{k,i}} \times \left(1 - e^{\left(-K_{DOC_k} \times F_T(T_{soil})_i\right)}\right) \quad \textit{(eq.10)}$$

where $S_{DOCi}$ is the DOC pool size ($k$ for labile or recalcitrant) in kg C m$^{-2}$ and $K_{DOCk}$ *is* the basal decomposition rate of the dissolved DOC ($k$ for labile or recalcitrant pool) (in day$^{-1}$) and $F_T(T_{soil})_i$ is the soil temperature rate modifier within each soil layer (i) same as in eq.4.

Part of decomposed DOC is respired ($R_{DOC}$ in kg C m$^{-2}$ day$^{-1}$, arrow g Fig. 1) and the rest returns to the BIO carbon pool ($F_{BIO\,IN}$ in kg C m$^{-2}$ day$^{-1}$, arrow h Fig. 1) from each soil layer

(i) and DOC pools (k). This proportion is controlled by a CUE parameter (Kalbitz *et al.*, 2003) which is set to 0.5 as a default as in Manzoni et al. (2012).
Hence distribution of decomposed DOC to the BIO pool and respiration will be:

$$F_{BIO_{IN}{}_i} = (1 - CUE) \times \sum F_{D}{}_{k,i} \quad \textit{(eq.11)}$$

$$R_{DOC}{}_{k,i} = CUE \times \sum F_{D}{}_{k,i} \quad \textit{(eq.12)}$$

For adsorption/desorption, a constant sorption equilibrium distribution coefficient ($K_D$) is used to partition DOC in dissolved and adsorbed phases. The assumption is that DOC in the labile or recalcitrant pool is proportionally distributed between adsorbed DOC ($S_{DOCad}$) and dissolved DOC pools ($S_{DOC}$ in soluble phase) depending on $K_D$ from each soil layer(i) and DOC pool (k). Hence if the potentially adsorbed DOC fraction ($AD\_pot_i$) compared to the size of the actually adsorbed DOC ($S_{DOC_{ad}{}_{k,i}}$) is positive then this fraction will be adsorbed and added to the adsorbed DOC pool, and if it is negative then this fraction will be desorbed and added to dissolved DOC pool per model time step.
These terms for DOC labile and recalcitrant pools in JULES-DOCM are as follow (arrow: i and j, Fig. 1):

$$AD\_pot_i = S_{DOC}{}_{k,i} \times K_D \times \frac{BK}{\theta v_i} \quad \textit{(eq.13)}$$

$$S_{DOC}{}_{k,i} = S_{DOC}{}_{k,i} - \left(AD\_pot_i - S_{DOC_{ad}{}_{k,i}}\right) \quad \textit{(eq.14)}$$

$$S_{DOC_{ad}{}_{k,i}} = S_{DOC_{ad}{}_{k,i}} + \left(AD\_pot_i - S_{DOC_{ad}{}_{k,i}}\right) \quad \textit{(eq.15)}$$

where $S_{DOCk,i}$ is dissolved labile and recalcitrant DOC pools in kg C $m^{-2}$, $K_D$ is the distribution factor ($m^3$ water $kg^{-1}$ soil), BK is bulk density (kg soil $m^{-3}$) and $\theta_{vi}$ is the volumetric soil moisture ($m^3$ $m^{-3}$) and it is considered to be same for DOC labile and recalcitrant pools.
DOC diffusion ($F_{Diff\,i,j}$) in kg C $m^{-2}$ $day^{-1}$ between the layers is based on Fick's second law and it is the function of the diffusion coefficient (D) in $m^2$ $day^{-1}$, concentration of labile or recalcitrant DOC at different soil depths ($C_{DOCk,i,j}$) in kg C $m^{-2}$ and the distance ($z_{i,j}$) between midpoints of soil layers (i: downward flow; j: upward flow) in m (arrow k, Fig. 1):

$$F_{Diff_{i,j}} = \mathrm{D} \times \frac{\partial^2 C_{DOC_{k,i,j}}}{\partial z_{i,j}^2} \qquad \textit{(eq.16)}$$

Leaching of the DOC is considered to occur from all 4 DOC soil layers. The top DOC is defined as the first two layers representing the first 35 cm of the soil. The lower two DOC layers represent the sub-soil from 35 cm down to 3 m. Soil leaching at the top DOC layer is dependent on the surface runoff whereas subsurface leaching is dependent on the subsurface runoff. However subsurface runoff is also representing the drainage from the bottom of the 3m soil column, and thus mimics the groundwater base flow, in terms of water as well as in terms of DOC exports. More information on the hydrology of model is given in Gedney & Cox (2003); Clark & Gedney 2008). Both DOC layers leaching fluxes are based on the concentration of dissolved DOC in the soil water. Hence leaching of DOC (*L*) from the dissolved labile and recalcitrant pool within the top (sum of first and second soil layer) - and sub-soil (sum of third and fourth soil layer) (T and S) in kg C $m^{-2}$ $day^{-1}$ is calculated as follows (arrow l, Fig.1):

$$L_T = S_{DOC_{k,h}} \times \frac{Roff_{surf}}{T_{s_i}} \qquad \textit{(eq.17)}$$

$$L_S = S_{DOC_{k,h}} \times \frac{Roff_{sub}}{T_{s_i}} \qquad \textit{(eq.18)}$$

where $S_{DOC_{k,h}}$ is the DOC quantity in the dissolved labile and recalcitrant pool (*h* for top or sub soil), $Roff_{surf}$ is the surface runoff, $Roff_{sub}$ is the subsurface runoff (both kg $m^{-2}$ $day^{-1}$) and $T_{si}$ (defined in code as $\theta_s$) is the soil moisture in each soil layer (i) (kg $m^{-2}$).
Hence dissolved and adsorbed DOC pools are updated as follow:

$$\frac{\Delta S_{DOC_k}}{\Delta t} = F_{P_{k,i}} + AD\_pot_i + F_{Diff_i} - F_{D_{k,i}} - L_T - L_S \qquad \textit{(eq.19)}$$

Values of the default DOC model parameters are given in Table 1.

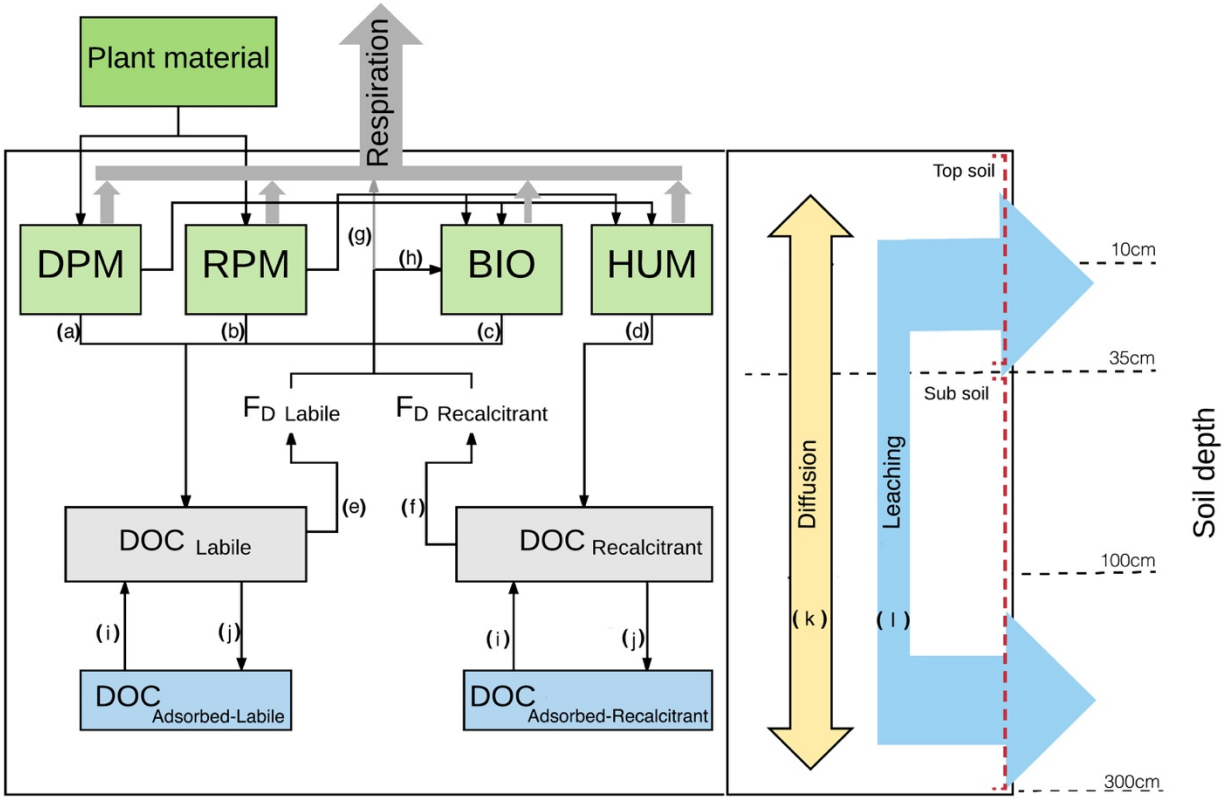


Figure 1. JULES-DOCM model structure

**Table 1.** DOC-relevant parameters in the JULES-DOCM model.

| Parameter | Description | Value | Unit | Sensitivity test values (±) | |
|---|---|---|---|---|---|
| | | Carbon parameters | | | |
| $z_0$ | *e*-folding depth of carbon content within 1 m of soil[a] | Values range (65.68–167.13) | $m^{-1}$ | PFT based | 109.55 |
| $\tau_\zeta$ | Decay of carbon decomposition with depth (z)[b] | 2 | $m^{-1}$ | 3 | |
| | | DOC parameters | | | |
| $K_P$ | Rate constant for DOC production specific to each carbon pool[c] | $1 \times 10^{-4}$, $5 \times 10^{-6}$, $5 \times 10^{-5}$, $2 \times 10^{-6}$ | $day^{-1}$ | – | – |
| $K_{DOC\ (labile)}$ | Basal decomposition rate of dissolved DOC labile pool[d] | 3 Value range (0.46–100) | days | 4.5 | 1.5 |
| $K_{DOC\ (recalcitrant)}$ | Basal decomposition rate of dissolved DOC recalcitrant pool[e] | 600.0 Value range (66–5000) | days | 900 | 300 |
| Slope parameter of $D_f$ | Slope parameter controlling DOC production and decomposition modifier depending on clay and silt fraction[f] | 0.75 | – | 1 | 0.5 |
| CUE | Carbon use efficiency[g] | 0.5 | – | 0.75 | 0.25 |
| $K_D$ | Distribution coefficient of of adsorbed DOC[h] | $8.05 \times 10^{-6}$ | $m^3$ water $kg^{-1}$ soil | $1.21 \times 10^{-4}$ | $4.03 \times 10^{-6}$ |
| $D$ | DOC diffusion coefficient[i] | $1.06 \times 10^{-5}$ | $m^2\ day^{-1}$ | $1.59 \times 10^{-5}$ | $5.31 \times 10^{-6}$ |

[a] Jobbágy and Jackson (2000). [b] Koven et al. (2013), Burke et al. (2017). [c] Smith et al. (2010). [d] Kalbitz et al. (2003), Turgeon (2008). [e] Kalbitz et al. (2003), Turgeon (2008). [f] Parton et al. (1987). [g] Manzoni et al. (2012). [h] Moore et al. (1992). [i] Ota et al. (2013).

Table 2. Symbols definition and units

| Symbol | Units | Definition |
|---|---|---|
| $BK$ | kg $m^{-3}$ | Bulk density |
| $\boldsymbol{B_R}$ | | Fraction of soil respiration which is respired |
| $\boldsymbol{\beta_z}$ | $m^{-1}$ | Carbon distribution with depth, depending on biome |
| CUE | | Carbon use efficiency |
| $C_{DOC}$ | kg C $m^{-2}$ | Amount of DOC subjected to transport by diffusion |
| D | $m^2$ $day^{-1}$ | DOC diffusion coefficient |
| $D_f$ | | DOC production / decomposition modifier depending on clay and silt fraction |
| $dz$ | m | Soil layer thickness |
| $\Delta S_{C_{BIO}}$ | kg C $m^{-2}$ $day^{-1}$ | Biomass carbon pool update |
| $\Delta S_{C_{DPM}}$ | kg C $m^{-2}$ $day^{-1}$ | Decomposable plant material carbon pool update |
| $\Delta S_{C_{HUM}}$ | kg C $m^{-2}$ $day^{-1}$ | Humus carbon pool update |
| $\Delta S_{C_{RPM}}$ | kg C $m^{-2}$ $day^{-1}$ | Resistant plant material carbon pool update |
| $\Delta S_{DOC}$ | kg C $m^{-2}$ $day^{-1}$ | Labile and recalcitrant DOC pools update |
| $AD\_pot$ | kg C $m^{-2}$ $day^{-1}$ | Adsorbed/desorbed DOC from labile and recalcitrant pools |
| $F_{BIO_{IN}}$ | kg C $m^{-2}$ $day^{-1}$ | Decomposed DOC flux from labile and recalcitrant pool into biomass pool |
| $F_D$ | kg C $m^{-2}$ $day^{-1}$ | Labile and recalcitrant decomposed DOC flux |
| $F_{Diff}$ | kg C $m^{-2}$ $day^{-1}$ | Flux of DOC transported by diffusion |
| $F_{P_{BIO}}$ | kg C $m^{-2}$ $day^{-1}$ | DOC flux originated from biomass carbon pool |
| $F_{P_{DPM}}$ | kg C $m^{-2}$ $day^{-1}$ | DOC flux originated from decomposable plant material carbon pool |
| $F_{P_{HUM}}$ | kg C $m^{-2}$ $day^{-1}$ | DOC flux originated from humus carbon pool |
| $F_{P_{RPM}}$ | kg C $m^{-2}$ $day^{-1}$ | DOC flux originated from resistant plant material carbon pool |
| $F_S(s)$ | kg $m^{-2}$ | Soil moisture rate modifier |
| $F_T(T_{soil})$ | K | Soil temperature rate modifier |
| $F_v(v)$ | | Fractional coverage of a vegetation type |

| Symbol | Units | Definition |
|---|---|---|
| $f_{dpm}$ | | Fraction of litter that is decomposable plant material |
| $K_P$ | $day^{-1}$ | Rate constant for DOC production specific to the pool |
| $K_{DOC}$ | days | Basal decomposition rate of dissolved DOC labile and recalcitrant pools |
| $K_D$ | $m^3$ water $kg^{-1}$ soil | Distribution coefficient of adsorbed DOC |
| $\Lambda_c$ | kg C $m^{-2}$ $day^{-1}$ | Litterfall rate |
| $L_T$ | kg $m^{-2}$ $day^{-1}$ | Leaching from labile and recalcitrant DOC pools in top soil |
| $L_S$ | kg $m^{-2}$ $day^{-1}$ | Leaching from labile and recalcitrant DOC pools in sub soil |
| m | | DOC decomposition rate type (labile or recalcitrant) |
| $R_{BIO}$ | kg C $m^{-2}$ $day^{-1}$ | Respiration from biomass carbon pool |
| $R_{DPM}$ | kg C $m^{-2}$ $day^{-1}$ | Respiration from decomposable plant material carbon pool |
| $R_{DOC}$ | kg C $m^{-2}$ $day^{-1}$ | Respiration from labile and recalcitrant DOC pools |
| $R_{HUM}$ | kg C $m^{-2}$ $day^{-1}$ | Respiration from humus carbon pool |
| $R_{RPM}$ | kg C $m^{-2}$ $day^{-1}$ | Respiration from resistant plant material carbon pool |
| $Roff_{surf}$ | kg $m^{-2}$ $day^{-1}$ | Surface Runoff |
| $Roff_{sub}$ | kg $m^{-2}$ $day^{-1}$ | Sub-Surface Runoff |
| $S_C$ | kg C $m^{-2}$ | Soil carbon storage |
| $T_s$ | kg $m^{-2}$ | Soil moisture content |
| $S_{DOC}$ | kg C $m^{-2}$ | Labile and recalcitrant DOC storages |
| $S_{DOC_{ad}}$ | kg C $m^{-2}$ | Adsorbed labile and recalcitrant DOC storages |
| $\theta_v$ | kg $m^{-3}$ | Volumetric Soil moisture content |
| $\tau_z$ | $m^{-1}$ | Decay of Carbon decomposition with depth |
| $z$ | m | Soil depth |
| $z_0$ | m | e-folding depth of carbon content within 1 meter of soil |

## 2.3 Sites description

Two data levels were provided in order to test the model performance. Level 1, including Hainich, Carlow and Brasschaat which included the carbon fluxes and continuous DOC measurements from soil water from 3 to 10 years period, and level 2, including Turkey Point 89 (TP89) and Guandaushi with fewer C fluxes measurements and discontinuous DOC measurements (Table 3). Location of sites are given in Figure 2.

### 2.3.1 Hainich

The site "Hainich", located in Germany – National park Hainich, (51°04′ 45″N, 10°27′07″E), is covered by an old-growth deciduous forest dominated by *Fagus sylvatica* and intermixed with *Fraxinus excelsior* and *Acer pseudoplatanus* (Mund *et al.*, 2010). The soil class at this site is Eutric Cambisol with a high clay content and high biological activity, as illustrated by a mull or F-Mull organic layer (Table 4). The mean annual air temperature is 7.5-8°C and the annual precipitation is in the range of 750-800 mm $yr^{-1}$ (Kutsch *et al.*, 2010). At this site, soil solution samples were taken at three depths (5, 10 and 20 cm) using ceramic suction plates positioned at four different plots within the site. Samples were obtained by applying a tension of 100 hPa after each bi-weekly sampling occasion.

### 2.3.2 Carlow

The site "Carlow" is located in Ireland – County Carlow, (52° 52'N, 6° 54'W). The land cover is grassland, the soil class is Calcic Luvisol. This sandy loamy soil has a uniform profile and is well-drained (Table 4). The climate is characterized by a mean annual air temperature of 9.3°C and a mean annual precipitation of 823 mm $yr^{-1}$ (Walmsley *et al.*, 2011). DOC samples were collected from at two locations separated 150 m from each other, using 20 suction cups per location, with ten of these cups installed directly beneath the rooting zone and the other ten at a depth of 0.7 m. Samples were obtained by applying a tension of 400 hPa after each bi-weekly sampling occasion (Walmsley, 2009).

### 2.3.3 Brasschaat

The site “Brasschaat” is located in Belgium and covered by mixed coniferous/deciduous (De Inslag) forest, (51°18’33" N, 4°31’14" E) with stands of old Scots Pine (*Pinus sylvestris)* (Janssens *et al.*, 1999). The temperate maritime climate is characterized by a mean annual air temperature of 11.1°C and a mean annual precipitation of 824 mm $yr^{-1}$ (Gielen *et al.*, 2010). The soil class was defined as Albic Hypoluvic Arenosol (Table 4). The profile usually exhibits a high soil moisture, but due to the sandy texture and rapid hydraulic conductivity in upper horizons, it is rarely saturated (Gielen *et al.*, 2011).

DOC samples were collected at three horizons of Al/Ap, A/E and Cg (Soil Classification Working Group, 1998) referred to 10,35 and 75cm depth, by means of ceramic suction cups on a biweekly interval. Two days prior to sample collection a tension of 600 hPa was applied to each suction cup. Samples were collected at three locations and pooled into one composite sample per layer for analysis (Gielen *et al.*, 2011).

### 2.3.4 Turkey Point 89

The site “Turkey Point 89 (TP89)”, located in southern Ontario – Canada, (42°77′57″N, 80°45′09″E), is covered by an evergreen needleleaf forest dominated by Eastern White pine *(Pinus strobus* L.*)* mixed with few stands of Oak, Paper birch, Wild black cherry and Red pine (Peichl and Arain, 2006) established in 1989 on agricultural lands (Peichl *et al.*, 2010). The mean annual air temperature is 8.1°C and mean annual precipitation is 832 mm $yr^{-1}$ (Peichl and Arain, 2006). The soil class at this site is Gleyed Brunisolic Luvisol and due to the high sand content, it is well drained and has a low to moderated water holding capacity (Presant, E.W., Acton, 1984; Peichl *et al.*, 2010). DOC sampling was attempted in monthly intervals at three depths of 25, 50 and 100 cm by means of porous suction cups, however, due to the dry sandy soils, samples could only be retrieved for 5 separate days of sampling after heavy rain fall events on 29-Nov-2004, 3-May-2005, 16-Jun-2005, 29-Jun-2005, 14-Oct-2005 (Peichl *et al.*, 2007).

### 2.3.5 Guandaushi

The site “Guandaushi” is located in central Taiwan, (23° 8'N, 120° 8'E). The climate is characterized by distinct rainy and dry seasons and a mean annual air temperature of 22.4°C and annual precipitation in the range of 2300 to 2700 mm $yr^{-1}$. The land cover is subtropical mixed hardwood forest including three stands of natural hardwood and secondary hardwood on light loam textured soil and Chinese fir (*Cunninghamia lanceolate)* on heavy clay textured soil. DOC samples were collected at three depths of 15, 30 and 60 cm in three locations at bi-weekly interval by means of ceramic suction cups.

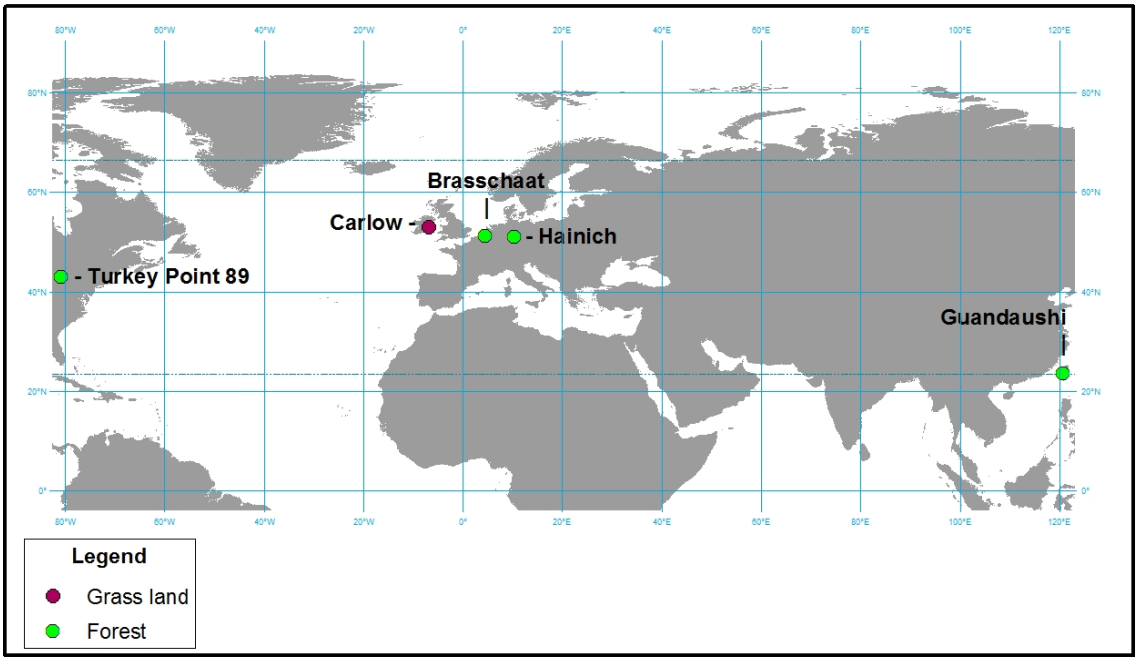


Figure 2. Study sites

Table 3. Data availability for model evaluation at different

| **Sites** | Brasschaat[1] | Carlow[1] | Guandaushi[2] | Hainich[1] | Turkey-point89[2] |
|---|---|---|---|---|---|
| | | | **Carbon fluxes** | | |
| *GPP* | 2000-2006 | 2008 | | 2000-2012 | 2005-2008 |
| *NPP* | 2000 | | | 2000-2007 | 2005-2008 |
| *Soil respiration* | 2000-2006 | | | 2000-2007 | 2005-2008 |
| *C content* | 1995-1998 | 2006-2009 | | 2000-2007 | 2004-2006 |
| | | | **DOC measurements** | | |
| *1 year* | | | 1999 | | |
| *1 to 5 years* | | 2006-2009 | | | 2004-2005 |
| *5 to 10 years* | 2000-2008 | | | 2001-2014 | |

1. level 1 site 2. Level 2 site

Table 4. Evaluation Level 1-sites characteristics

| | **Site** | | |
|---|---|---|---|
| | **Brasschaat** | **Carlow** | **Hainich** |
| | **Characteristics** | | |
| **Ecosystem** | Evergreen forest | Grassland | Deciduous forest |
| **Soil classification** | Arenosol | Luvisol | Cambisols |
| **BK (kg m-3)** | 1.4 | 1.07 | 1.2 |
| **Clay (fraction)** | 0.034 | 0.22 | 0.589 |
| **Sand (fraction)** | 0.8912 | 0.51 | 0.031 |
| **Silt (fraction)** | 0.0748 | 0.27 | 0.38 |
| | **Measurement depth (cm)** | | |
| **Carbon content** | 100[1] | 50[2] | 60[3] |
| **DOC concentration** | 10,35,75 | 5,10,20 | 10-77 |
| | **FLUXNET meteorological observations** | | |
| **Period** | 1996-2014 | 2004-2014 | 2004-2009 |

1. Janssens et al. 1999 2. Kindler & Siemens 2010 3. Schrumpf et al. 2011

## 2.4 Model input and setting

Model performance was tested against observed data from Guanduashi and four FLUXNET sites (Hainich, Carlow, Brasschaat and Turkey Point-89). The FLUXNET database provides on-site meteorological data for each site that could be used as forcing for simulations in JULES, However, we had to use the global WATCH dataset (Weedon et al. 2010) as forcing for Guandaushi site where no on-site data was available. However, both forcing data were checked for any missing data and it was gap filled by linear interpolation. The meteorological forcing is provided at the measurement site level (no explicit spatial resolution) and includes the downward shortwave and longwave radiation at the surface (W m-2), rainfall (kg m-2 s-1), snowfall (kg m-2 s-1), wind speed (m s-1), atmospheric temperature (K), atmospheric specific humidity (kg kg-1) and air pressure at the surface (Pa) at half an hour time step (Best et al. 2011).

For Brasschaat, additional model parameters such as BK and clay were taken from Janssens et al. (1999). The model was first spun-up looping over period 1996 to 2014 until all the soil variables reached a steady state. For Hainich, site parameters were taken from Kutsch et al. (2010). The spin-up was run looping 300 times over the years 2004 to 2014. For Carlow, site parameters were taken from Walmsley (2009) and Kindler & Siemens (2010). The spin-up was run looping 300 times over the years 2004-2009. For Turkey Point-89, site parameters were taken from Peichl & Arain (2006) and spin-up was run looping 300 times over the years 2002-2007. For Guandaushi, site vegetation parameters were taken from Liu & Sheu (2003) and soil parameters from HWSD global data (Nachtergaele *et al.*, 2010) and spin-up was run looping 300 times over years 1990 to 2000. The evaluation of model was performed on plot-scale, using climate forcing data, soil and land cover consistent with the site, no horizontal spatial dimension was involved.

## 2.5 Sensitivity test

In order to test the sensitivity of DOC related model parameters on the DOC concentration in different depths of the soil profile, simulations were performed with varying values for $z_0$, $\tau_z$ and DOC controlling parameters such as $K_{DOC\ (labile)}$, $K_{DOC\ (recalcitrant)}$, slope parameter of $D_f$, *CUE*, $K_D$ and D (Table 1).

In total, 16 runs were performed by modifying each parameter once by increasing it 50% and once by decreasing it by 50%, except for the slope parameter controlling $D_f$ (eq. 5) which was changed by 33% to remain within the physical boundaries. In order to do the comparison with measurements, runs were performed for 3 meters soil depth for the periods that measurements were available. Hence, Brasschaat runs were performed for the years 2006-2010, Hainich runs for the years 2005-2014 and Carlow runs for the years 2006-2008.

### 2.6 Statistical analysis

In order to test the model performance, with regard to simulated C stock and fluxes, we used an ANOVA (Analysis of variance) test to compare the model results from the default set of parameters against measurements. In order to test the parameter impact on the simulated DOC concentrations, we computed the RMSE values from each set of model parameter configurations.

## 3 Results

### 3.1 Validation of carbon concentration and fluxes

To examine the performance of soil DOC simulations, it is first necessary to explore other carbon fluxes which link to soil DOC pools. The first flux to be validated is the gross primary production (GPP), for which we have observed values (Table 3). The modelled mean GPP for Brasschaat and Carlow was significantly lower than measurements with 867±25 g C $m^{-2}$ $year^{-1}$ compared to 1173.3±91 g C $m^{-2}$ $year^{-1}$and 903.2 g C $m^{-2}$ $year^{-1}$ compared to 1165.3 g C $m^{-2}$ $year^{-1}$ ($p < 0.05$, Table S3), respectively. For Turkey Point 89 and Hainich, the measured GPP was in line with our model results with 1731.5±108 g C $m^{-2}$ $year^{-1}$ and 1606.74±101 g C $m^{-2}$ $year^{-1}$ compared to 1635.1± 62 g C $m^{-2}$ $year^{-1}$ and 1455±167 g C $m^{-2}year^{-1}$ ($p = 0.162$, Table S3). The modelled NPP was higher than observed values for Hainich and for Turkey Point-89, while it was lower than observed values for Brasschaat (Table 5).

Total soil respiration measurements were available for Brasschaat, Hainich and Turkey Point-89 (Table 3) and were compared with the modelled outputs. The simulated values were close to observed values at Hainich, while the modelled values for Brasschaat were significantly higher (p-value < 0.05, Table S3) and for Turkey Point-89 higher (p-value = 0.0896, Table S3), than the observed values (Table 5).

Finally, we compared the SOC in measurements and model outputs, where the measurements from Brasschaat for 100 cm, Hainich for 60 cm, Carlow for 50 cm and Turkey Point-89 for 15cm (A-horizon) of soil were available. The modelled SOC stock for Brasschaat in the first 100 cm and for Hainich down to 60 cm were slightly lower than the observations, while for Carlow the simulated stocks down to 50 cm and for Turkey Point-89 the simulated stocks down to 15 cm were higher than the observed stocks (Table 5).

## 3.2 DOC simulations

In general, JULES-DOCM was capable of reproducing the DOC concentrations at all the tested sites using the default set of parameters (Table 1) chosen as representative for the top soil (Fig. 3 Level 1 sites, Fig. 4 level 2 sites). For Hainich, the simulated average values and value range were close to observed values at 10 cm and 20 cm (Table 5, RMSE values for 10 cm and 20 cm are 3.0 and 2.5 mg $L^{-1}$ respectively). For Brasschaat, the simulation underestimated DOC concentrations at all depths, but with an increasing underestimation with soil depth (Table 5, RMSE values for 10, 35 and 75 cm are 22.9, 18.4 and 16.8 mg $L^{-1}$ respectively). For Carlow, the modelled and measured values were close at depths of 10 cm and 77 cm, but strongly underestimated at the intermediate depth of 28 cm (Table 5, RMSE values for 10, 10-38 and 28-77 cm are 3, 10.2 and 1.5 mg $L^{-1}$ respectively). At Turkey Point-89, the modelled and observed values were close at 25cm depth, but the DOC concentration average over the profile down to 100 cm was overestimated (Table 5). For Guandaushi, DOC measurements from three different stands (Natural hardwood, secondary hardwood and Chinese fir) values were compared with modelled values. The model values for a depth of 15 cm were closer to observed values for Chinese fir than for natural hardwood or secondary hardwood sites. For 30cm depth, the simulated DOC concentration was substantially lower than the measured DOC averaging over three stands in Guandaushi (Table 5).

Overall, the model was capable of reproducing the seasonality of DOC concentrations for the European sites where long-term observation data are available (Fig. 5). However, at Braschaat the simulated DOC peaked from April-July while observed DOC peaked from July-September. We also examined the hydrology of the model and its interaction with DOC concentration and leaching (e.g. Hainich - Fig. 6; other sites are plotted in Fig. S3). It can be seen for the period 2005 to 2014 that during heavy precipitation, high runoff was produced which caused the higher leaching, and the consequence was a drop in the DOC concentration in 3 meters of soil.

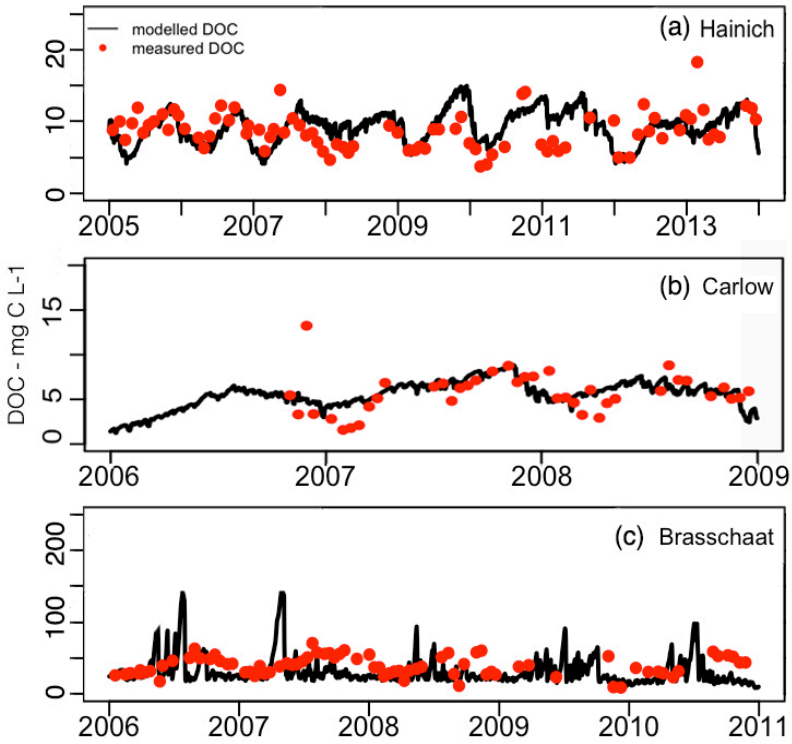


Figure 3. DOC concentration (mg C $L^{-1}$) at 10 cm depth measured (red dots) and simulated (black lines) for (a) Hainich, (b) Carlow, and (c) Brasschaat. Results for other depths are given in Figure S2.

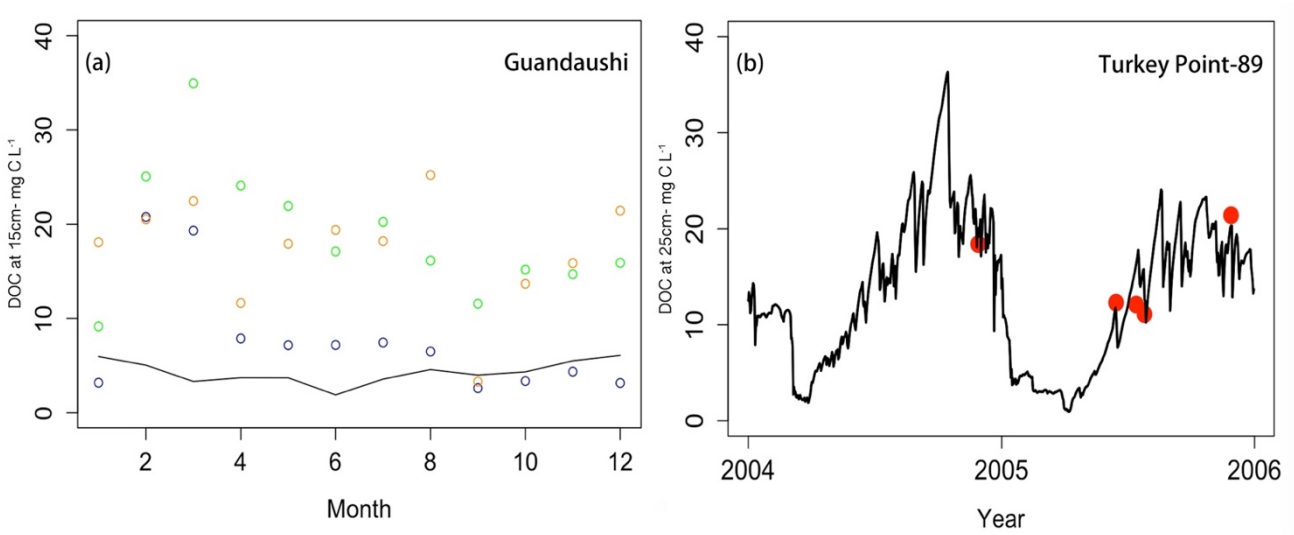


Figure 4. DOC concentration (mg C $L^{-1}$) for (a) Guandaushi at 15 cm measured (black circle: Chinese Fir, green circle: natural hardwood, orange circle: secondary wood) and simulated (black lines) and for (b) Turkey Point 89 at 25 cm measured (red dots) and simulated (black lines). Results for other depths are given in Figure S2.

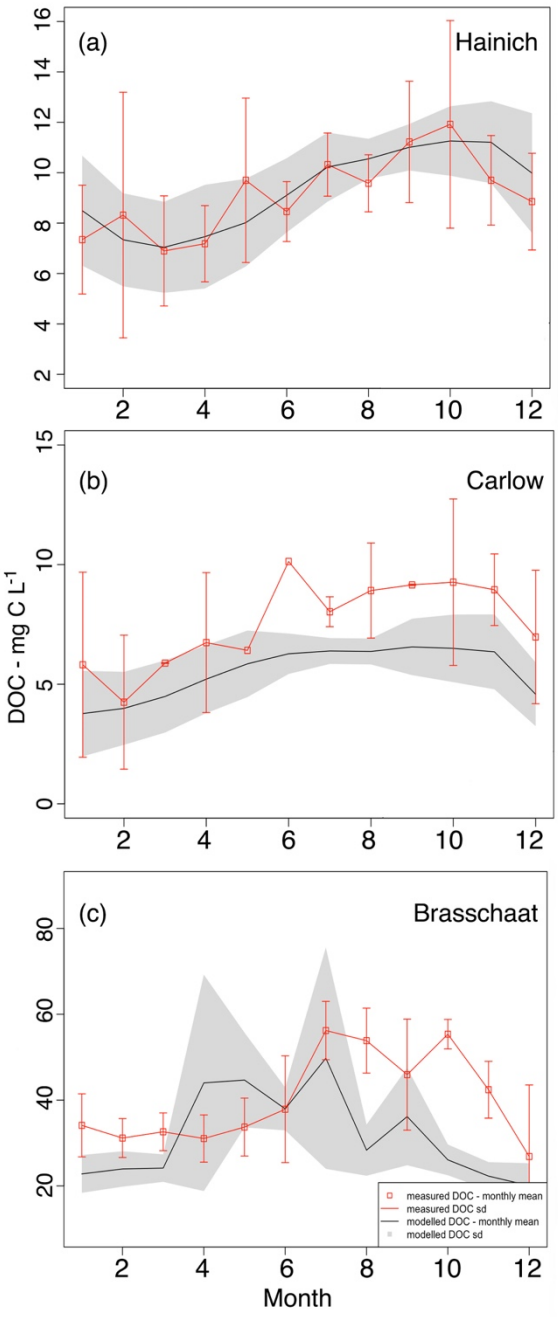


Figure 5. a) Monthly DOC (mg C $L^{-1}$) at 10 cm in Level 1- sites modelled (black line: mean, grey line: standard deviation) versus measured (red square: mean, red line: standard deviation) for studied period (a) Hainich averaging from 2005-2014 (b) Carlow, averaging from 2006-2008 (c) Brasschaat, averaging from 2006 –2010. Results for other depths are given in Figure S6.

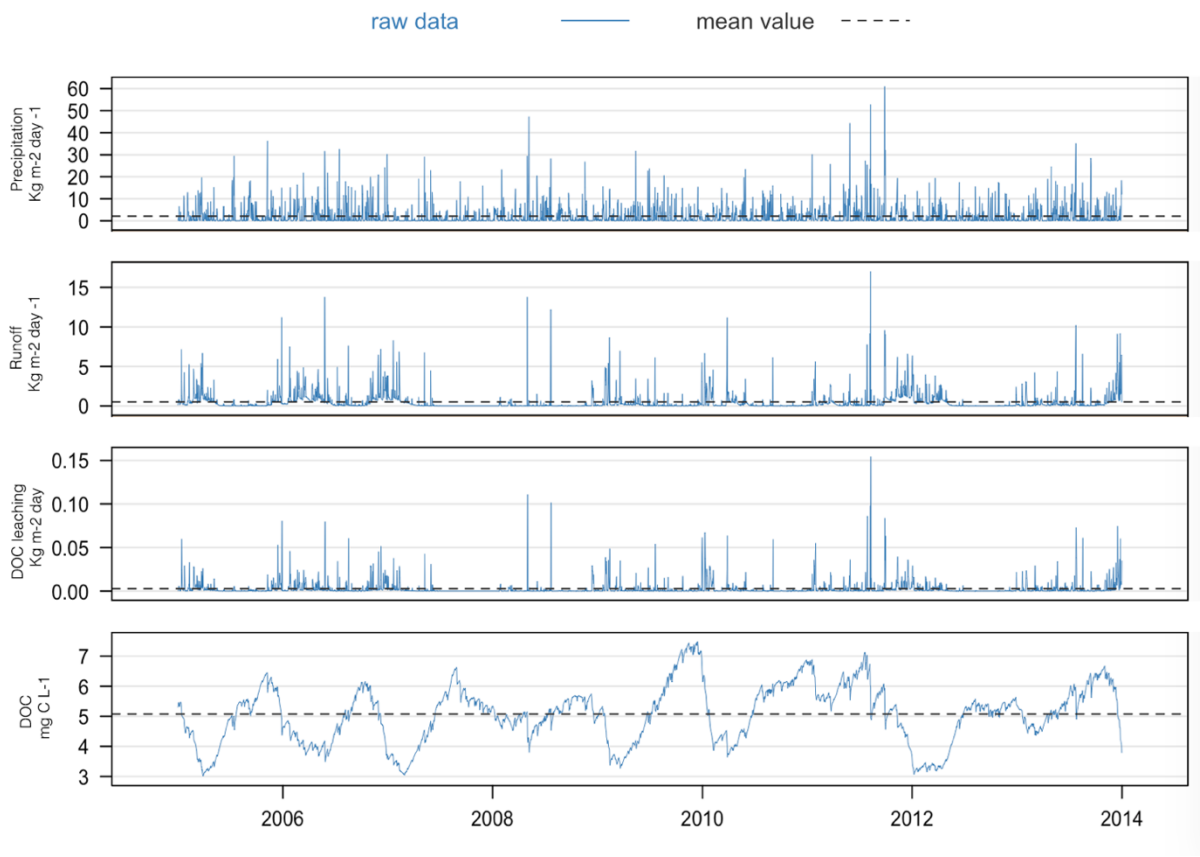


Figure 6. Observed precipitation, simulated runoff, DOC leaching and DOC concentration in Hainich from 2006 to 2013 indicating the relation between the averaged DOC concentrations at 3 m of soil with leaching as a result of runoff that follows large precipitation events.

## 3.3 Sensitivity tests

Sensitivity to model parameters was tested on the three European sites where a representative time-series of observed DOC concentrations was available (e.g. Hainich-10cm, Fig. 7). The results indicate that among all the parameters in all three sites, the model shows the highest sensitivity to SOC vertical profile, controlled by parameter $z_0$ (eq. 1), and the changing of SOC decomposition rate with soil depth, parameter, $\tau_z$ (eq. 4) (p-values < 0.05, Table S6). Among the DOC controlling parameters, the model shows the highest sensitivity to the basal decomposition rate of recalcitrant DOC ($K_{DOC\ (\text{recalcitrant})}$) (eq.10), which is the inverse of the residence time of DOC in the recalcitrant pool.

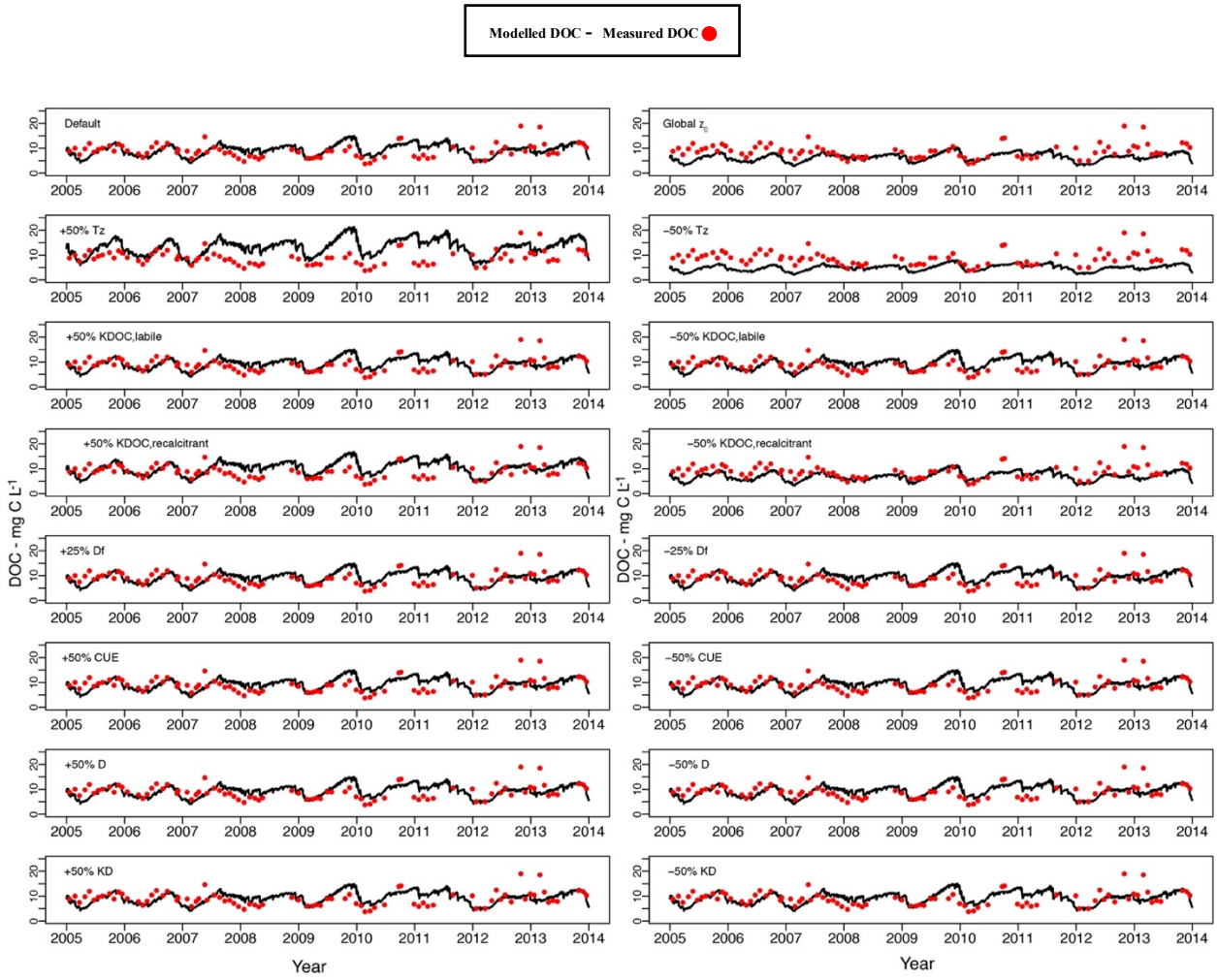


Figure 7. DOC concentration (mg C $L^{-1}$) simulated with sensitivity parameter sets (black line) versus measured (red dot) at 10 cm depth in Hainich for period 2004-2013. Parameter sets description and values are given in Table 1. Results for other sites are given in Figure S1.

The sensitivity of the model to each of these parameters was different at each site. For Hainich, the highest sensitivity was assigned to $\tau_z$. Here, a change in $\tau_z$ by 50% leads to a 36% change in the mean DOC within 3 m, while a 50% change in $K_{DOC\,(\text{recalcitrant})}$ leads to a 29% change and global $z_0$ leads to a 25% change in simulated DOC concentrations (Fig 8a). The closest value for the mean DOC in 10 cm in Hainich (8.8 mg $L^{-1}$) to the measurement was produced by the default set (8.9 mg $L^{-1}$), while the highest value for DOC was reached with the 50% increase in $\tau_z$ (12.7 mg $L^{-1}$) and the lowest DOC value was produced with 50% decrease in $\tau_z$ (4.7 mg $L^{-1}$). In contrast to that, at a depth of 20 cm, the closest value to the mean of measured DOC (5.6 mg $L^{-1}$) was produced by 50% decrease in $K_{DOC\,(recalcitrant)}$ (4.9 mg $L^{-1}$) (Fig. 9-a).

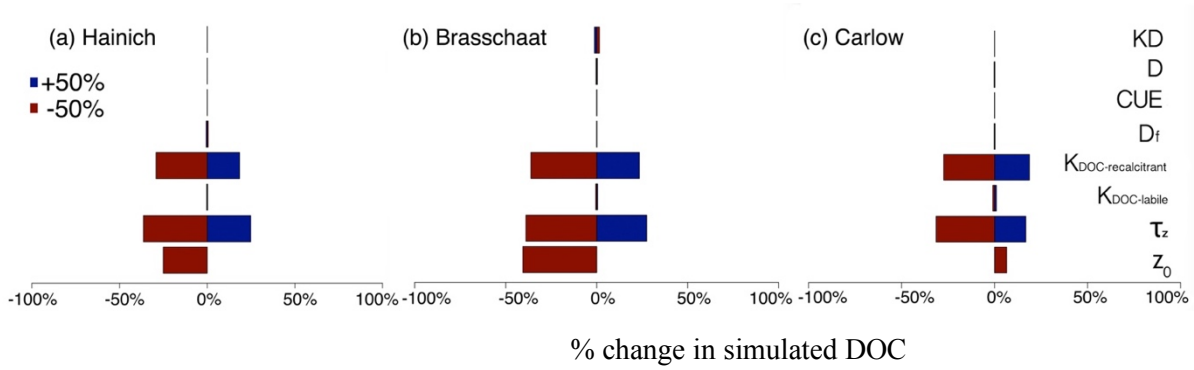


Figure 8. Relative change in simulated DOC (%) for a +50% (blue) and -50% (red) change in each parameter for level 1- sites: (a) Hainich, (b) Brasschaat and (c) Carlow. Values are given in Table S5.

In Brasschaat, the highest sensitivity was to $z_0$, closely followed by $\tau_z$ and $K_{DOC\ (recalcitrant)}$. A 50% change in each of these parameters led to a 36-40% change in DOC concentration over the 3 meters of soil profile (Fig. 8-b). At 10 cm, the closest value to measurements mean (39.4 mg $L^{-1}$) was produced by 50% increase in $\tau_z$ (39.2 mg $L^{-1}$). At 35 cm depth, the closest value to mean measurement (29.3 mg $L^{-1}$) was calculated by 50% increase in $K_{DOC\ (recalcitrant)}$ (16.2 mg $L^{-1}$) which was also the highest simulated value as well. At 75 cm, the closest value to mean of DOC measurement (22.0 mg $L^{-1}$) was produced by 50% increase in $K_{DOC\ (recalcitrant)}$ (8.1 mg $L^{-1}$) as it was the highest of the simulated values (Fig. 9-b).

For Carlow, the most sensitive parameters were $\tau_z$ and $K_{DOC\ (recalcitrant)}$: a 50% change in those parameters leads to a 31.5% and 27.4% in simulate DOC. In contrast to the other sites, global $z_0$ leads to a low but still significant positive change of 6.5% in simulated DOC within 3 meters of soil (p-value <0.05, Table S6) (Fig. 8-c). In 10cm, the closest modelled value to the mean measurement (5.7 mg $L^{-1}$) was produced by default parameter set (5.8 mg $L^{-1}$). Between 10 to 28 cm all the parameter sets underrepresented the DOC concentration mean measurement (13.1 mg $L^{-1}$) and the closest and highest value was produced by 50% in $\tau_z$ (3.8 mg $L^{-1}$). For 28 to 77cm, the closest value to the measurement (4.8 mg $L^{-1}$) was calculated by increasing $\tau_z$ by 50% (4.5 mg $L^{-1}$) (Fig. 9-c).

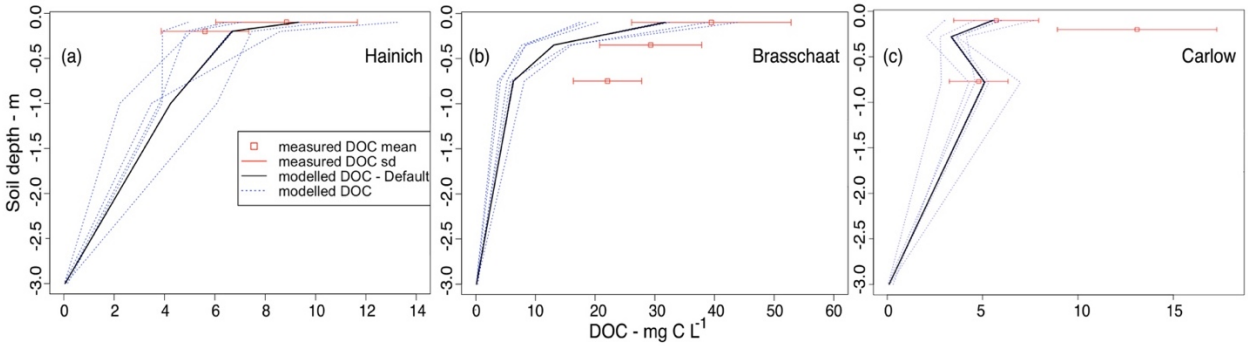


Figure 9. DOC concentration (mg C $L^{-1}$) in 3 m soil depth at level 1-sites modelled (black line: default parameter set; blue dashed line: sensitivity test parameter set) vs. measured (red square: mean; red line: standard deviation) for (a) Hainich (b) Brasschaat (c) Carlow. Plot of each parameter in 3 m soil depth in Figure S5.

# 4 Discussion

## 4.1 Measurements versus model simulations

Overall, JULES-DOCM reproduced the range of GPP for most of our sites to an acceptable degree. At some sites, due to over/underestimated autotrophic respiration, the NPP and total respiration values were slightly different than measurements. Consequently, the modelled carbon stocks were different from the measurements in most of the sites, but yet capable of representing the general patterns that were observed in the measurements.

In Brasschaat, the modelled SOC was lower than the measurements, which could be due to the underestimated NPP (Table 5) and, as a consequence, the underestimated litter input, but also due to the overestimated soil respiration and SOC decomposition rates. The underestimation of SOC as a source of DOC led to a general underestimation of DOC. Nevertheless, the decrease of relative DOC concentration through soil is consistent with the observations.

In Hainich, a slightly overestimated NPP partly counter-balanced the overestimated soil respiration. Nevertheless, the SOC concentration simulated down to 60 cm was lower than the measurement at this depth. As we did not have observations of SOC down to 3 meters, we cannot certainly say if the simulated total SOC stock (13.7 kg C $m^{-2}$) over the whole soil column is close to the reality or not. Some of the controlling parameters like DOC basal decomposition rates are kept constant over the soil profile in our simulation, while they are maybe not constant with depth in the real world, perhaps due to priming effects (Guenet *et al.*, 2010). That could

explain why at Hainich, the simulated and observed DOC concentrations are very close at 10 cm depth, while they differ more at 20 cm depth.

In Carlow, the slight overestimation of GPP led to the overestimated SOC concentrations down to 50 cm, whilst again we cannot say with certainty that the whole SOC stock is overestimated, as the SOC stock has not been measured down to three meters. Some sources suggest that the SOC in Carlow grassland could be higher than the reported value in our reference, if we calculate the C in soil based on the fraction of loss of ignition (LOI) (Walmsley, 2009; Hoogsteen *et al.*, 2015). As Carlow is our only grassland biome site, additional data from different study sites would be valuable to achieve a more representative parametrization of soil carbon processes under grassland. One of the parameters to be optimized for such sites could be CUE which has a strong impact on the stocks and fluxes. Also, since the measured values for NPP or soil respiration for this site were not available to us, we were unable to assess whether we over- or underestimated these fluxes and if this could have potentially biased our SOC stock simulations. DOC measurements were provided from two plots which were placed on different terrain positions. The measurements from plot 2 (150 meter in south-westerly direction from plot 1) at 10 to 28 cm depth had a higher DOC concentration than plot 1 at the 10 cm (Walmsley, 2009). This could be the result of small scale variations related to terrain position, which can be related to different soil moisture regimes and lateral import of DOC. It is not possible to represent such small-scale variation in global models like JULES-DOCM.

At Turkey Point-89, the simulated GPP is close to the observations, while NPP is slightly overestimated. The simulated soil respiration and decomposition rates are higher than observed values. The overestimated SOC concentration in the top soil could be the result of an overestimated depth gradient in SOC concentration, which in our simulations is derived from global data (Jobbágy and Jackson, 2000). Also, we simulated the steady state SOC profile for forest vegetation, whereas the forest stand at the site is relatively young and succeeded agricultural land use in 1989, and thus, the SOC profile is likely not representative for a forest site. The overestimated DOC concentration for 100 cm depth may be due to this change in land use, which was not taken into account during simulations, providing more C input for DOC production. At this site, the observed higher soil moisture in the deeper profile could indicate a potentially high advection of DOC to the lower layers (Peichl, Arain and Brodeur, 2010). This could be another reason for the lower DOC in 100 cm from measured compared to the modelled results.

In Gundaushi due to the lack of SOC, or vegetation carbon fluxes measurements from the site, we have no information on SOC concentrations and stocks. The lower values of DOC from our model compared to the measurements could be due to: Firstly, the high temporal variability of observed concentrations (large standard deviation for all the depths from the three stands). Second, the high value of DOC input from rainfall, which is not represented in JULES-DOCM (Liu and Sheu, 2003). Recent studies have indicated that including this flux in models can have a significant impact on the DOC in soil (Lauerwald *et al.*, 2017).

As there are no measurements of lateral leaching of DOC from soil to the river, our evaluation of this flux is based on the simulated DOC concentration and runoff. Hence as the simulated hydrology of the JULES model has been evaluated previously (Gedney, N. , Cox, 2003; Clark and Gedney, 2008), in this study, we assume that we will get robust estimates of DOC leaching by multiplying simulated concentration by runoff, as long as simulated DOC concentrations can be validated.

Overall, besides over/underestimation of DOC at some sites, the model was capable of representing the trend of DOC concentration at different depths when comparing to the measurements at all the sites.

**Table 5.** The measured (Obs.) versus the modelled (Mod.) carbon fluxes, SOC concentration, and soil DOC concentration at different soil depths in five study sites.

| Variables | Level 1 | | | | | | Level 2 | | | |
|---|---|---|---|---|---|---|---|---|---|---|
| | Brasschaat | | Carlow | | Hainich | | Turkey Point 89 | | Guandaushi | |
| | Obs. | Mod. | Obs. | Mod. | Obs. | Mod. | Obs. | Mod. | Obs. | Mod. |
| | Carbon fluxes ($g\,C\,m^{-2}\,yr^{-1}$) and SOC ($kg\,C\,m^{-2}$) | | | | | | | | | |
| GPP | 1173 ± 92 | 867 ± 25 | 903 | 1165 | 1606 ± 102 | 1455 ± 168 | 1732 ± 108 | 1635 ± 63 | – | – |
| NPP | 850 | 596.1 | – | – | 673 ± 33 | 833 ± 153 | 814 ± 51 | 1013 ± 92 | – | – |
| Soil res* | 411 ± 34 | 625 ± 54 | – | – | 883 ± 206 | 909 ± 66 | 693 ± 16 | 1006 ± 142 | – | – |
| SOC | 11.47 | 8.01 | 2.3 | 4.17 | 11.75 | 8.63 | 1.85 | 3.39 | – | – |
| | DOC concentration ($mg\,C\,L^{-1}$) | | | | | | | | | |
| 10 cm | 39 ± 15 | 28 ± 13 | 7 ± 3 | 6 ± 1 | 9 ± 3 | 9 ± 2 | – | – | – | – |
| 15 cm | – | – | – | – | – | – | – | – | nh: 19 ± 12<br>sh: 17 ± 12<br>cf: 8 ± 15 | 4 ± 1 |
| 20 cm | – | – | – | – | 6 ± 2 | 7 ± 2 | – | – | – | – |
| 25 cm | – | – | – | – | – | – | 15 ± 4.5 | 16 ± 4 | – | – |
| 10–28 cm | – | – | 13 ± 4 | 4 ± 1 | – | – | – | – | – | – |
| 30 cm | – | – | – | – | – | – | – | – | nh: 9 ± 7<br>sh: 15 ± 8<br>cf: 7 ± 17 | 3 ± 1 |
| 35 cm | 29 ± 2 | 13 ± 9 | – | – | – | – | – | – | – | – |
| 75 cm | 22 ± 1 | 6 ± 6 | – | – | – | – | – | – | – | – |
| 28–77 cm | – | – | 5 ± 2 | 5 ± 0.2 | – | – | – | – | – | – |
| 100 cm | – | – | – | – | – | – | 2.2 ± 0.2 | 7.9 ± 2 | – | – |

* Soil respiration, nh: natural hardwood; sh: secondary hardwood; cf: Chinese fir.

## 4.2 Sensitivity analysis

The sensitivity tests indicate that the parameters controlling SOC concentrations in the soil profile ($Z_0$ and $\tau_z$) and the recalcitrant DOC residence time ($K_{DOC\ (recalcitrant)}$) have the most significant effect on soil DOC concentration, which indicates the importance of factors controlling DOC sources. Nevertheless, DOC related model parameters such as basal DOC decomposition rate are constant over different depths, which could be the reason for the difference between the modelled and measured values, especially in the deeper soil layers. Hence, it is important to introduce a depth-dependence decay rate for these parameters.
One limitation in our simulation is that we use a single, calibrated value for recalcitrant DOC residence time, which is the most sensitive DOC controlling parameter. It has been shown that this parameter can vary with biodegradability of SOC and litter under different PFTs and at different sites (Kalbitz et al. 2003; Turgeon 2008). However, more detailed data for different biomes is needed for calibrating different residence times for different PFTs. We note that our sensitivity analysis, changing one parameter at a time, does not investigate the potential interactions between different parameters.

# 5 Conclusion

Applying a carbon cycle model that integrates the whole continuum from land to ocean to atmosphere provides a better understanding of the Earth's carbon cycle and makes more reliable future projections. In this study, we presented DOC related processes in JULES, JULES-DOCM, which includes the DOC produced in the soil down to three meters and its subsequent fate including its decomposition and release as $CO_2$ to the atmosphere, and its export to the river network via leaching in different ecosystems. Results show that the model is capable of representing the DOC stocks, processes and its export to the riverine systems from different ecosystems. In future, our developments in the representation of DOC leaching will lead to a model approach integrating terrestrial and aquatic C cycling. However, more field data are still required to improve the model parametrization and performance.

# Supporting document: Chapter 1 - Representation of dissolved organic carbon in the JULES land surface model (vn4.4_JULES-DOCM)

Table S1. $z_0$ values for each PFT

| PFT | $z_0$ |
|---|---|
| Boreal forest | 0.775625 |
| Crops | 1.13717 |
| Deserts | 1.67113 |
| Sclerophyllous shrubs | 1.22839 |
| Temperate deciduous forest | 0.725914 |
| Temperate evergreen forest | 0.857235 |
| Temperate grassland | 1.22839 |
| Tropical deciduous forest | 1.67113 |
| Tropical evergreen forest | 1.0188 |
| Temperate grassland/savana | 1.45185 |
| Tundra | 0.656898 |

Table S2. $z_0$ values for each PFT in JULES-DOCM

| JULES PFT | $z_0$ |
|---|---|
| Tropical broadleaf evergreen forest | 1.0188 |
| Temperate broadleaf evergreen forest | 0.857235 |
| broadleaf deciduous forest | 0.725914 |
| needle-leaf evergreen forest | 0.857235 |
| needle-leaf deciduous forest | 0.725914 |
| C3 grass | 1.13717 |
| C4 grass | 1.13717 |
| Evergreen shrubs | 1.22839 |
| Deciduous shrubs | 1.22839 |

Table S3. Anova test results for Carbon fluxes (Df: Degree of freedom, Sum sq: sum of squares, Mean sq: mean of squares, Pr: p-value)

ANOVA

| | Df | Sum sq | Mean Sq | F value | Pr(>F) |
|---|---|---|---|---|---|
| GPP | | | | | |
| Hainich | 1 | 102955 | 102955 | 5.352 | 0.0343 |
| | 16 | 307785 | 19237 | | |
| Brasschaat | 1 | 280924 | 280924 | 62.27 | 1.33E-05 |
| | 10 | 45117 | 4512 | | |
| Turkey Point-89 | 1 | 9295 | 9295 | 4.714 | 0.162 |
| | 2 | 3943 | 1972 | | |
| NPP | | | | | |
| Hainich | 1 | 88254 | 88254 | 7.222 | 0.0362 |
| | 6 | 73323 | 12220 | | |
| Turkey Point-89 | 1 | 39632 | 39632 | 7.154 | 0.116 |
| | 2 | 11080 | 5530 | | |
| SOIL RESPIRATION | | | | | |
| Hainich | 1 | 1400 | 1400 | 0.06 | 0.815 |
| | 6 | 140896 | 23483 | | |
| Brasschaat | 1 | 160497 | 160947 | 77.44 | 1.40E-06 |
| | 12 | 24870 | 2073 | | |
| Turkey Point-89 | 1 | 98114 | 98114 | 9.687 | 0.0896 |
| | 2 | 20256 | 10128 | | |

We include all the sensitivity runs for Level-1 sites: Hainich, Brasschaat and Carlow for all the depths where the measurements were available. Red points are indicating measurements where black points are values from model (Fig. S2). Also representing Level-2 sites: Turkey Point 89 and Guandaushi comparison of modelled DOC versus measured in deeper soil depths (Fig. S3).

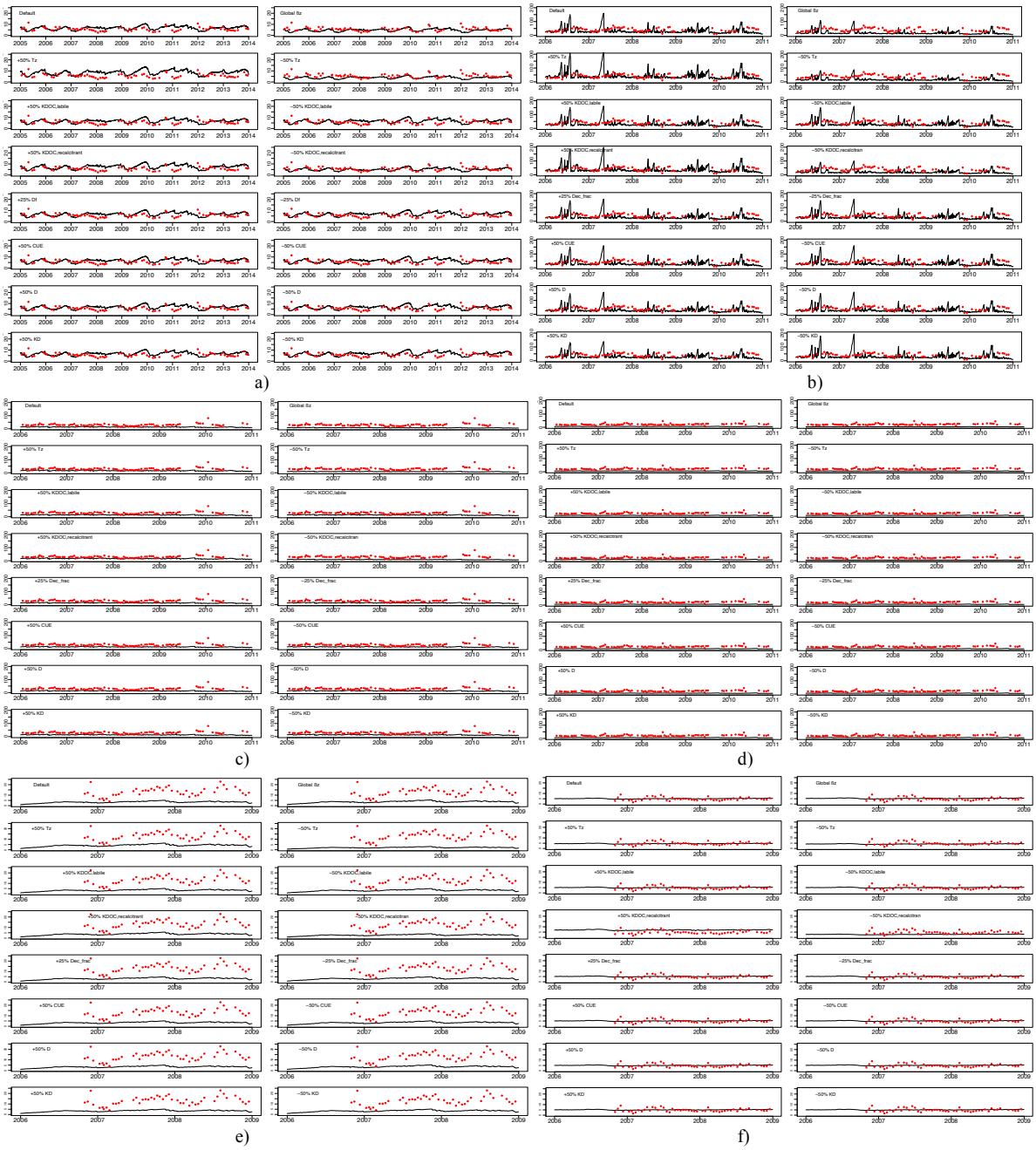


Figure S1. Sensitivity tests (black line) versus measurements (red dot) at a) 20cm depth – 2004-2013, Hainich b) 10cm depth – 2006-2010, Brasschaat c) 35cm depth – 2006-2010, Brasschaat d) 75cm depth – 2006-2010, Brasschaat e) 10 to28cm depth – 2006-2009, Carlow f) 28 to78cm depth – 2006-2009, Carlow; X axis is year and Y axis is DOC concentration in mg C $L^{-1}$. Parameter sets description and values in Table 1

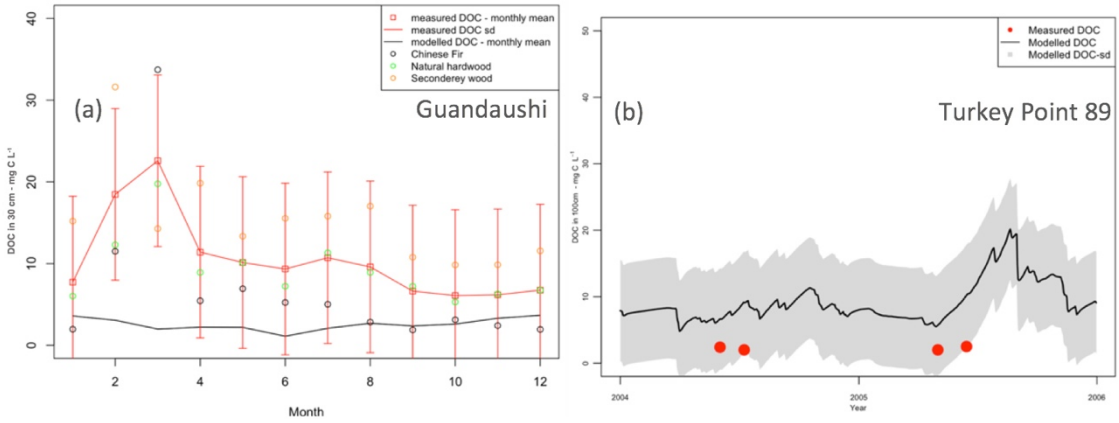


Figure S2. DOC concentration (mg C L-1) for (a) Guandaushi at 30 cm measured (black dot: Chinese Fir, green dot: natural hardwood, orange dot: secondary wood, red square: mean, red line: standard deviation) and simulated (black lines) and for (b) Turkey Point 89 at 100 cm measured (red dots) and simulated (black lines, grey line: standard deviation).

We examine the hydrology of the model and its interaction with DOC concentration and leaching for Level-1 sites: Carlow and Brasschat (Fig. S3) and overall model performance in DOC representation in all depths by comparing modelled versus measurements during study period in Hainich, Brasschaat and Carlow (Fig. S4).

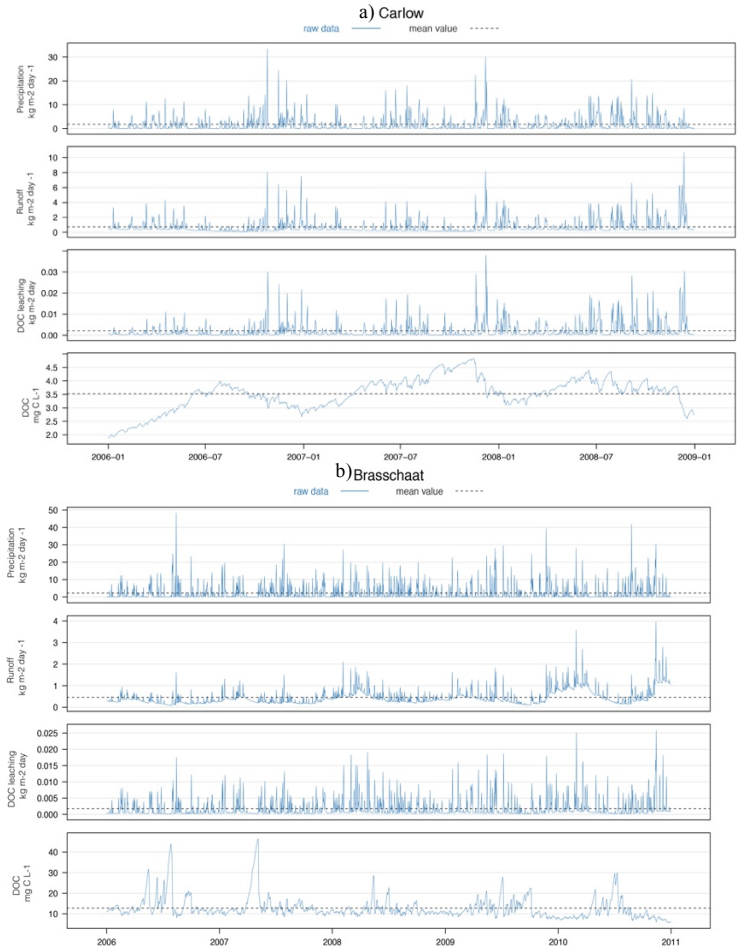


Figure S3. a) Precipitation, runoff, DOC leaching and DOC concentration (down to 3 m averaged) in Carlow from 2006 to 2009 b) in Brasschaat from 2006 to 2010 simulated data with JULES-DOCM

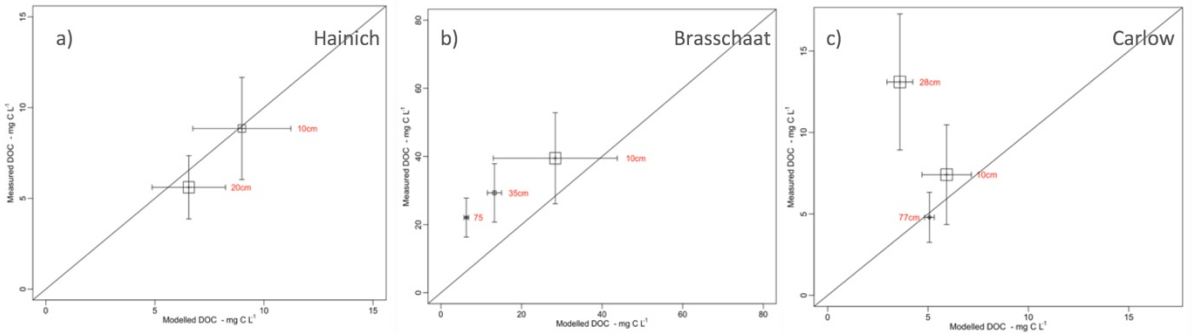

Figure S4. a) Measured vs modelled DOC (mg C L-1) with default set in Hainich from 2006 to 2013 at 10 and 20cm b) in Brasschaat from 2006 to 2010 at 10,35 and 75cm c) in Carlow from 2006 to 2009 at 10,10 to 28 and 28 to 78cm

Sensitivity of model parameters (Table S4) was tested in Level-1 Sites for the depths where the DOC measurements where available (Fig. S5) and the results were reported in percentage of change compared to default parameters set (Table S5). Anova test was used in order to determine each parameter's impact significance on DOC representation (Table S6).

Table S4. JULES-DOCM parameters set for sensitivity test

| *ID* | *Description* |
|---|---|
| *SET-1* | *PFT based* $z_0$ |
| *SET -2* | *Global* $z_0$ |
| *SET -3* | *+50%* $\tau_z$ |
| *SET -4* | *-50%* $\tau_z$ |
| *SET -5* | *+50%* $K_{DOC,\ labile}$ |
| *SET -6* | *-50%* $K_{DOC,\ labile}$ |
| *SET -7* | *+50%* $K_{DOC,\ recalcitrant}$ |
| *SET -8* | *-50%* $K_{DOC,\ recalcitrant}$ |
| *SET -9* | *+25%* $D_f$ |
| *SET -10* | *-25%* $D_f$ |
| *SET -11* | *+50% CUE* |
| *SET -12* | *-50% CUE* |
| *SET -13* | *+50% D* |
| *SET -14* | *-50% D* |
| *SET -15* | *+50%* $K_D$ |
| *SET -16* | *-50%* $K_D$ |

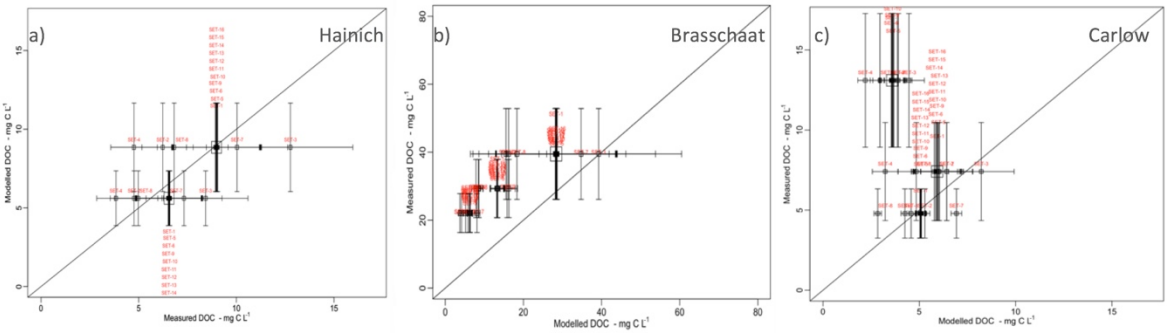


Figure S5. a) Measured (X axis) vs modelled (Y axis) DOC sensitivity runs (Table1) in Hainich from 2006 to 2013 at 10 and 20cm b) in Brasschaat from 2006 to 2010 at 10,35 and 75cm c) in Carlow from 2006 to 2009 at 10,10 to 28 and 28 to 78cm

Table S5. Relative change in simulated DOC (%) for a +50% and -50% changes in model parameters for Hainich, Carlow and Brasschaat

| **HAINICH** | $Z_0$ | $\tau_Z$ | $K_{DOC\text{-}LABILE}$ | $K_{DOC\text{-}RECALCITRANT}$ | $D_F$ | **CUE** | **D** | $K_D$ |
|---|---|---|---|---|---|---|---|---|
| **50%** | **- (PFT based $z_0$)** | **24.82748** | **0.2746118** | **18.51532** | **-0.590175** | **-0.06117** | **-0.04519973** | **-0.05364935** |
| **-50%** | **-25.12175 (global $z_0$)** | **- 36.45213** | **-0.2729602** | **-29.18424** | **0.586697** | **0.06068464** | **0.04545651** | **0.05483722** |
| **CARLOW** | | | | | | | | |
| **50%** | **- (PFT based $z_0$)** | **16.81662** | **0.9795210** | **18.77268** | **-0.2522954** | **-0.08957044** | **0.1873639** | **-0.05575369** |
| **-50%** | **6.52764 (global $z_0$)** | **-31.50205** | **-0.9754175** | **-27.40512** | **0.2517171** | **0.08983245** | **-0.2774403** | **0.05659863** |
| **BRASSCHAAT** | | | | | | | | |
| **50%** | **- (PFT based $z_0$)** | **27.52056** | **0.5294166** | **23.45682** | **-0.1300973** | **-0.1176923** | **-0.3806475** | **-1.256365** |
| **-50%** | **-40.6144 (global $z_0$)** | **-38.92471** | **-0.5120930** | **-36.20752** | **0.1305755** | **0.1183834** | **0.3794148** | **1.571266** |

Table S6. Anova test results for sensitivity test of Level-1 sites

ANOVA

| DOC Hainich | Df | Sum sq | Mean Sq | F value | Pr(>F) |
|---|---|---|---|---|---|
| set-2 | 1 | 10686 | 10686 | 1066 | **2.00E-16** |
| set-3 | 1 | 10437 | 10437 | 491.9 | **2.00E-16** |
| set-4 | 1 | 22499 | 22499 | 2572 | **2.00E-16** |
| set-5 | 1 | 1 | 1.277 | 0.094 | 0.759 |
| set-6 | 1 | 1 | 1.267 | 0.093 | 0.76 |
| set-7 | 1 | 5805 | 5805 | 382.7 | **2.00E-16** |
| set-8 | 1 | 14422 | 14422 | 1322 | **2.00E-16** |
| set-9 | 1 | 6 | 5.898 | 0.437 | 0.508 |
| set10 | 1 | 6 | 5.828 | 0.427 | 0.514 |
| set11 | 1 | 0 | 0.063 | 0.005 | 0.946 |
| set12 | 1 | 0 | 0.062 | 0.005 | 0.946 |
| set13 | 1 | 0 | 0.035 | 0.003 | 0.96 |
| set14 | 1 | 0 | 0.035 | 0.003 | 0.96 |
| set15 | 1 | 0 | 0.049 | 0.004 | 0.952 |
| set16 | 1 | 0 | 0.049 | 0.004 | 0.952 |

ANOVA

| DOC Carlow | Df | Sum sq | Mean Sq | F value | Pr(>F) |
|---|---|---|---|---|---|
| set-2 | 1 | 116 | 115.98 | 20.27 | **6.81E-06** |
| set-3 | 1 | 770 | 769.7 | 109.73 | **2.00E-16** |
| set-4 | 1 | 2701 | 2701.1 | 703.7 | **2.00E-16** |
| set-5 | 1 | 3 | 2.611 | 0.486 | 0.486 |
| set-6 | 1 | 3 | 2.59 | 0.49 | 0.484 |
| set-7 | 1 | 959 | 959.2 | 145.6 | **2.00E-16** |
| set-8 | 1 | 2044 | 2044.2 | 488.3 | **2.00E-16** |
| set-9 | 1 | 0 | 0.173 | 0.033 | 0.857 |
| set10 | 1 | 0 | 0.172 | 0.032 | 0.857 |
| set11 | 1 | 0 | 0.022 | 0.004 | 0.949 |
| set12 | 1 | 0 | 0.022 | 0.004 | 0.949 |
| set13 | 1 | 0 | 0.096 | 0.018 | 0.894 |
| set14 | 1 | 0 | 0.096 | 0.018 | 0.894 |
| set15 | 1 | 0 | 0.008 | 0.002 | 0.968 |
| set16 | 1 | 0 | 0.008 | 0.002 | 0.968 |

ANOVA

| DOC Brasschaat | Df | Sum sq | Mean Sq | F value | Pr(>F) |
|---|---|---|---|---|---|
| set-2 | 1 | 98664 | 98664 | 5924 | **2.00E-16** |
| set-3 | 1 | 45301 | 45301 | 126.7 | **2.00E-16** |
| set-4 | 1 | 90625 | 90625 | 585.2 | **2.00E-16** |
| set-5 | 1 | 17 | 16.76 | 0.069 | 0.792 |
| set-6 | 1 | 16 | 15.69 | 0.065 | 0.798 |
| set-7 | 1 | 32911 | 32911 | 109.1 | **2.00E-16** |
| set-8 | 1 | 78414 | 78414 | 462.8 | **2.00E-16** |
| set-9 | 1 | 1 | 1.01 | 0.004 | 0.948 |
| set10 | 1 | 1 | 1.02 | 0.004 | 0.948 |
| set11 | 1 | 1 | 0.83 | 0.003 | 0.953 |
| set12 | 1 | 1 | 0.83 | 0.003 | 0.953 |
| set13 | 1 | 9 | 8.67 | 0.036 | 0.849 |
| set14 | 1 | 9 | 8.61 | 0.036 | 0.85 |
| set15 | 1 | 94 | 94.41 | 0.415 | 0.519 |
| set16 | 1 | 148 | 147.7 | 0.566 | 0.452 |

Seasonality of DOC concentration in different depths of Level-1 sites (Hainich, Carlow and Brasschaat) was tested by comparing monthly modelled DOC means versus measurements (Fig. S6).

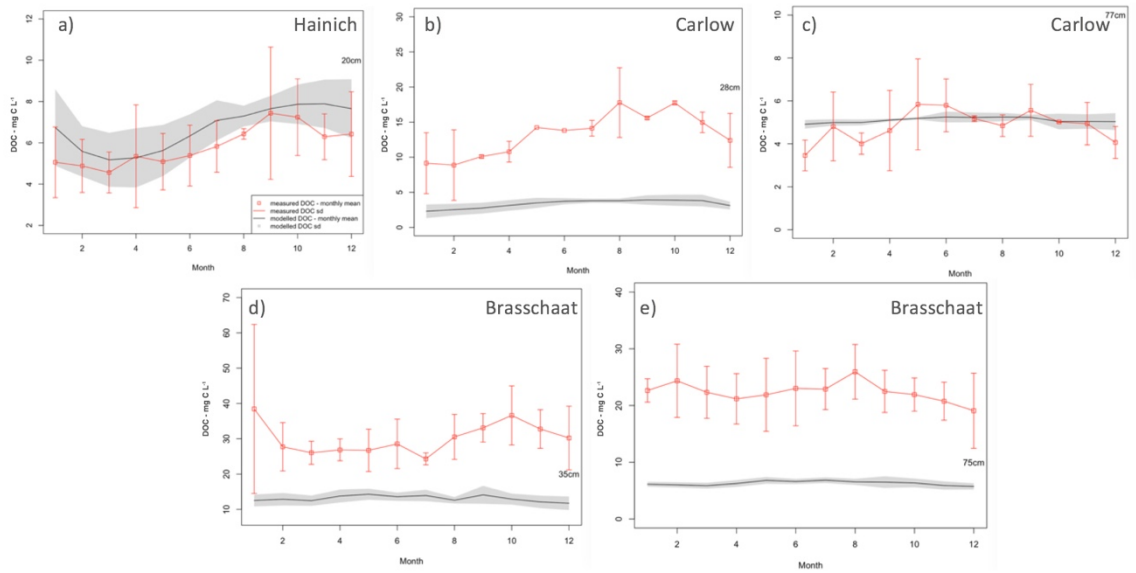


Figure S6. Monthly DOC means modelled versus measured (mg C L-1) for studied period at a) 20cm of Hainich b)10 to 28cm of Carlow c) 28 to 77 cm of Carlow d) 35cm of Brasschaat e) 75cm of Brasschaat

# Chapter 2

# Chapter 2 - Soil dissolved organic carbon leaching is a minor source to inland water carbon budget

This chapter presents the global simulation performed with JULES-DOCM and their implication for the role of DOC in the global carbon budget. It has been submitted to Nature Geoscience and is reproduced here as a chapter.

Mahdi Nakhavali, Ronny Lauerwald, Pierre Regnier, Bertrand Guenet, Sarah Chadburn and Pierre Friedlingstein, Soil dissolved organic carbon leaching is a minor source to inland water carbon budget, Nature Geosciences, *submitted, May 6th 2019.*


**Abstract**

**The lateral transfer of carbon (C) from vegetation and soils to rivers plays a significant role in ecological processes in both the terrestrial and aquatic ecosystems[1,2]. This flux is poorly constrained at the global scale and has so far only been diagnosed from global budget calculations involving the riverine C exports to the coast and estimates of $CO_2$ emissions from inland waters and C burial in aquatic sediments, all of these terms having large uncertainties[3,4]. Dissolved organic carbon (DOC) is generally considered to be a significant contributor of the lateral C flux[3]. However, measurements of DOC concentrations in runoff and drainage are scarce and highly skewed across the globe and thus the contribution of terrestrial DOC leaching to the global-scale C balance of aquatic ecosystems remains poorly constrained. Here, using a process-based, integrative modelling approach to upscale from existing observations, we estimate a global terrestrial DOC leaching flux of 0.44+/- 0.07 Gt C/yr. This estimate only represents about 6-17 % of the C inputs required to sustain the previously estimated $CO_2$ evasion and C exports to the ocean reported in the literature[4] and suggests that the soil-derived DOC flux is a minor component of the aquatic C budget.**


The land-ocean transfer of terrestrial organic carbon through the river network is an important link in the global C cycle and an important process for the assessment of terrestrial and aquatic C budgets [3,5]. It has been hypothesized that the exclusion of lateral C transfers in land surface components of Earth System Models (ESMs) implies that soil heterotrophic respiration and/or C accumulation in the soil could be significantly overestimated in global C budgets accounting[6,7], with state-of-the-art ESMs such as those used for the 5th assessment report of the IPCC[8] yielding a biased quantification of the land C sink and its response to changing $CO_2$ and climate[3,9,10].

Dissolved organic carbon (DOC), which has been estimated to make up about 37% of the terrestrial C export to the oceans[11–13], represents often the more reactive fraction of this lateral C flux feeding in-stream respiration and $CO_2$ emission from inland waters[14]. Empirical

approaches can predict fluvial DOC fluxes from a variety of allochthonous sources based on catchment properties[12,13,15,16], implicitly treating riverine DOC as a conservative tracer. While DOC loss from the river network due to decomposition and adsorption[16] in transit and in-stream production from submerged litter decomposition[17] are thought to be important components of the river DOC budget, it is not yet possible to quantify these terms at global scale[16] using empirical models. Similarly, a quantitative assessment of DOC transfers through the terrestrial-aquatic interface is currently critically missing due to the scarcity of direct observations. Arguably, the only way to assess global DOC leaching, its spatio-temporal variations and its response to environmental change is to rely on a process-based modelling approach that explicitly represents the production and cycling of DOC within the soil column as well as the subsequent DOC leaching fluxes from terrestrial ecosystems to inland waters[18].

Although several models have been developed and tested successfully to simulate DOC dynamics at plot to regional scales[10,19–22], none of these models have so far addressed DOC cycling at the global scale and its sensitivity to large scale spatial patterns in climate, vegetation and soil properties. Here we use the recently upgraded Joint UK Land Environment Simulator (JULES) to simulate the global distribution of soil DOC stocks and leaching fluxes[23]. In short, JULES-DOCM represents the vegetation dynamics for nine distinct plant functional types (PFTs)[24], simulates photosynthesis, plant and soil respiration and allows quantifying the Net Biome Production (NBP) as a function of climate, atmospheric $CO_2$ and land cover change. SOC processes are represented following the RothC model[25], which distinguishes four carbon pools with different turnover-times[26]. Soil DOC cycling is simulated for each model grid-cell over a 3 m soil profile vertically discretized into four soil layers, including the production associated with SOC decomposition, and losses by respiration, biological consumption and leaching[23]. DOC production associated with litter and SOC pools decomposition depends on temperature, moisture, vegetation type and soil texture, while DOC respiration is only a function of temperature. DOC leaching is diagnosed from soil DOC concentrations and simulated runoff and drainage. A full description of the model is available in ref. 23.

To constrain JULES-DOCM with observations, for the recent period (1980-2010), we compiled the largest global dataset of measured soil DOC concentrations (n= 92), which we then partitioned according to the different JULES PFTs (supporting document: Table S1). All top soil layer DOC measurements within one model grid-cell (1.25° latitude, 1.875° longitude) were aggregated and the resulting grid-cell average observed DOC concentration (n = 27) was then used for optimisation of the model (see Suppl. Info.). To complement our analysis of soil DOC, we further confronted the model results against observed DOC concentration in bottom soil layers when available as well as DOC concentration within headwater streams to evaluate our simulated DOC leaching fluxes. River DOC concentrations in low order streams is a good integrator of the soil DOC leached in the draining catchments[21], hence we compared simulated DOC concentrations in runoff across the United States with observed riverine DOC concentrations (n = 623) from the GloRiCh database [27] where the higher data density was available and yet covered different biomes. Where instantaneous discharge measurements were also reported in GloRiCh, we directly compared DOC leaching fluxes as well. Further details on model-data comparison are provided in section process optimization of SI.

Figure 1a shows measured DOC concentration in the top and bottom soil layers against the simulated values while Figure 1b compares measured DOC concentration and DOC leaching fluxes in headwater streams against simulated ones. Results show that simulated DOC concentration in the soil column ($r^2$ of 0.99, p value of 0.002 for top-soil and $r^2$ of 0.97, p value of 0.008 for bottom-soil) correlate reasonably well with observed DOC concentrations.

Furthermore, our results show that the simulated DOC leaching fluxes are overall in good agreement with observed fluvial DOC exports ($r^2$ of 0.58 and p-value of 0.01), the slight underestimation in the model being mainly due to the lower runoff in the simulations compared to measured discharges (Figure S4). The calibrated version of JULES-DOCM is then used to spatially upscale from the few DOC measurements to biome scales and to the globe.

The globally simulated soil DOC concentration averages to 29.3±2.4 mg C $L^{-1}$ in the top-soil and 8.3±1.4 mg C $L^{-1}$ in the bottom-soil. Temperate and tropical zones exhibit the highest soil DOC concentration in the top soils as already reported in previous studies[26], followed by sub-tropical and boreal zones (Table S3). Note that the observed DOC concentrations in the boreal biome reported in Figure 1a originate exclusively from needle-leaved evergreen (NET) forest ecosystems while the global-scale simulation of DOC concentration for this biome encompasses other important PFTs such as needle-leaved deciduous forest (NDT) and C3 grass. This explains why the globally simulated DOC concentration in the boreal biome (Table S3) is substantially lower than would have been expected from the observed data used for calibration alone (Figure 1a). The mean DOC stocks per unit surface area are highest in temperate regions (4.4±0.3 g C $m^{-2}$), intermediate in the tropics (2.9±0.2 g C $m^{-2}$) and lowest in the boreal (2.1±0.3 g C $m^{-2}$) and sub-tropical (1.1± 0.1g C $m^{-2}$) zones (Table S4).

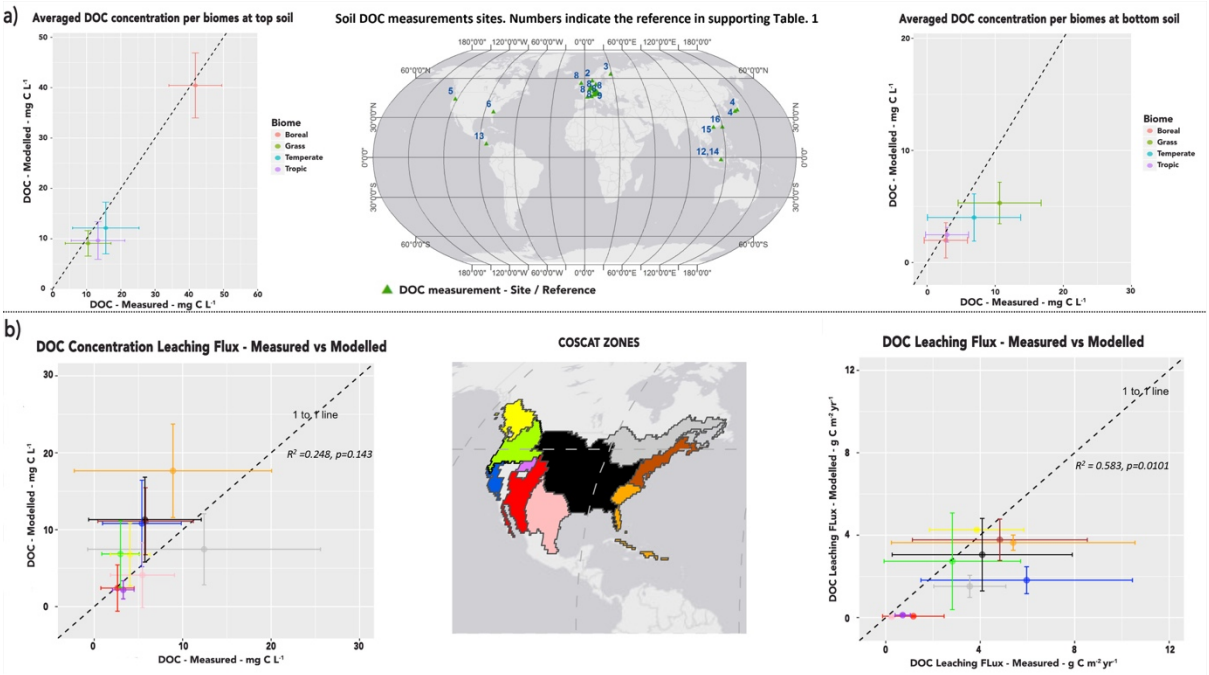


Figure 1. a) Averaged measured vs. modelled soil DOC concentration in top (left) and bottom (right) soil layers at measurement sites averaged at four biome regions (middle). b) Measured DOC concentration (left) and leaching fluxes in headwater streams (right) against simulated values aggregated at the scale of the COSCAT regions across the United States (middle) [28]. Colours on the plots correspond to those indicated on the map.

The spatial patterns in simulated soil DOC stocks (Figure 2a) are significantly correlated to those of SOC stocks (Figure 2b), as further evidenced by the statistics reported for the scatter plots shown in Figure S6. However, this correlation has only a $r^2$ of 0.48, which indicates that other factors also play a role in determining the global distribution of soil DOC stocks in the

model. The spatial distribution of the DOC leaching flux (Fig. 2c) is to a large extent controlled by the distribution of runoff, and hence precipitation, across the globe (Fig. 2d, Fig. S7).

However, to better understand the partial spatial decoupling between SOC stocks, DOC soil concentration and DOC leaching flux, we compute three time constants from our model results, which are related to depth-integrated DOC production rate ($K_{prod}$=DOC production flux/SOC stocks), DOC decomposition rate ($K_{dec}$=DOC decomposition flux/DOC stocks) and DOC leaching rate ($K_{leach}$= DOC leaching flux/DOC stocks) (Table S5). Based on these definitions, the simulated residence time ($\tau_{DOC}$) of DOC in the soil column is given by $\tau_{DOC}=1/(K_{dec}+K_{leach})$. The DOC production rate is controlled by temperature and moisture while temperature is the only climatic driver of the decomposition rate, runoff being the main climatic driver of the leaching flux rate.

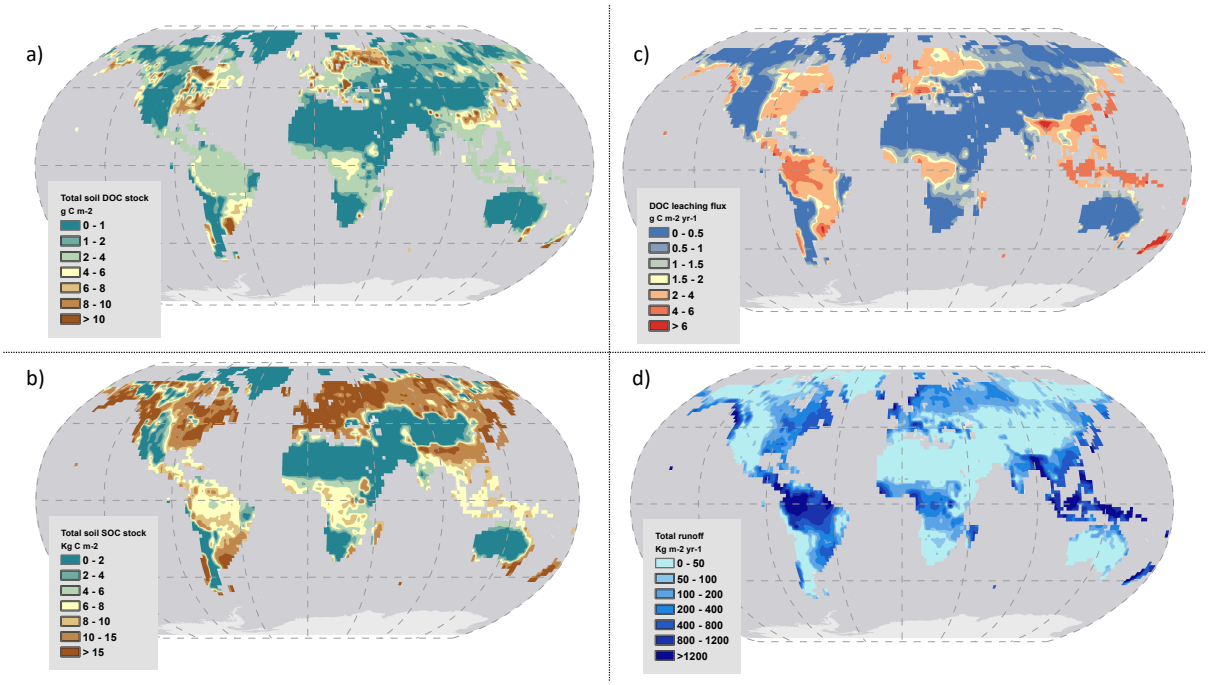


Figure 2. Simulated present-day a) soil DOC stock (g C $m^{-2}$) b) soil SOC stock (kg C $m^{-2}$), c) DOC leaching fluxes (g C $m^{-2}$ $y^{-1}$), and d) runoff (kg $m^{-2}$ $y^{-1}$)

The DOC production rate ($K_{prod}$) has largest values in tropical regions, despite having comparatively lower SOC stocks than other latitudinal bands, which is due to both moisture and temperature having a positive effect on the DOC production rate (Figure 3a), and, overall, $K_{prod}$ increases by at least one order of magnitude from high to low latitudes.
The DOC leaching rate ($K_{leach}$), is strongly spatially correlated with runoff. This is evidenced on Figure 3b which reveals a steady increase of DOC leaching at low to intermediate runoff values, with lower increase at high runoff level, where available DOC stocks becomes a limiting factor for leaching (Figure 3c). This pattern is typical of a transition from transport limited to substrate limited behaviour which can also be seen from the ratio of leached NPP as DOC to the river system (Figure 3d). In addition, as high runoff rates are typically found in the tropics, the accompanying high temperatures lead to high DOC decomposition rates in the soil, further decreasing DOC concentrations in runoff from soil. Despite these effects, the fluxes per unit area are overall higher in the tropics, the lower DOC stocks in this latitudinal band being largely compensated by the much higher runoff. In contrast, many regions of low runoff are also areas of particularly low DOC stocks and, thus, limited leaching. Regionally, areas on land that show the highest DOC leaching fluxes include SE Asia, New-Zealand and a small portion

of the South American continent where both drivers (runoff and DOC stocks) are high. Other hotspot areas include the Amazon, and to a lesser extent, the Congo basins, as well as Western Europe and large portions of the Eastern part of North America.

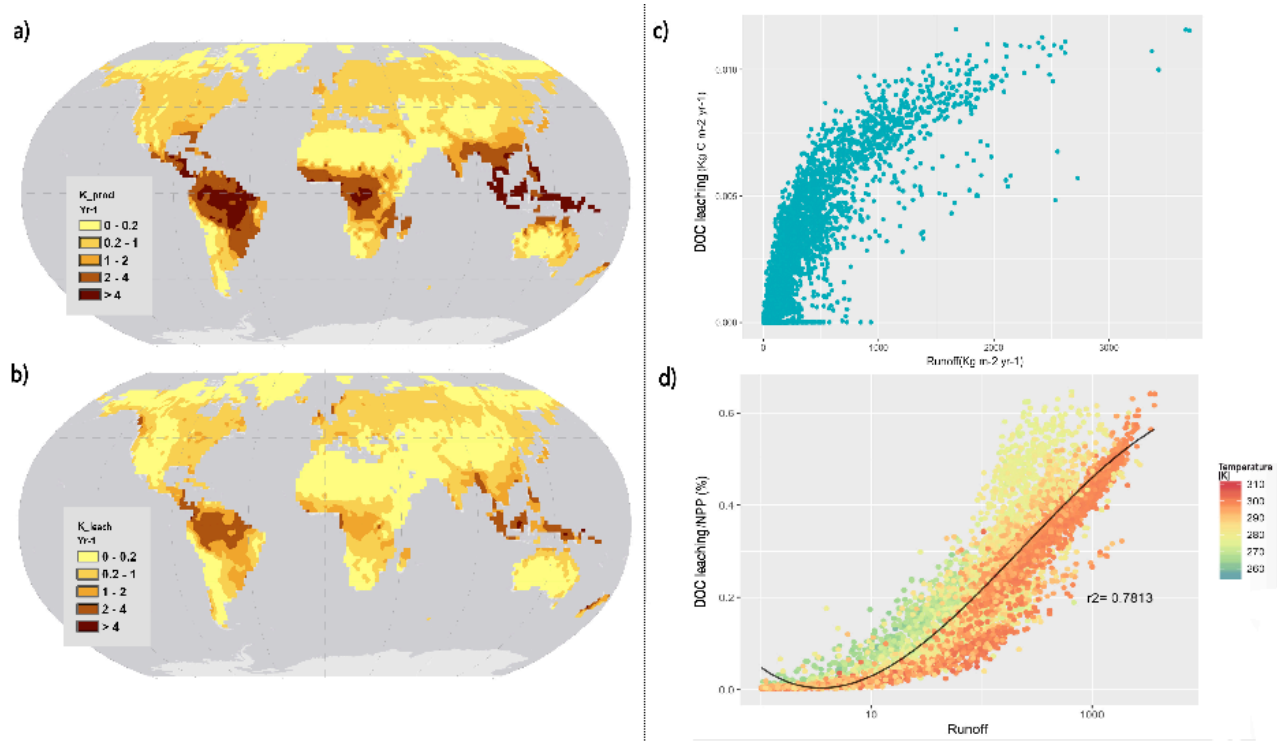


Figure 3. Global distribution of the time constants for dissolved organic carbon a) production rate ($K_{prod}$) ($yr^{-1}$) and b) leaching rate ($K_{leach}$) ($yr^{-1}$) . Also shown, the relationship between DOC leaching flux (Kg C $m^{-2}$ $yr^{-1}$) against runoff (Kg $m^{-2}$ $yr^{-1}$) (panel c), and the relationship between the DOC leaching to terrestrial NPP ratio (%) against runoff (Kg $m^{-2}$ $yr^{-1}$) and temperature (K) (panel d). Note the log scale for the X-axis in panel d.

The simulated DOC residence time in the soil column ($\tau_{DOC}$), increases from a few weeks in tropical soils to more than a year in the boreal region (Figure S8e), a result which is in line with previous studies[29–31]. Altogether, the first-order latitudinal pattern in DOC stock results from the partly opposing effects of SOC stocks that are highest in boreal and temperate regions and of the ratio $K_{prod}/(K_{leach}+K_{dec})$, which is highest in the (sub)-tropics (Figure S8h). This explains why the marked latitudinal gradient in SOC stock between tropical and boreal zones is not as prominent for DOC stocks (supporting document: Figure S8).

Globally, we estimate the production of DOC from litter and SOC decomposition to amounts to about 1.4 Gt C ±0.1 per year, out of which 40% (0.5±0.03 Gt C $yr^{-1}$) is mineralized in the soil and released back as $CO_2$ to the atmosphere, 40% is transformed back into SOC, and only about 20% (0.3±0.1 Gt C $yr^{-1}$) is leached to aquatic systems. Our global estimate of DOC leaching directly originating from soils is thus equal to 0.3±0.1 Gt C $yr^{-1}$ (Figure 4a). The present-day global DOC stock stored in soils is estimated at 0.3±0.04 Gt C, of which 30% is concentrated in the top 10 cm (Fig. S5).The globally-averaged residence time of soil DOC is remarkably short, only of the order of 4 months. When integrated over larger biomes, the total soil DOC stocks are highest in the tropical region (101±6 Tg C), followed by the temperate (97±11.6 Tg C), boreal (70±10.3 Tg C) and subtropical (70±9.3 Tg C) zones.

Consistent with these stocks, biome-averaged DOC production is also highest for the tropics (858±15.4 Tg C $yr^{-1}$), followed by the sub-tropical (273±19 Tg C $yr^{-1}$), temperate (244±26 Tg C $yr^{-1}$) and boreal (104±14.8 Tg C $yr^{-1}$) regions (Fig. 4b). The same decreasing order is simulated for the DOC mineralization fluxes, while for leaching fluxes about 60 % occurs in the tropical band, a result in agreement with the very high river $CO_2$ emission rate in this region[17]. DOC leaching in temperate areas is slightly higher than in the subtropics and is lowest in the boreal region. Despite much smaller absolute fluxes, the boreal region exhibits a slightly higher export to production ratio (23 %) than the sub-tropics (16 %) and tropics (19 %) due to the highest residence time and lowest decomposition rate in the boreal biome. This result is consistent with the higher proportion of NPP leached as DOC already reported by other studies for the boreal zone [21].

Our global-scale soil-derived DOC leaching flux is estimated only at 0.3±0.1 Gt C $yr^{-1}$. However, two other significant terrestrial sources of DOC that can possibly contribute to aquatic DOC fluxes are not explicitly considered in the present study. First, plant litter fall can directly support in-stream DOC production from litter decomposition. As a first order assessment, using litter production computed by JULES and an estimate of the global areal coverage of streams and rivers[16,32], we quantify the DOC production flux from litter decomposition at 0.12 Gt C $yr^{-1}$. Assuming a carbon use efficiency of 0.5[38], half of this decomposed litter material would directly be oxidized to $CO_2$, while the remainder, about 0.06 Gt C $yr^{-1}$ would be transformed into DOC feeding in the global river network (Fig. 4a). Second, JULES does not account for wetlands and peatlands, which together represent an estimated C stock and C accumulation rate of 110-455 Gt C $yr^{-1}$ and 45-210 Tg C $yr^{-1}$ [33], respectively. These ecosystems are potentially significant, yet highly uncertain sources of DOC to the river network. Previous model estimates from GlobalNEWS-2 suggest that wetlands could contribute up to about 20% of fluvial DOC export to the coast[13,34]. Assuming that this ratio also holds for DOC exported from wetlands to aquatic systems, that is, assuming that DOC from all terrestrial sources have similar reactivity within aquatic systems, we estimate a global wetland DOC flux into inland waters of about 0.1 Gt C $yr^{-1}$ as a very first-order assessment. This can be considered as an upper bound value as wetland derived DOC is known be more recalcitrant to in-stream respiration than DOC derived from other terrestrial sources[5].

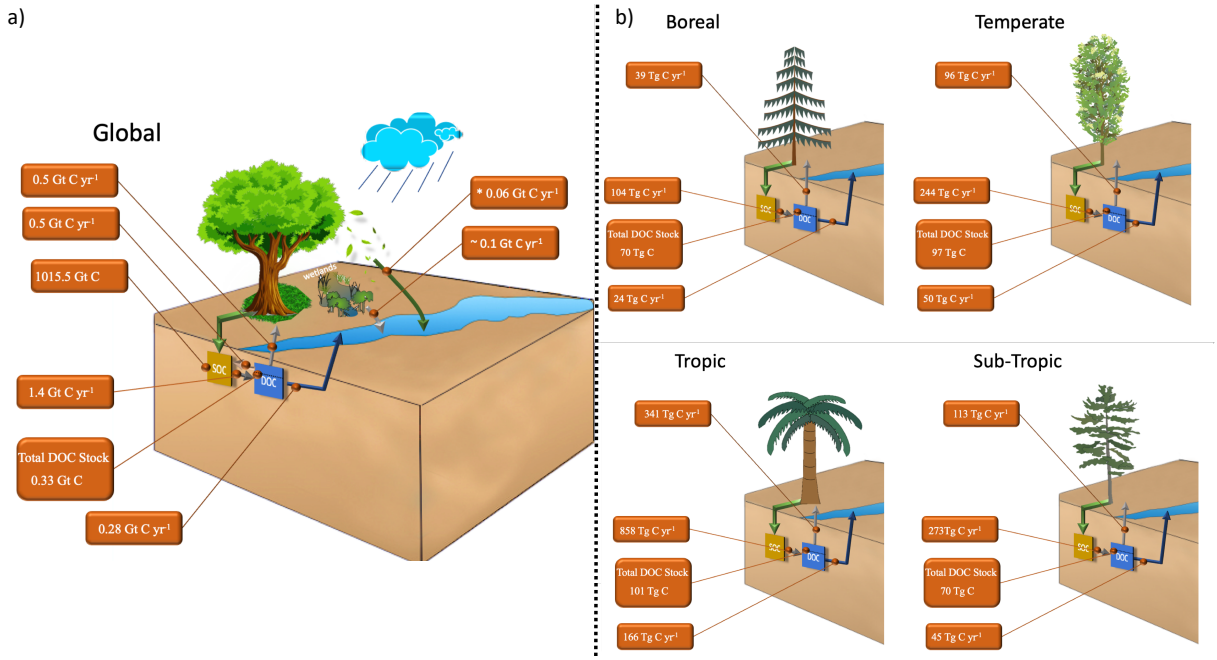

Figure 4. Global and regional DOC stocks and fluxes. Units are Gt C and Gt C $yr^{-1}$ for global, and Tg C and Tg C $yr^{-1}$ for regional estimates

Therefore, the inclusion of estimates of DOC inputs from litter fall and wetlands leads to a total global DOC leaching flux from terrestrial ecosystems to aquatic systems that does not exceeds 0.5 Gt C $yr^{-1}$, significantly lower than previous estimates[4]. Until now, these previous estimates, were all relying on a C budget closure for the inland waters where the soil C leaching term is diagnosed as the sum of fluvial C exports to oceans, C burial in aquatic sediments and $CO_2$ outgassing from inland waters, each of which entail high uncertainties. Using such an approach, quantitative estimates of C transfers from land to inland waters are in the range 1.9 Gt C $yr^{-1}$-5.1 Gt C $yr^{-1}$ [35,36] . Such quantification includes all C forms (dissolved organic as we estimate here, but also dissolved inorganic as well as particulate for both inorganic and organic material) and we are not aware of any estimate for DOC-only leaching from terrestrial to aquatic systems. Hence it is impossible to directly compare these estimates to our DOC only leaching flux of less than 0.5 Gt C $yr^{-1}$. However, Meybeck et al.[11] assessed that DOC represents about 37% of all total C exported from land to the coastal ocean. If we were to assume a similar ratio for soil leaching, our global estimate of total C export from soils would be about 1.4 Gt C $yr^{-1}$. This flux should be seen as an upper estimate of total C leached from soils given the larger reactivity of DOC compared to other forms of riverine C. It is thus lower by up to a factor of 4 than previously published estimates[4,5], indicating that upland terrestrial ecosystems (soils and litter combined) are probably not able to sustain such high leaching fluxes. Indeed, the range of published estimates of total C leaching represents about 3 to 8% of global terrestrial NPP, an order of magnitude higher than what our DOC-only model suggest. Our results imply that other sources or processes such as sewage input, leaching from eroded soils, autotrophic production in fringing wetlands and riparian ecosystems or algae bloom[3], not accounted here, could potentially also provide significant DOC inputs to inland waters. Furthermore, our analysis suggest that more conservative estimates of land to ocean C fluxes, most notably $CO_2$ outgassing and C burial are needed in order to reconcile the carbon cycle along the aquatic continuum.

**Method**

Studies show that vegetation controls the quality and concentration of DOC in soil [2,37,38] as well as the DOC leaching out of the soil [16]. Hence the DOC decomposition and leaching rate are affected by the dominant vegetation type(s) which could be related to the lignin and polyphenols [2,39]. Thus, our database of soil DOC observations was first partitioned according to the different plant functional types (PFTs) for which measurements were available (Table S1). Because of limited data coverage, the nine PFTs of JULES-DOCM were further aggregated into four broad categories: boreal; temperate; subtropical and tropical; and grassland and croplands.

The DOC production ($F_{p_{k,i}}$) in each soil layer (i) and for each pool (k) in our model is represented as:

$$F_{p_{k,i}} = S_{c_k} \times \left(1 - e^{(-K_P \times ratemodifiers_i)}\right) \qquad \text{Eq. 1}$$

where $S_{Ck}$ is SOC content in soil, $K_P$ is the basal DOC production rate based on the C pool source, and the rate modifiers$_i$ includes production rate dependence on temperate, moisture, vegetation and soil texture, estimated for each soil layer.
DOC decomposition ($F_{D_{k,i}}$) in the model is represented as:

$$F_{D_{k,i}} = S_{DOC_{k,i}} \times \left(1 - e^{(-K_{DOC_k} \times FT_i)}\right) \qquad \text{Eq. 2}$$

where $S_{DOCk,i}$ stands for the DOC content in soil, $K_{DOCk}$ is the basal decomposition rate of DOC and $FT_i$ is a rate modifier that only depends on temperature in each soil layer.
In this revised version of JULES-DOCM we modified the DOC production and decomposition by making the parameters $K_P$ and $K_{DOC}$ dependent on the dominant PFT. $K_{DOC}$ is calculated as the inverse of the residence time of labile or recalcitrant DOC. Taken that the model is not sensitive to the labile DOC residence time [23], we specified only a range of values for recalcitrant DOC residence times per PFT based on literature values (Table. S2). In order to recalibrate the $K_P$ and $K_{DOC}$ values, we applied the Latin hypercube method [40] using the Latin hypercube package in R (ihs) [41] to select random values of $K_P$ and $K_{DOC}$ covering the whole range of probable values.
Our global simulation follows the TRENDY protocol[42], based on the global simulation data setting and method provided for JULES (see Harper et al, 2016[24]) at N96 spatial resolution (1.875◦ longitude×1.25◦ latitude). Meteorological data from CRU-NCEP version 4 was used as climate forcing[43]. In addition, the model was forced with observed atmospheric $CO_2$ and land cover change [44]. Prior to DOC processes optimization, we compared simulated global gross primary production (GPP) and net primary production (NPP) against data from the model tree ensemble (MTE) and MODIS 17 [45,46], respectively. We also compared simulated total SOC stocks against the HWSD at the global scale.
As the SOC needs several thousands of years to reach an equilibrium state in JULES, we used an accelerated spin-up method, which only requires 200-300 years of spin-up [24]. This method assumes that the decomposition rate of the most recalcitrant C pools (resistant plant material, soil biomass and humus) is identical to the decomposition rate of the most labile litter pool. This was achieved by scaling the pool sizes of resistant plant material, soil biomass and humus by a factor of 33, 15 and 500, respectively. Each simulated C pool was then multiplied by the same scaling factors. A final spin up with the actual decomposition rate for each pool was then performed for another 300 years to ensure the simulated SOC stocks are in equilibrium.
Because the DOC optimization process requires 30 random samples for each of the 27 grid-cells with observations (note that, only top-soil DOC observations were used for model calibration), 810 simulations were performed, starting from the spin-up described above. The best pair of $K_p$ and $K_{DOC}$ values was then retained for each PFT and used to calculate DOC stocks and fluxes globally at the spatial resolution of JULES-DOCM.
An uncertainty analysis on estimated DOC stocks was also performed, by repeating the simulation with the observation-based WATCH meteorological forcing data[47], instead of CRU-NCEP. Furthermore, we also ran the model with the CRU-NCEP configuration and the second-best combination of $K_P$ and $K_{DOC}$ with regard to RMSE as well as a parameter set using as $K_P$ and $K_{DOC}$ for the PFTs, which were not calibrated, the recalibrated $K_P$ and $K_{DOC}$ values from the PFTs that were most similar to them (as opposed to keeping the default parameters for non-calibrated PFTs). That means in detail that we applied the best parameter set from broadleaf evergreen tropical trees to broadleaf evergreen temperate trees, the one from needle leaf evergreen trees to needle leaf deciduous trees, and the one from C3 grass for C4 grass to

deciduous and evergreen shrubs. We calculated standard deviation of the global DOC stocks and concentration from these three runs in order to assess the uncertainty.

# Supporting document: Chapter 2 - Soil leaching as minor source to inland water carbon budget

In JULES-DOCM, we modified the RothC scheme and distributed the simulated SOC pools vertically over 4 soil layers (from top to bottom: 0-10 cm, 10-35 cm, 35-100 cm, and 100-300 cm), assuming an exponential decay of SOC with depth (Jobbágy & Jackson, 2000). The main source for DOC is SOC and litter decomposition (Eq.1), a process that is controlled by soil moisture, temperature, vegetation cover and soil texture (clay and silt content). These environmental factors are collectively referred to as "rate modifier" in Eq.1. Two DOC pools are distinguished, depending on whether they are derived from labile or recalcitrant SOC and litter pools. These DOC pools then decompose at a rate controlled by their respective reactivity and the temperature in each soil layer (Eq.2). A fraction of the decomposed DOC, defined by the Carbon Use Efficiency (CUE) parameter (Kalbitz *et al.*, 2000; Manzoni *et al.*, 2012) returns to the SOC pool while the remainder is released to the atmosphere as $CO_2$.

Each of the two DOC pools can exchange between a dissolved and an adsorbed phase, and the adsorption isotherm depends on soil texture and pH (Moore et al. 1992). In addition, the model represents the diffusive transport of dissolved DOC, including leaching. Diffusion between layers depends on the DOC concentration gradient and a molecular diffusion coefficient (Ota et al, 2013) while leaching of dissolved DOC from the soil column is related to surface and subsurface runoff. Adsorbed DOC is assumed inert and immobile. All these processes are calculated for each soil layer and at a 30 min time-step. For further details, refer to Nakhavali et al. 2018.

**Process optimization**

**Table S1.** Dissolved Organic Carbon measurements from literature and database

| SITE | DOC in soil- Annual mean (mg C $L^{-1}$) | Depth of measurement (cm/horizon) | Reference |
|---|---|---|---|
| **Boreal Forest** | | | |
| Coulissenheib | 24.7 | 20 | 1 |
| Coulissenheib | 5.0 | 90 | 1 |
| Bikenes | 50.6 | 9 | 2 |
| Waldstein | 47.8 | 12 | 2 |
| Kangasvaara | 38.5 | E horizon* | 3 |
| Kangasvaara | 0.5 | B horizon | 3 |
| **Temperate forest** | | | |
| Nagano | 3.23 | O,A horizons | 4 |
| Tango | 20.95 | O,A horizons | 4 |
| Tango | 2.3 | B horizon | 4 |
| Kyoto | 14.7 | O,A horizons | 4 |
| Kyoto | 4.3 | B horizon | 4 |

| | | | |
|---|---|---|---|
| Oregon | 40 | 10 | 5 |
| Oregon | 25.5 | 20 | 5 |
| Oregon | 15.75 | 30 | 5 |
| Oregon | 0.5 | 70 | 5 |
| South Carolina | 19.22 | 15 | 6 |
| South Carolina | 1.39 | 50 | 6 |
| South Carolina | 0.97 | 175 | 6 |
| South Carolina | 0.82 | 600 | 6 |
| BITÖK | 17.8 | 20 | 7 |
| BITÖK | 5.7 | 60 | 7 |
| Søro | 22.9 | 15 | 8 |
| Søro | 14.1 | 100 | 8 |
| Laois | 10.9818 | 15 | 8 |
| Laois | 3.2 | 70 | 8 |
| Loobos | 32.1 | 5 | 8 |
| Loobos | 5.6 | 120 | 8 |
| Wetzsein | 43.1 | 20 | 8 |
| Wetzsein | 17.6 | 90 | 8 |
| Hainich | 7.5 | 10,20 | 9 |
| Brasschaat | 34 | 10,35 | 10 |
| Brasschaat | 22 | 75 | 10 |
| Ebrach | 23.1 | 20 | 11 |
| Ebrach | 9.9 | 120 | 11 |
| Freising | 6.6 | 30 | 11 |
| Freising | 3.0 | 140 | 11 |
| Mitterfels | 1.3 | 30 | 11 |
| Mitterfels | 1.2 | 120 | 11 |
| Ebersberg | 7.5 | 30 | 11 |
| Ebersberg | 3.6 | 100 | 11 |
| Flossenbürg | 3.3 | 20 | 11 |
| Flossenbürg | 4.3 | 120 | 11 |
| Goldkronach | 4.9 | 20 | 11 |
| Goldkronach | 3.0 | 120 | 11 |
| Kreuth | 5.2 | 20 | 11 |
| Kreuth | 2.4 | 120 | 11 |
| Rothenkirchen | 5.5 | 30 | 11 |
| Rothenkirchen | 2.9 | 80 | 11 |
| Sonthofen | 5.8 | 20 | 11 |
| Sonthofen | 4.7 | 120 | 11 |
| Zusmarshausen | 4.5 | 30 | 11 |
| Zusmarshausen | 2.4 | 130 | 11 |
| Landau | 13.0 | 30 | 11 |

| | | | |
|---|---|---|---|
| Landau | 6.7 | 130 | 11 |
| Riedenburg | 5.4 | 30 | 11 |
| Riedenburg | 5.0 | 120 | 11 |
| Würzburg | 3.0 | 30 | 11 |
| Würzburg | 7.7 | 110 | 11 |
| Altdorf | 7.3 | 140 | 11 |
| Dinkelsbühl | 6.2 | 30 | 11 |
| Dinkelsbühl | 7.2 | 120 | 11 |
| Pegnitz | 15.4 | 20 | 11 |
| Pegnitz | 6.4 | 120 | 11 |
| **TROPICAL FOREST** | | | |
| Bukit Soeharto | 25.95 | O,A horizons | 12 |
| Bukit Soeharto | 9.9 | B1 horizon | 12 |
| Bukit Bankirai | 21.85 | O,A horizons | 12 |
| Bukit Bankirai | 6 | B1 horizon | 12 |
| La Selva | 3.9 | 25 | 13 |
| La Selva | 0.7 | 150 | 13 |
| Kuaro_KR1 | 13.4 | A1 | 14 |
| Kuaro_KR1 | 5.4 | B1 | 14 |
| Kuaro_KR2 | 5.7 | A | 14 |
| Kuaro_KR2 | 1.7 | Bt1 | 14 |
| Kuaro_KR3 | 10.1 | A | 14 |
| Kuaro_KR3 | 2.8 | Bt1 | 14 |
| **SUBTROPICAL FOREST** | | | |
| Dinghushan | 22.66 | 0:20 | 15 |
| Guandaushi | 12.5 | 15 | 16 |
| Guandaushi | 10.3 | 30 | 16 |
| **Grassland** | | | |
| Carlow | 13 | 10:28 | 17 |
| Carlow | 5 | 28:79 | 17 |
| Easter Bush | 17.1 | 30 | 8 |
| Easter Bush | 16.3 | 100 | 8 |
| Früebüel | 3.7 | 30 | 8 |
| Früebüel | 12.3 | 100 | 8 |
| Laqueuille | 2.0455 | 30 | 8 |
| Laqueuille | 1.7 | 90 | 8 |
| **Cropland** | | | |
| Carlow | 4.2 | 0:40 | 17 |
| Klingenberg | 13.9 | 35 | 8 |
| Klingenberg | 10.1 | 75 | 8 |
| Grignon | 17.3 | 0:40 | 8 |
| Grignon | 13.8 | 90 | 8 |

1. Michalzik et al. (1999)(Michalzik et al., 1999)(Michalzik et al. 1999) 2.Mulder et al. (2000) 3.Piirainen et al. (2004) 4.Fujii, Funakawa, et al. (2011) 5. Yano et al. (2004) 6. Markewitz & Richter (1998) 7.Solinger et al.( 2001) 8. Kindler & Siemens (2010) 9. Kutsch et al. (2010) 10. Gielen et al. (2011) 11.Borken et al. (2011) 12.Fujii et al. (2009) 13. Schwendenmann & Veldkamp (2005) 14.Fujii, Hartono, et al. (2011) 15.Fang et al. (2009) 16.Liu & Sheu (2003) 17.Walmsley et al. (2011)

* Horizons O, A and E are treated as top soil (down to 35 cm) and Horizon B is treated as bottom soil (from 35 cm down to 3 m)

Note however, the observed data for boreal zone only covers needle-leaf evergreen trees (NET) which cover a large proportion of the boreal biome. Needle-leaf deciduous forest (NDT) which covers another important portion of boreal biome is not covered by our literature database. Hence, we used the default DOC residence time and production for NDT, which is about 1/5 of the NET residence time (simulation results with parameter sets from the calibrated PFTs that were most similar to uncalibrated PFTs in Table. S5).

Next, for each of these four categories, the kinetic parameters for DOC production and decomposition rates were calibrated through an optimization procedure minimizing the mismatch between observed and modelled DOC concentrations. The calibration of JULES-DOCM was based on top-soil concentrations (0-35 cm) only, because data density is significantly higher for shallow soils and sampling depths are more consistently defined across the globe for this layer. The resulting PFT-dependent kinetic parameters for soil DOC production and decomposition are reported in supporting document Table S2. Observed sub-soil DOC concentrations (35-300 cm) were only used for model validation. In addition, we also compared simulated and measured SOC concentrations for all grids for which DOC measurements were available. Where measured SOC data was not reported, we compared simulated SOC concentrations against values reported in the Harmonized World Soil Database (HWSD)(Nachtergaele *et al.*, 2010).

In this revised version of JULES-DOCM we modified the DOC production and decomposition by making the parameters $K_P$ and $K_{DOC}$ dependent on the dominant PFT. $K_{DOC}$ is calculated as the inverse of the residence time of labile or recalcitrant DOC. Taken that the model is not sensitive to the labile DOC residence time (Nakhavali *et al.*, 2018), we specified only a range of values for recalcitrant DOC residence times per PFT based on literature values(Johnson *et al.*, 2000; Kalbitz *et al.*, 2003; Yule and Gomez, 2009)

In order to recalibrate the $K_P$ and $K_{DOC}$ values, we applied the Latin hypercube method (Stein, 1987) using the Latin hypercube package in R (ihs) (Davis, 2015) to select random values of $K_P$ and $K_{DOC}$ covering the whole range of probable values. This method requires selection of a number of random samples at least ten times larger than the number of variables to be tested. In this work, we thus defined, for each PFT, 25 random combinations of $K_P$ and $K_{DOC}$ values within the observed ranges and 5 additional values outside of the observed ranges.

Next, we performed a cross validation (Refaeilzadeh et al, 2009), by splitting the pool of observed soil DOC concentrations for each PFT between calibration and validation sites. For boreal and tropical/subtropical forests where observations are rather limited (<5), we used all possible combinations of sites, each time using three quarter of the observation sites as calibration data and keeping one quarter as validation data. For temperate forests and grass/croplands, the high number of observation sites (> 5) precludes calculations for all possible combinations of sites. Here, we selected instead ten and eight random combination of sites for temperate forests and for grass/croplands, respectively, using the SAMPLE function in R (R-Documentation, 2016). Based on each pair of $K_P$ and $K_{DOC}$ values, we calculated the average RMSE for both calibration and validation sites. As the RMSE results from the various cross validation sets were not showing a significant difference, we used all the top soil DOC

observations per PFT for our final parameter calibration, choosing the combination of $K_P$ and $K_{DOC}$ which gave the lowest RMSE.
In addition to the DOC concentration in soils, we further used observed DOC concentration in headwater streams to validate simulated DOC leaching fluxes. River DOC is a good integrator of the soil DOC leached in the draining catchments and we compared simulated DOC concentrations in runoff with observed riverine DOC concentrations from the GloRiCh database (Hartmann et al, 2014). Where instantaneous discharge measurements were available in GloRiCh, we validated DOC leaching fluxes as well (Fig.2).

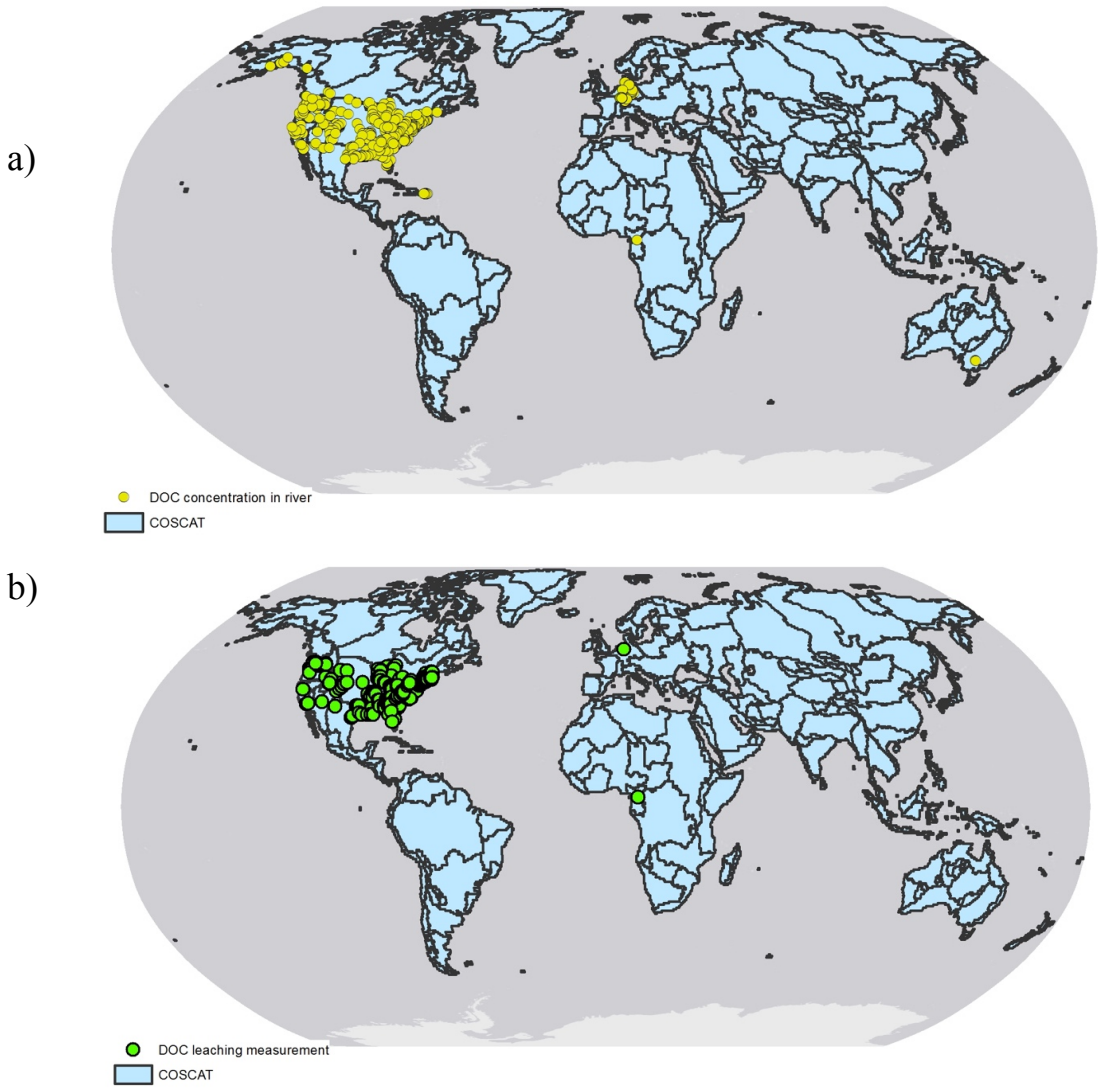


**Figure S1.** Locations of measurements of dissolved organic carbon a) concentration in runoff in mg C $L^{-1}$ b) leaching flux (calculated from measured DOC concentration and instantaneous discharge) in g C $m^{-2}$ $yr^{-1}$, using the COSCAT (costal segmentation and related catchments, (Meybeck, Dürr and Vörösmarty, 2006)) scheme for regionalisation. Yellow and green points indicate the measurements from GloRiCh database (Hartmann, Lauerwald and Moosdorf, 2014). Black lines with blue area indicates COSCAT (costal segmentation and related catchments, (Meybeck, Dürr and Vörösmarty, 2006)

## Optimization results

The vegetation of each grid cell is represented in the model as an ensemble of different PFTs of which each is assigned an areal proportion. In order to make the simulated soil DOC concentrations per pixel more comparable to literature values in the recalibration of $K_p$ and $K_{DOC}$, we prescribed a single PFT for each site used in the calibration process, which corresponded to the dominant land cover type that was described for the observed sites. Prescribing theses single PFTs together with the default parameterisation of JULES-DOCM (Nakhavali et al., 2018) leads to a general underestimation of DOC stocks in the top soil layer but already a statistically significant correlation between modelled and observed values (p-values <0.001, $R^2$ values of 0.51).

As a next step, we varied the rates of DOC production and decomposition using the Latin hypercube method and using RMSE values in cross-validation for best parameters combination at each site. Cross validation results reveal that different combinations of calibration and validation sets do not have a significant impact on the absolute model residuals, indicating that the calibration was robust for all four PFTs. Therefore, for the final model parameter calibration we used all the top-soil measurements. The averaged RMSE in top-soil DOC concentration is 2.84 mg C $L^{-1}$ for boreal forest, 10.83 mg C $L^{-1}$ for temperate forest, 9.04 mg C $L^{-1}$ for subtropical/tropical forest and 6.77 mg C $L^{-1}$ for grass/croplands.

In the final calibration, the RMSE is not significantly different from the initial parametrisation from Nakhavali et al. (2018) with prescribed PFTs for sub-tropical forests, tropical forests and grass/croplands. However, the recalibration markedly reduces the absolute model residuals for these three PFTs. For temperate forests, the average RMSE for the final calibration is always slightly higher than the one using default parameters values. This can be explained by the fact that the model was initially developed using sites from temperate ecosystems only (Carlaw, Braaschaat, etc)(Nakhavali *et al.*, 2018). Hence the default set of parameters is already giving the best results. We hence kept these parameter values for temperate forests.

We illustrate as density plots the dependence of the average RMSE per PFT on the selected $K_P$ and $K_{DOC}$ values when using all the observed top-soil DOC concentrations (Fig S2). The darker coloured areas indicate zones of low RMSE, the red symbol defining the minimum after final calibration while the white symbol corresponds to the RMSE for the default model configuration.

Table S2. PFT-dependent kinetic parameters for soil DOC production and decomposition

| Final model parameters (unit in years) | | | | | | | | | |
|---|---|---|---|---|---|---|---|---|---|
| | BET-TR | BET-TE | BDT | NET | NDT | C3 | C4 | DSH | ESH |
| 1/KDOC | 635.5799 | 600 | 610.6468 | 3283.84 | 600 | 600.7512 | 600 | 600 | 600 |
| 1/KP | 1.902623 | 1 | 0.9926714 | 1.238146 | 1 | 1.19097 | 1 | 1 | 1 |

Tropical broadleaf evergreen trees (BET-TR), Temperate broadleaf evergreen trees (BET-TE), Broadleaf deciduous trees (BDT), Needle-leaf evergreen trees (NET), Needle-leaf deciduous trees (NDT), C3 grass (C3), C4 grass (C4), Evergreen shrubs (ESH), Deciduous shrubs (DSH)

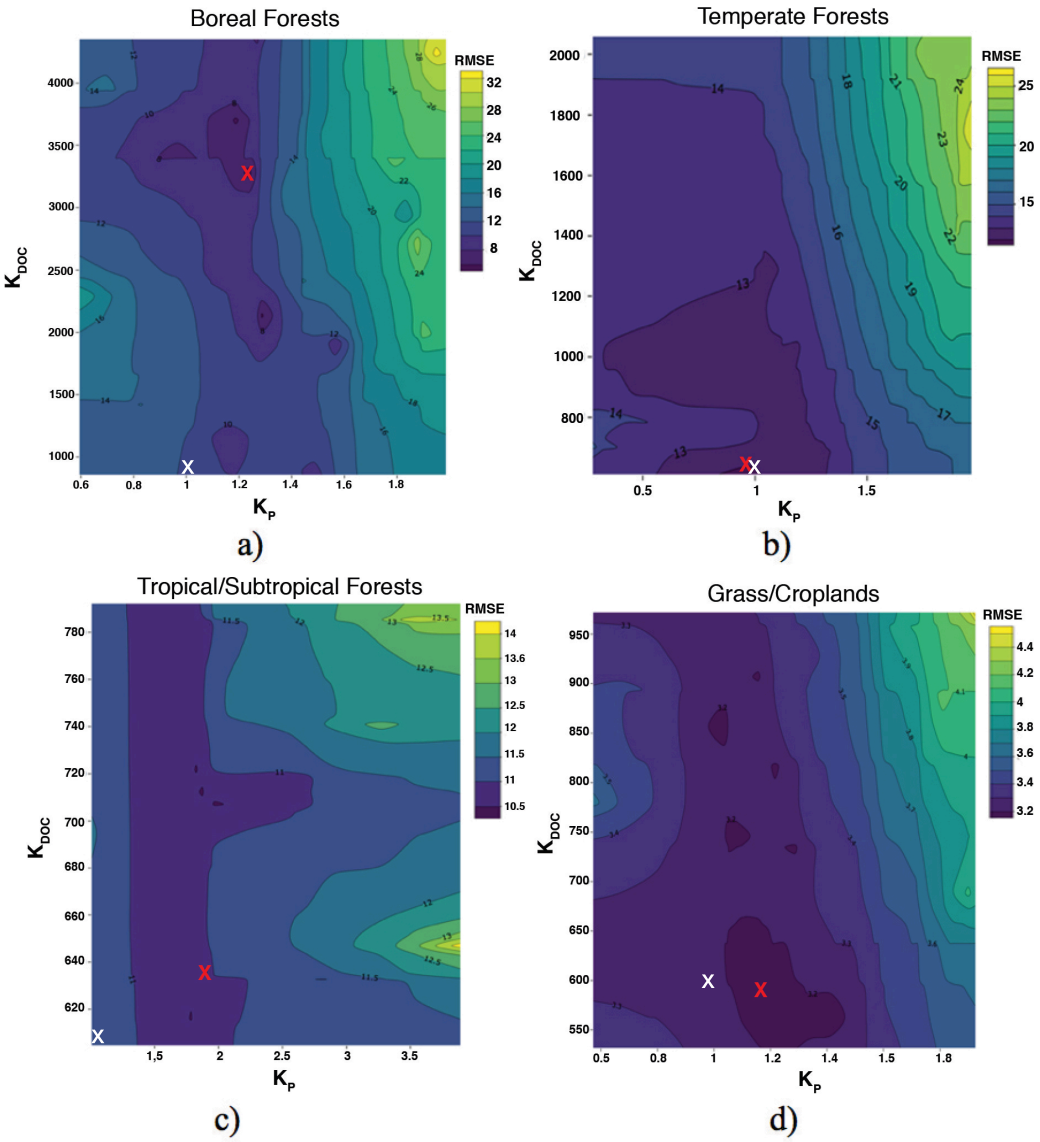


Figure S2. RMSE of simulated vs measured DOC, for varying values of DOC decomposition and production rates in a) Boreal forests b) Temperate forests c) Tropical and subtropical forests and d) Grasslands and croplands. Red X indicated the simulated combination of $K_{DOC}$ and $K_P$ parameters that leads to the lowest RMSE. $K_{DOC}$ and $K_P$ unit is day. White X indicated the default values of $K_{DOC}$ and $K_P$ parameters. We used the initial values from historical global scale simulation for the site level simulation. Before the main 10 years of simulation we performed an additional 10 years of spin up for the same period of the main simulations.

Figure S3 represents the correlation between modelled and observed DOC concentrations for top and bottom soil, per site and aggregated per PFT after recalibration. For the top-soil, there is a highly significant (p-values <0.001, $R^2$ value 0.40) correlation between observed and modelled average DOC concentrations.

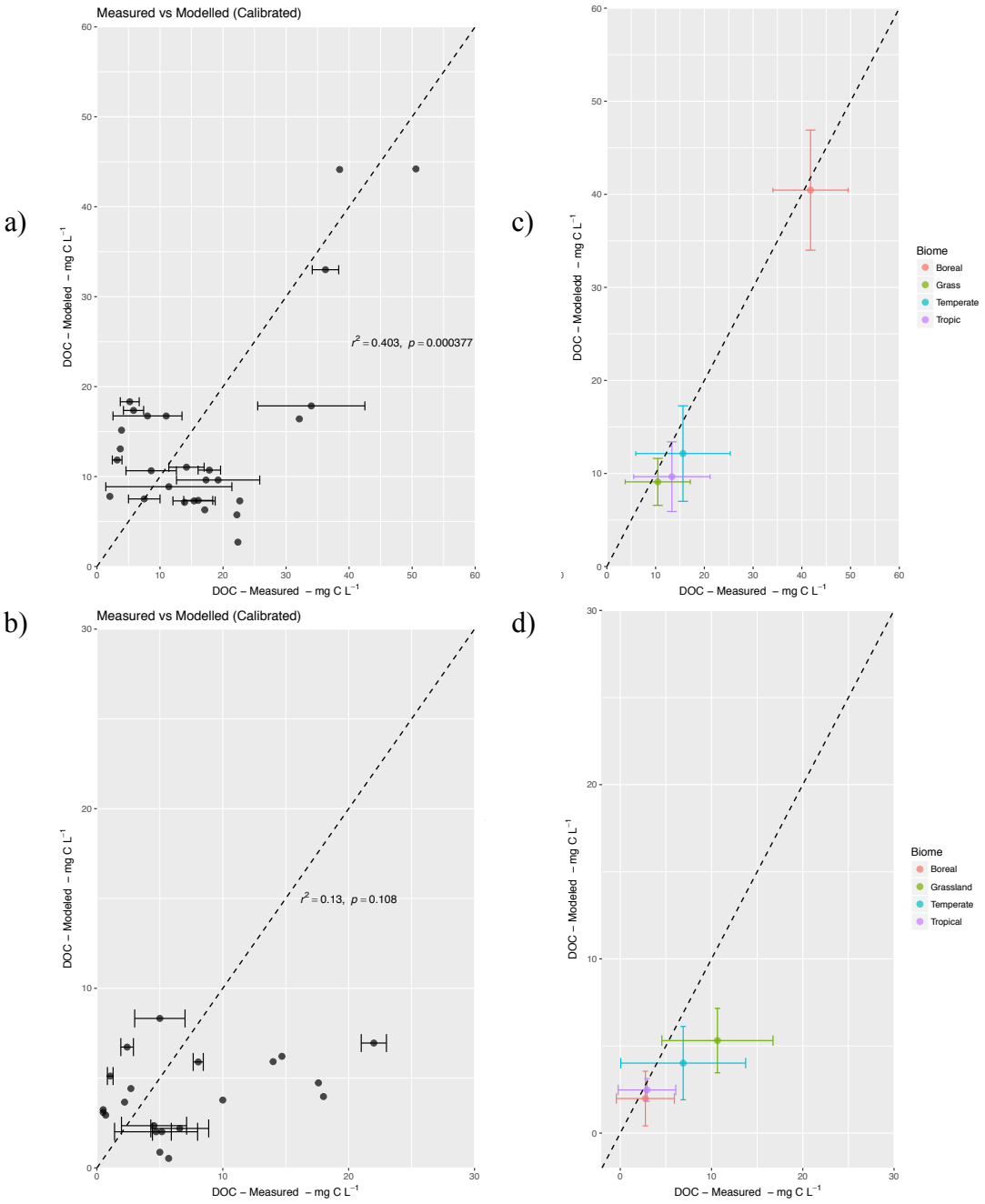


Figure S3. Calibrated model results. Modelled versus measured DOC concentration (in mg C L-1) at a) top soil b) bottom soil. Standard deviations of the measurements whenever available are reported on the plot. Averaged DOC per biomes and spatial standard deviation of measurements and simulation in each biome at c) top soil d) bottom soil. Dashed line indicates 1 to 1 line.

In order to further evaluate the model performance, we compared observed and simulated bottom soil DOC concentrations, for which no separate calibration was performed. A first comparison was made for simulations using the default parametrisation of JULES-DOCM and unique PFT for each observation site. Results showed a consistent underestimation in modelled bottom soil DOC, with no significant correlation between observed and simulated values ($R^2$ value of 0.08, p=0.209). The final calibration configuration yielded a slightly more significant correlation between modelled and observed subsoil DOC concentrations ($R^2$ value of 0.13, p=0.108) (Fig. S3).

## DOC leaching

Although we retained only small rivers in the analysis, in which the DOC concentrations should be closely related to that of the runoff, such comparison is not straightforward as model results do not account for potentially important in-stream sources of DOC by, e.g. litter decomposition, or sinks of DOC by decomposition. Simulations also ignore the distinct DOC dynamics in saturated soils along the riparian zone, which may hamper an accurate reproduction of river DOC fluxes.

Nevertheless, our results show that the simulated DOC leaching flux show a fair correlation ($r^2$ of 0.58 and p-value of 0.01) and only slightly underestimate the observed fluvial DOC exports, mainly due to the lower runoff in the simulations compared to measured discharges (Fig. S4).

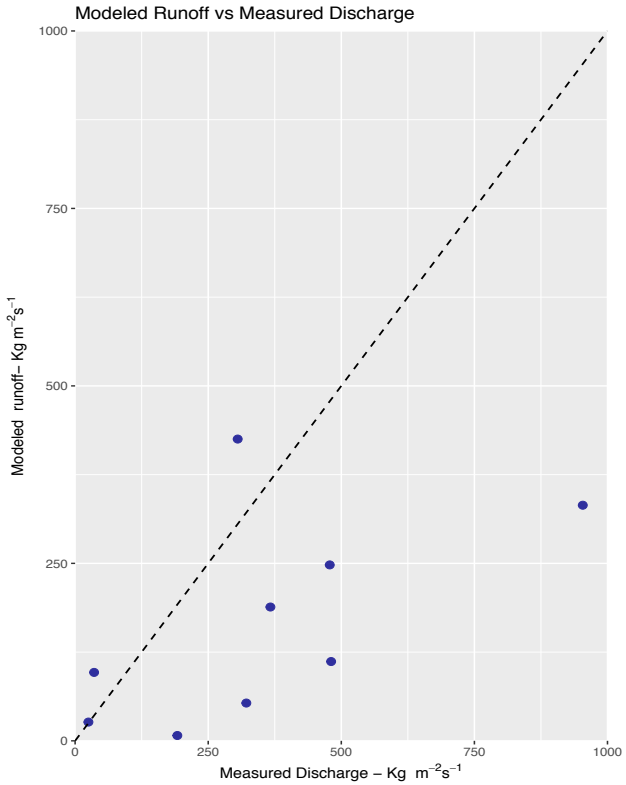


**Figure S4.** Comparison of modelled runoff against measured discharge from GloRiCh data (units in Kg $m^{-2}$ $s^{-1}$)

## Global distribution of soil DOC stock & concentration and DOC leaching

Using the optimised, PFT-specific values for the DOC production and decomposition parameters, we performed global simulations to estimate the global top-soil DOC stock (top 35 cm) and in the bottom soil column (35cm to 3 meters) (Fig. S5). Our estimates are slightly different when using the WATCH forcing data or when using the two-alternative parametrisation, i.e. the second-best combination of $K_{DOC}$ and $K_P$ and the application of the recalibrated $K_{DOC}$ and $K_P$ to the remaining not calibrated PFTs based on apparent physiological similarities (cf. last subsection of methodology) (Table S7).

a)

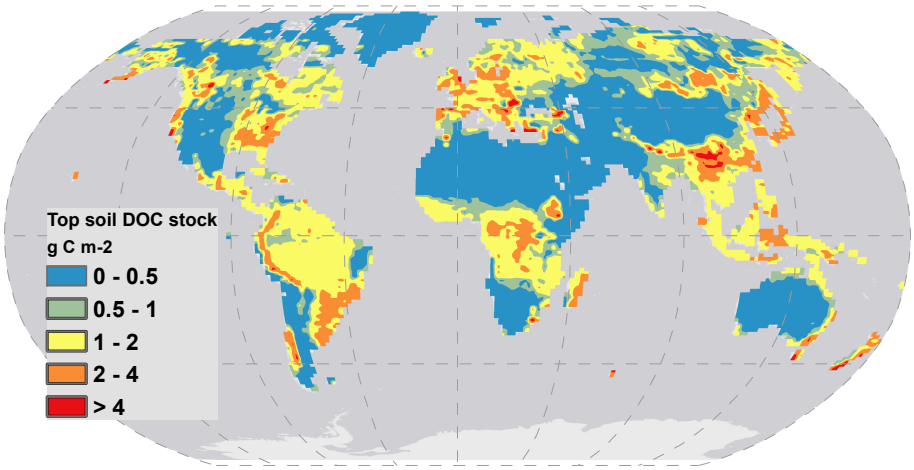


b)

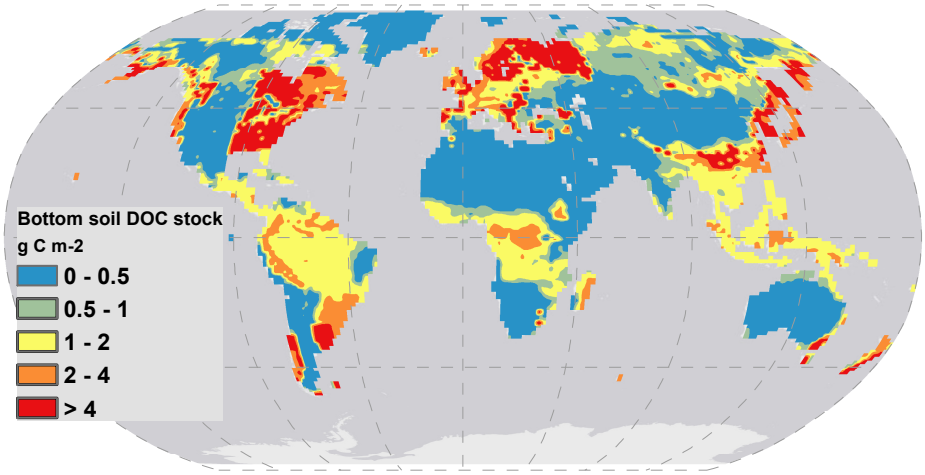


**Figure S5.** Global map of soil DOC stock at a) top b) bottom soil layers.

**Table S3.** DOC concentration and fluxes, precipitation and runoff fluxes

| | Averaged SOC/DOC stock | | | Averaged DOC leaching flux |
|---|---|---|---|---|
| | TOTAL SOC (Kg C $m^{-2}$) | TOP DOC stock (g C $m^{-2}$) | TOTAL DOC stock (g C $m^{-2}$) | Flux (g C m-2 yr-1) |
| Boreal | 9.3 | 0.75 | 2.15 | 0.69 |
| Temperate | 12.2 | 1.3 | 3.5 | 1.76 |
| Tropic | 7.2 | 1.45 | 2.9 | 4.78 |
| Sub-tropic | 3.4 | 0.5 | 1.15 | 0.71 |

**Table S4.** DOC production, decomposition and leaching rate per major climate zones

| | DOC production/decomposition | | | | |
|---|---|---|---|---|---|
| | DOC production (g C $m^{-2}$ $yr^{-1}$) | DOC decomposition (g C $m^{-2}$ $yr^{-1}$) | DOC leaching divided production | decomposition | NPP |
| Boreal | 3.13 | 1.17 | 23.07 | 61.51 | 0.31 |
| Temperate | 8.46 | 3.29 | 20.5 | 52.03 | 0.28 |
| Tropic | 24.77 | 9.85 | 19.34 | 48.68 | 0.37 |
| Sub-tropic | 4.32 | 1.77 | 16.48 | 39.82 | 0.26 |

**Table S5.** Production ratio ($K_{prod}$), decomposition ratio ($K_{dec}$), leaching ratio ($K_{leach}$) and residence time ($\tau_{DOC}$) per major biomes

| | Kpd-avg | Kd-avg | Kh-avg | rt-avg |
|---|---|---|---|---|
| Boreal | 0.30 | 0.63 | 0.30 | 0.93 |
| Temperate | 0.69 | 1.30 | 0.48 | 0.69 |
| Sub-tropic | 1.28 | 2.19 | 0.28 | 0.51 |
| Tropic | 3.17 | 3.34 | 1.54 | 0.23 |

**Table S6.** DOC stock in top and total soil and DOC leaching per major climate zones

| | DOC concentration bottom | DOC concentration top | DOC concentration in flux | avg. precipitation | total. precipitation | avg. runoff | total runoff |
|---|---|---|---|---|---|---|---|
| Boreal | 8 | 18 | 7.23 | 403.57 | 12058.24 | 108.48 | 3415.78 |
| Temperate | 4 | 40.5 | 10.74 | 752.73 | 21882.81 | 198.83 | 5644.36 |
| Tropic | 13 | 40 | 9.89 | 1801.3 | 62324.58 | 615.65 | 21380.6 |
| Sub-tropic | 8 | 19 | 4.33 | 460.43 | 28694.8 | 72.82 | 4569.87 |

**Table S7.** Simulation results by using WATCH and CRU_NCEP with default, second best model parameter set and parameter set for all PFTs

| |
|---|
| WATCH |
| Top/total stock (Pg C $year^{-1}$) = 0.108 ; 0.22 |
| Top/Bottom concentration (mg C $L^{-1}$) = 28.64 ; 3.1 |
| CRU_NCEP default parameter set |
| Top/total stock (Pg C $year^{-1}$) = 0.142 ; 0.34 |
| Top/Bottom concentration (mg C $L^{-1}$) = 26.03 ; 7.62 |
| CRU_NCEP with 2nd best guess parameter set |
| Top/total stock (Pg C $year^{-1}$) = 0.170 ; 0.43 |
| Top/Bottom concentration (mg C $L^{-1}$) = 30.89 ; 10.19 |
| CRU_NCEP with parameter set for all PFTs |
| Top/total stock (Pg C $year^{-1}$) = 0.154 ; 0.37 |
| Top/Bottom concentration (mg C $L^{-1}$) = 29.04 ; 8.60 |

Using WATCH forcing, simulated top and total soil DOC stock are 0.11 Pg C and 0.22 Pg C, respectively, while DOC concentration averages 28.64 mg C L-1 in the top-soil and 3.1 mg C L-1 in the bottom-soil. Using CRU-NCEP with the second-best parameter set or the recalibrated parameters to all PFTs, the top soil DOC stock is estimated at 0.17 Pg C or 0.15 Pg C and the total DOC stock is estimated at 0.43 Pg C or 0.37 Pg C, respectively. Average DOC concentration is 30.89 and 29.04 mg C L-1 in top soil and as 10.19 and 8.60 mg C L-1 in bottom soil for second best parameter set and the application of recalibrated parameters to all PFTs, respectively. These difference between simulations indicate the need for more soil DOC measurements covering the broad range of climate and vegetation types to narrow down estimates.

Finally, we studied environmental factors that could have an impact on the spatial variability of DOC stocks in top soil. From all the studied factors, soil moisture, NPP and SOC stocks had the highest correlation with top soil DOC stock ($r^2$ of 0.24, 0.42 and 0.48 respectively) (Fig. S6). Although runoff had a high correlation with the DOC leaching flux (Fig. S7), it did not show a significant correlation to DOC stocks.

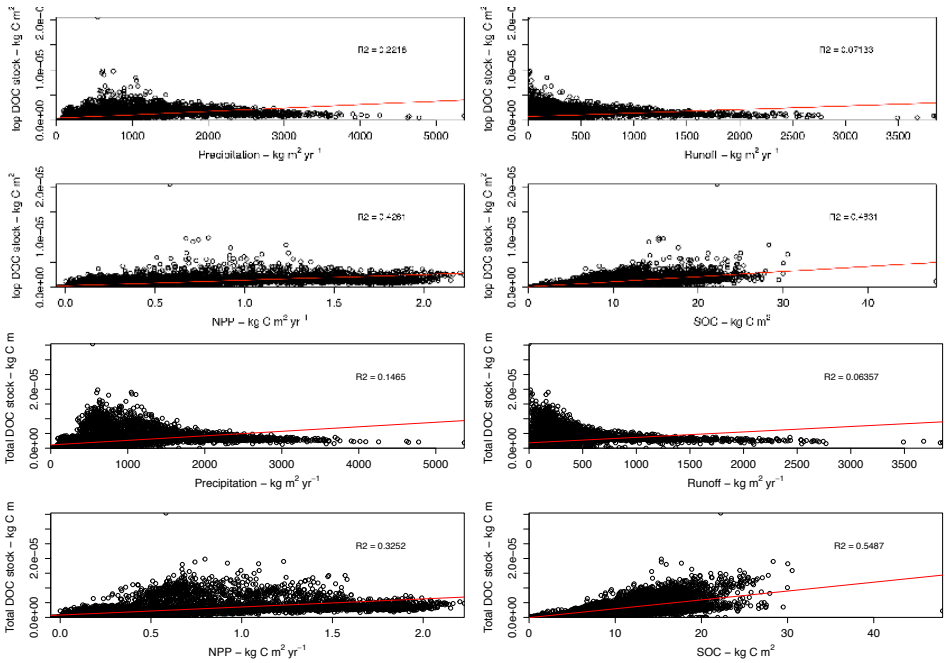


**Figure S6.** Top and total soil DOC stock vs environmental controllers for individual grid cells

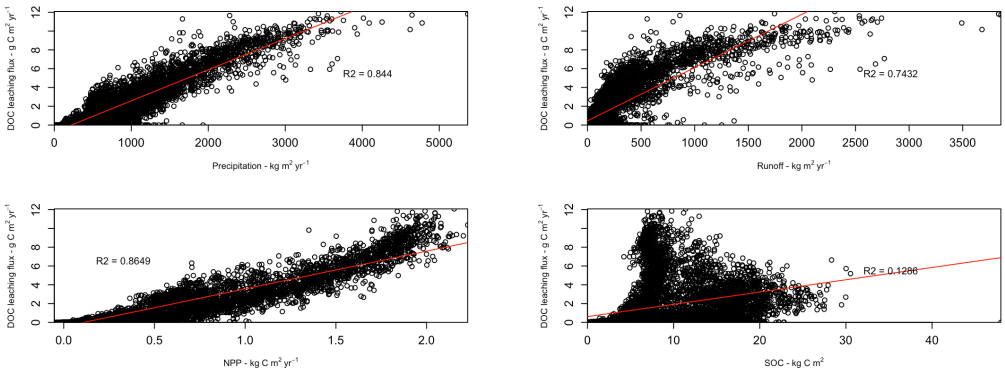


**Figure S7.** DOC leaching flux vs environmental controllers for individual grid cells

A multiple linear regression analysis confirmed that SOC is the main control of the spatial variations in soil DOC stocks (Table S8), NPP and soil moisture only adding little explanatory power. We thus conclude that the correlation between NPP or soil moisture and DOC is mainly due to the correlation of those variables with SOC.

However, closer inspection reveals that all regions of high DOC stocks correspond to regions of high SOC stocks. The most important are Western Europe and the Eastern part of North America, significant portions of South-East Asia, and for the Southern Hemisphere, New Zeeland, Eastern Australia and a portion of South America under subtropical to temperate climate. However, the converse is not true, and large portions of the globe with high to very high SOC stocks have low DOC stocks. This feature is most prominent in the broad boreal

region (most of Canada and Russia), but is also observable in arid parts of temperate to subtropical North America and Asia.

**Table S8.** Multiple linear regression of total DOC vs environmental controllers

multiple linear regression

| | r2 |
|---|---|
| Total DOC stock vs smcl*+npp+soc | 0.6174667 |
| Total DOC stock vs npp+soc | 0.6170734 |
| Total DOC stock vs smcl+soc | 0.596213 |
| Total DOC stock vs smcl+npp | 0.3429866 |

* smcl = soil moisture

In our soil DOC model, the DOC stock is equal to the product of the SOC stock times the dimensionless ratio of the time constants $K_{prod}/(K_{leach}+K_{dec})$. This dimensionless ratio (Figure S8f) is comprised between 0.06 and 1.5 per grid-cell and is lowest in the boreal region (0.36 on average) while the tropics and subtropics overall show highest values (0.68 and 0.59, respectively). Although there are some local exceptions, the temperate region is characterized by intermediate values (0.45). Therefore, the latitudinal pattern in $K_{prod}$ can also be observed in the dimensionless ratio $K_{prod}/(K_{leach}+K_{dec})$, but the variation is now significantly smaller (about a factor of 2). This result can be explained by the concomitant increase in $K_{dec}$ and $K_{leach}$ from high to low latitudes, the time constants scaling to temperature and runoff (Figure 3d), respectively.

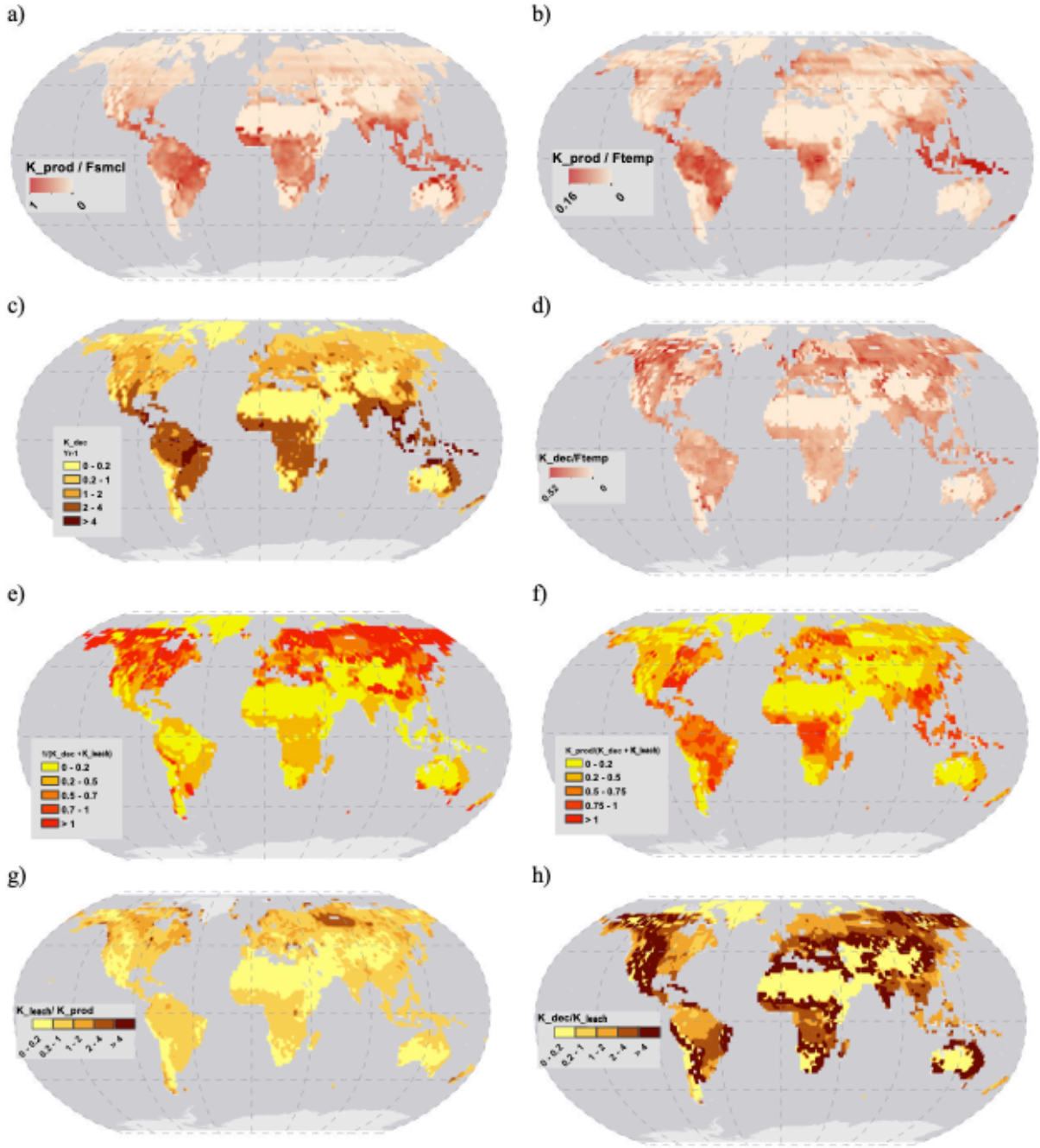


**Figure S8.** a) effect of temperature and b) moisture on DOC production, c) DOC decomposition time constant, d) effect of temperature on decomposition, e) residence time, f) production over loss terms, g) leaching over production rate and h) decomposition over leaching rate

# Chapter 3

# Chapter 3 - Historical trend of lateral export of dissolved organic carbon from soil to river system

This chapter presents historical trend of DOC transported from the soil to the river system, studying environmental changes impact on DOC stocks and leaching fluxes at the global scale and will be submitted to Global Biogeochemical Cycles soon.

## Abstract

Dissolved organic carbon (DOC) represents a significant proportion of terrestrial carbon inputs to aquatic ecosystem (Meybeck, 1993; Ludwig, Probst and Kempe, 1996; Harrison, Caraco and Seitzinger, 2005; Dai *et al.*, 2012), fuelling inland water net-heterotrophy and $CO_2$ emission (Battin *et al.*, 2008) and facilitating fluvial transfers of heavy metals (Ravichandran, 2004). It was shown that these C fluxes are non-negligible in the simulation of the contemporary terrestrial and oceanic C budget (Regnier *et al.*, 2013). Here we used the process based terrestrial ecosystem model JULES-DOCM to simulate spatial-temporal trends in DOC inputs from soil to the river system from 1860 to 2010 at global scale, quantifying the impacts of major environmental drivers such as $CO_2$ fertilization, climate and land use change. We estimated a global increase in terrestrial DOC inputs of 42 Tg C from 1860 to 2010, with a present day flux of 292 Tg C $yr^{-1}$. At the global scale, $CO_2$ fertilization of vegetation was identified as the main controller of increased DOC flux (due to increased biomass and hence soil carbon), with a smaller impact from climate and still smaller from land use change. Most of the DOC export originated from tropical ecosystems, increasing from 152 to 173 Tg C $yr^{-1}$ over the historical period, also primarily due to the increase in atmospheric $CO_2$. In the temperate and boreal zones, the role of climate change becomes increasingly important. Contrary to general assumptions, we find that land use changes only play a minor role in driving the changes in DOC leaching.

# 1. Introduction

The inland water network connects the terrestrial and oceanic systems in the global C cycle, but inland waters are at the same time biogeochemical reactors in which allochthonous C primarily fixed by terrestrial ecosystems is fuelling a strong net heterotrophy and net-emission of $CO_2$ to the atmosphere. The amounts of C exported from terrestrial ecosystems into the inland water network have so far only coarsely been estimated by closing a budget based on observed fluvial C exports to the coast and the still poorly constrained estimates of inland water $CO_2$ evasion and C burial in aquatic sediments (Battin *et al.*, 2008; Regnier *et al.*, 2013). The representation of lateral C exports will arguably help to improve the representation of soil C cycling and its response to climate change, land-use change and atmospheric $CO_2$ increase (Ciais *et al.*, 2013). Ignoring those exports has so far likely been compensated by an overestimation of heterotrophic soil respiration and/or C accumulation in the soil (Jackson, Banner and Jobbágy, 2002; Janssens *et al.*, 2003), potentially biasing future simulations of climate-C feedbacks.

DOC represents about 20% of the fluvial C export to the oceans (Dai *et al.*, 2012), but its proportion on the terrestrial C inputs into inland waters is likely higher (Nakhavali *et al.*, 2019) because of its higher reactivity compared to particulate organic C (POC), and which is thus a major contributor to the net-heterotrophy of inland waters and related $CO_2$ evasion(Battin *et al.*, 2008). An increase in terrestrial export of DOC from soils over the past decades have been described for the UK (Freeman *et al.*, 2001), Northern and Eastern United States (Stoddard *et al.*, 2003), Canada (Bouchard, 1997), Norway (Hongve, Riise and Kristiansen, 2004) and Czech Republic (Hejzlar *et al.*, 2003). Several potential drivers were suggested, which affect soil DOC production as well as soil organic C (SOC) as the primary source of DOC in soils: changes in temperature (Rind *et al.*, 1990; Freeman *et al.*, 2001), the fertilization effects of increasing atmospheric $CO_2$ concentrations (Clair, Ehrman and Higuchi, 1999), precipitation (Hongve, Riise and Kristiansen, 2004) , land use change (Brye *et al.*, 2001) and burning biomass (Clutterbuck and Yallop, 2010). Historical changes in runoff and river discharge have potentially led to changes in the fraction of soil DOC being laterally displaced through the river network(Ledesma, Köhler and Futter, 2012).

As highlighted in previous studies (Regnier *et al.*, 2013; Lauerwald *et al.*, 2017), the lack of empirical data and upscaling techniques leaves process based models as the only tool to assess

the magnitude and dynamics of DOC exports from soil to rivers at regional to global scales. Hence we recently developed a process-based model JULES-DOCM (Nakhavali *et al.*, 2018) for this purpose, which has been calibrated and successfully validated at global scale for present day conditions (Nakhavali *et al.*, 2019). Here, we use this model to simulate the spatio-temporal trends in soil-river DOC fluxes at the global scale over the historical period from 1860 to 2010, attributing temporal changes to the main environmental drivers: $CO_2$ fertilization, climate change and land use change. We highlight the differences in temporal trends and environmental driver attribution in four major climate zones: boreal, temperate, tropical and sub-tropical.

# 2. Methodology

In order to study the historical trend of DOC leaching from soils to the river network, we used the newly developed extension of the JULES land surface model version 4.4, JULES-DOCM(Nakhavali *et al.*, 2018), which additionally represents DOC cycling in the soil and its leaching out of the soil. Recently JULES-DOCM was calibrated and successfully validated to represent DOC stocks and leaching fluxes at the global scale.

For the historical simulation we followed the TRENDY protocol (Sitch *et al.*, 2015) and settings provided for JULES (Harper *et al.*, 2016) at N96 resolution (1.875◦ longitude×1.25◦ latitude). The climate forcing was CRUNCEP version 4 (Harris *et al.*, 2014) spanning from 1860 to 2010. Additionally, the model was forced by data on historical atmospheric $CO_2$ (Dlugokencky and Tans, 2013) and land cover data from HYDE v. 3.1 (Klein Goldewijk *et al.*, 2011).

In order to obtain a steady state for simulated SOC and DOC pools, we used an accelerated spin-up method, which only requires 200 to 300 years of spin-up instead of several thousand years (Harper *et al.*, 2016). In this method the decomposition rate of the most labile litter pool is used for all C pools. This was achieved by scaling the humus, biomass and resistant plant material decomposition rates, based on labile plant material pool, by a factor of 33, 15 and 500, respectively. Then the simulated C pools were rescaled by the same scaling factors. At the end another 300 years spin up with the actual decomposition rate of each pool was performed to reach the equilibrium. Finally, all simulations started in 1860 from an equilibrium state using pre-industrial climate, CO2 and land-cover.

For transient simulation over the historical period, the initial condition was defined by using the final results from steady state spin up. We then ran a transient simulation $S_{ALL}$ with time variant climate, land use and $CO_2$ forcing data. In order to attribute changes in DOC leaching to the three environmental drivers ($CO_2$ fertilization, land use change, climate change) we performed three additional experiments. For this, we ran three alternative simulations with fixed land use ($S_{LUC}$), atmospheric $CO_2$ ($S_{CO2}$), or climate ($S_{CLM}$) forcing. The impact of land use change was then calculated as the difference $S_{ALL}$-$S_{LUC}$, that of atmospheric $CO_2$ increase as $S_{ALL}$-$S_{CO2}$, and that of climate change as $S_{ALL}$-$S_{CLM}$. In order to analyse the temporal trends, we calculated the 10 year running means of the simulations results.

## 3. Results and Discussion

We estimated an average global DOC leaching of 292 Tg C $yr^{-1}$ for present day (2001 – 2010), 24 Tg C $yr^{-1}$ of which in the boreal, 49 Tg C $yr^{-1}$ in the temperate, 46 Tg C $yr^{-1}$ in the sub-tropical and 173 Tg C $yr^{-1}$ in the tropical zone (Table 1). According to our simulation, the average global DOC leaching for period 1861 - 1870 amounted to 250 Tg C $yr^{-1}$ and increased since then by 17%. Considering major climate zones, we simulated the highest relative increase of 28% in boreal zone, followed by an increase of 20% in the temperate zone and the sub-tropical zone, and the lowest percentage increase of 14% in tropical zone (Fig. 1).

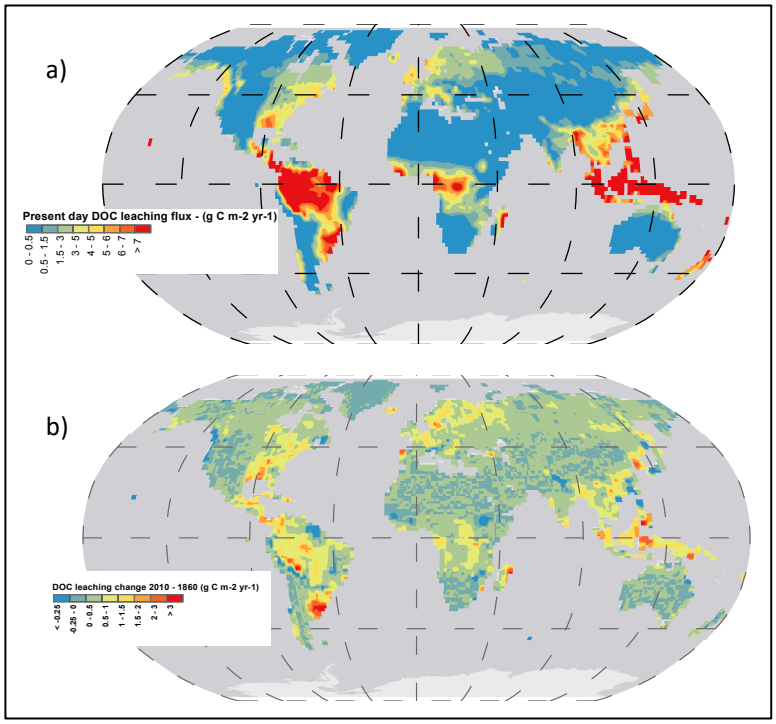


**Fig 1.** Dissolved organic carbon flux at a) present day b) changes from 1860 to 2010 in g C $m^{-2}$ $yr^{-1}$

**Table 1.** Dissolved organic carbon leaching changes

| | **Average 1860s** (Tg C yr-1) | **Average 2000s** (Tg C yr-1) | **Difference 2010s - 1860s** (Tg C yr-1) | **% increase** | **$CO_2$ imp. %** | **CLIM imp. %** | **LUC imp. %** |
|---|---|---|---|---|---|---|---|
| **Global** | 250 | 292 | 42 | 17 | 64 | 23 | 13 |
| **Boreal** | 19 | 24 | 5 | 28 | 30 | 65 | 5 |
| **Temperate** | 41 | 49 | 8 | 20 | 48 | 42 | 10 |
| **Tropics** | 152 | 173 | 21 | 14 | 75 | 10 | 15 |
| **Sub-tropics** | 38 | 46 | 8 | 20 | 60 | 28 | 12 |

Studying the drivers attribution to the DOC leaching, our results identify $CO_2$ fertilization as the strongest control on this increase at the global scale, contributing 64% of total changes (Fig. 2). Climate and land use change had a lower impact of 23% and 13% of total change, respectively (Fig. 3). Analysing the impact of these drivers in each major climate zone reveals significant differences. For the boreal zone, climate change has the highest impact on DOC leaching, contributing 65% of the total increase. This is in line with previous studies that highlighted the dominant role of temperature (Eimers *et al.*, 2008) and river flow (Worrall and Burt, 2007) in terrestrial exported DOC in that zone. A recent study in Sweden showed that increasing runoff is the main reason for the observed increase in DOC leaching (Nydahl, Wallin and Weyhenmeyer, 2017). $CO_2$ fertilization still plays a significant role contributing 30% to the simulated increase, while land use change contributes only 5% and has thus a lower impact on DOC leaching in the boreal zones.

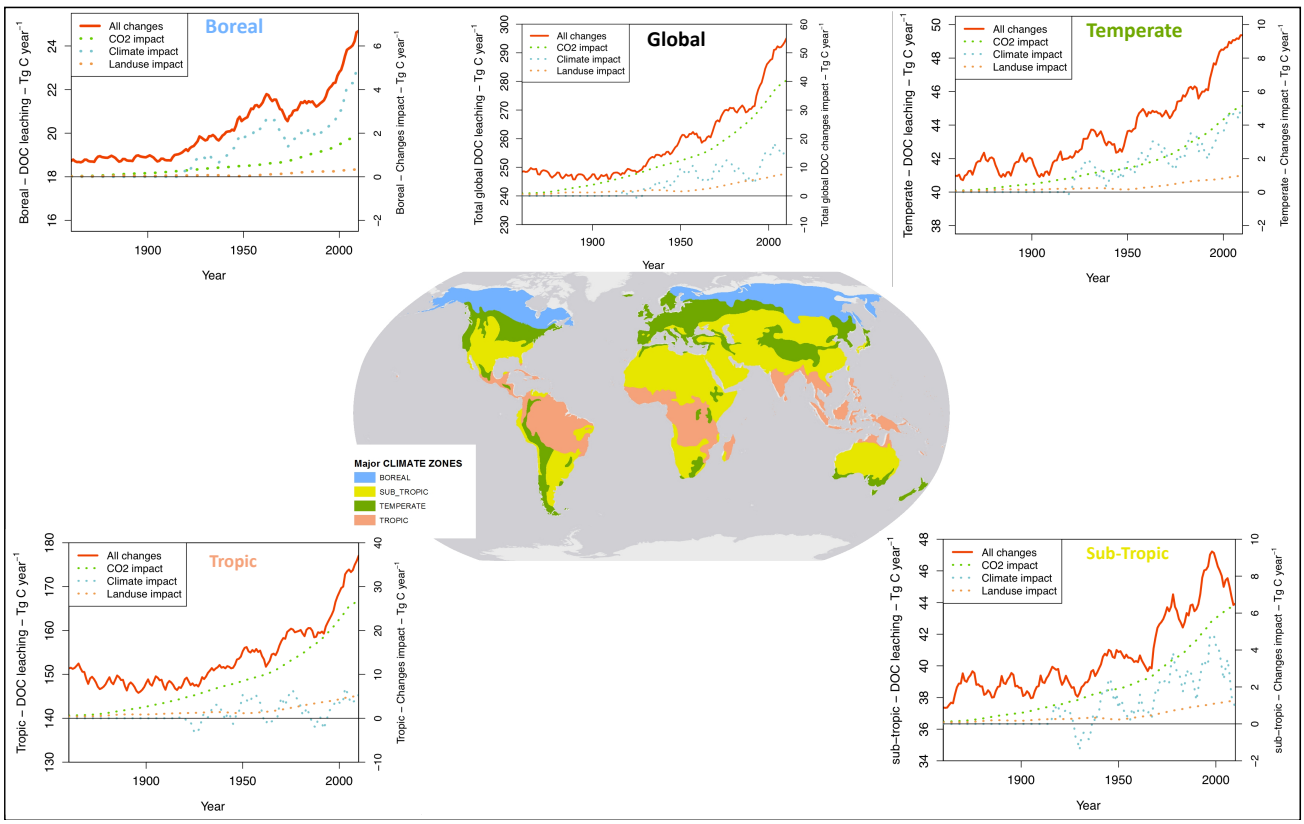


**Fig 2.** Dissolved organic carbon leaching controllers per major climate zones

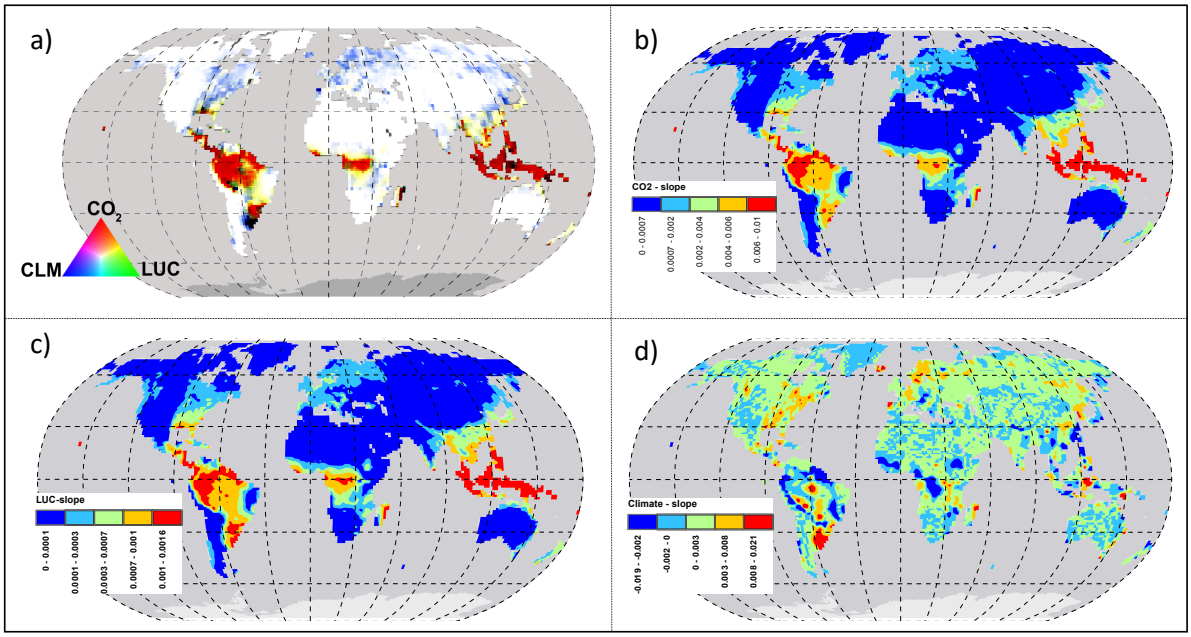


**Fig 3.** Patterns of global change impacts on DOC leaching. (a) Relative contribution of individual environmental drivers. Linear regression slope of impact of (b) atmospheric $CO_2$ increase, (c) impact

of climate change and (d) impact of land use (Linear regression P value of impact of (b) atmospheric CO2 increase, (c) impact of climate change and (d) impact of land use in Figure 4).

For the temperate zone, we simulate a similar impact of $CO_2$ fertilization and climate change which contribute 48% and 42%, respectively, to the increase in DOC leaching, while land use change contributes only 10% of total changes. However, our results shows a good correlation between DOC leaching and change in runoff (r2= 0.38) but no significant correlation between DOC leaching and temperature change (r2 < 0.001). Hence as the climate change impact in both boreal and temperate zones, the increase in runoff is the main control of the increase in leaching. Overall, in temperate regions, DOC leaching is transport limited rather than limited by production or decomposition rates (Nakhavali *et al.*, 2019).

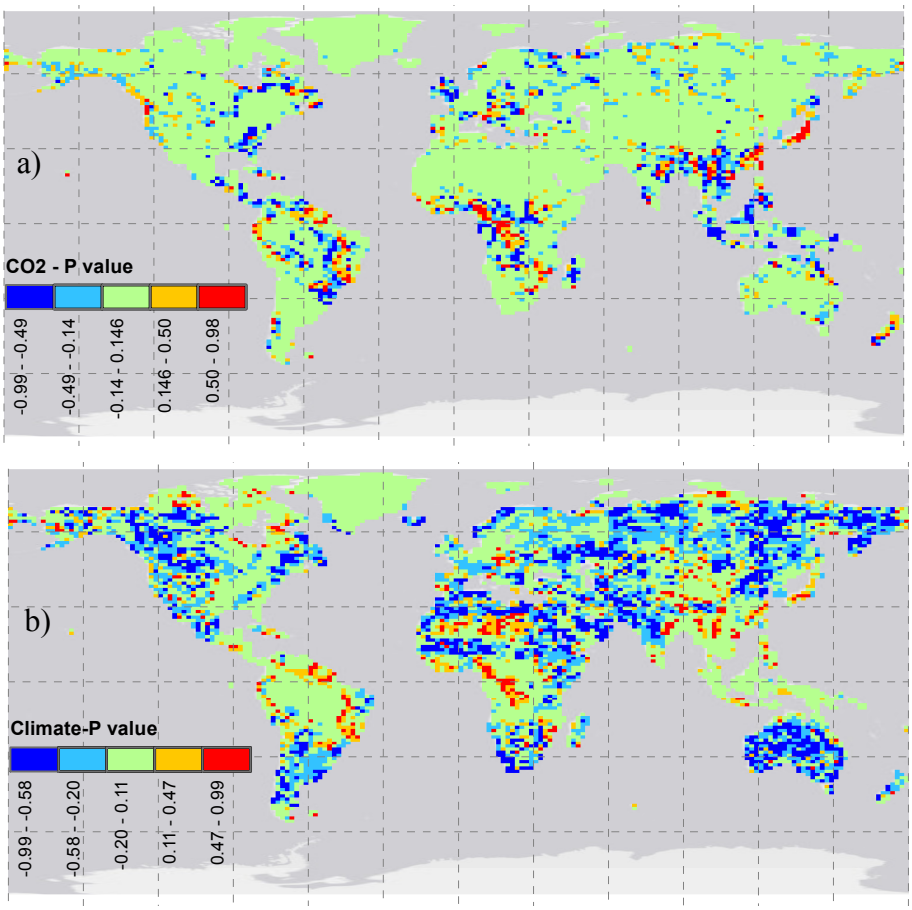

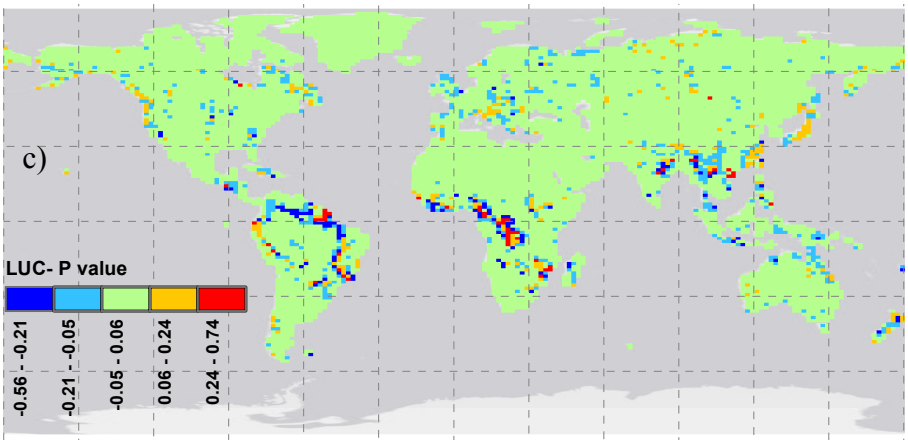


**Fig 4.** Linear regression P value of impact of (b) atmospheric $CO_2$ increase, (c) impact of climate change and (d) impact of land use

For the tropical zone, $CO_2$ fertilization was identified as the main control, contributing 75% of the increase in simulated DOC leaching. Land use and climate changes show a lower impact on tropical zone DOC leaching of respectively 15% and 10% of total changes. The tropical forests have the highest efficiency of C sequestration among other terrestrial ecosystems and capability of storing larger amounts of C in vegetation (Sitch *et al.*, 2003; Hirano *et al.*, 2009), which explains the highest response of the increased DOC leaching to $CO_2$ fertilization in tropical zone (Fujii *et al.*, 2009; Zhou *et al.*, 2016). The results for sub-tropical zone are similar to those of the tropical zone, with $CO_2$ fertilization as main control explaining 60% of the simulated increase in DOC leaching, climate and land use change contributing 28% and 12%, respectively.

However, effect of $CO_2$ and climate can be trusted a priori as they are mainly affecting processes such as production and decomposition/leaching of DOC which were calibrated in model previously (Nakhavali *et al.*, 2019). Regarding the land use change effect, as model only accounts for vegetation transitions and not representing processes such as increased soil erosion following deforestation, we probably underestimating land use change influence on DOC leaching.

We studied the impact of temperature and runoff as the main climate controllers of DOC leaching flux and its change between 1860 and 2010 (Fig. 5) and overall correlations (Fig, 7). The DOC leaching hotspots (Fig 5-c) of changes between this period are in close correspondence with the runoff hotspots (Fig 5-b) ($r^2$=0.38), which indicates runoff as key

influence on the leaching. Despite runoff, temperature shows no correlation with DOC leaching flux ($r^2$=2e-0.4).

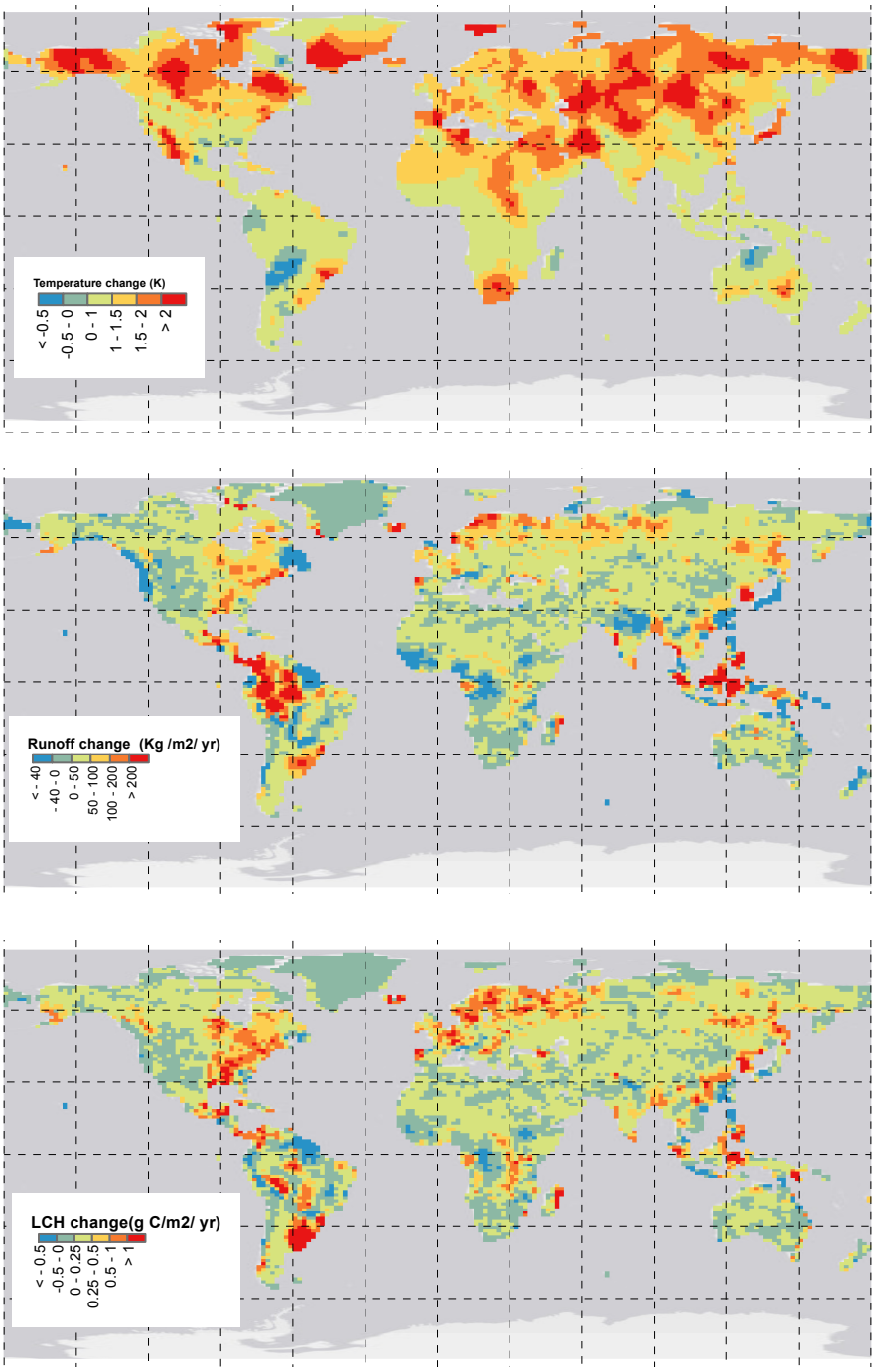


**Fig 5.** Changes between 1860 to 2010 in a) temperature b) runoff c) DOC leaching flux due to climate change

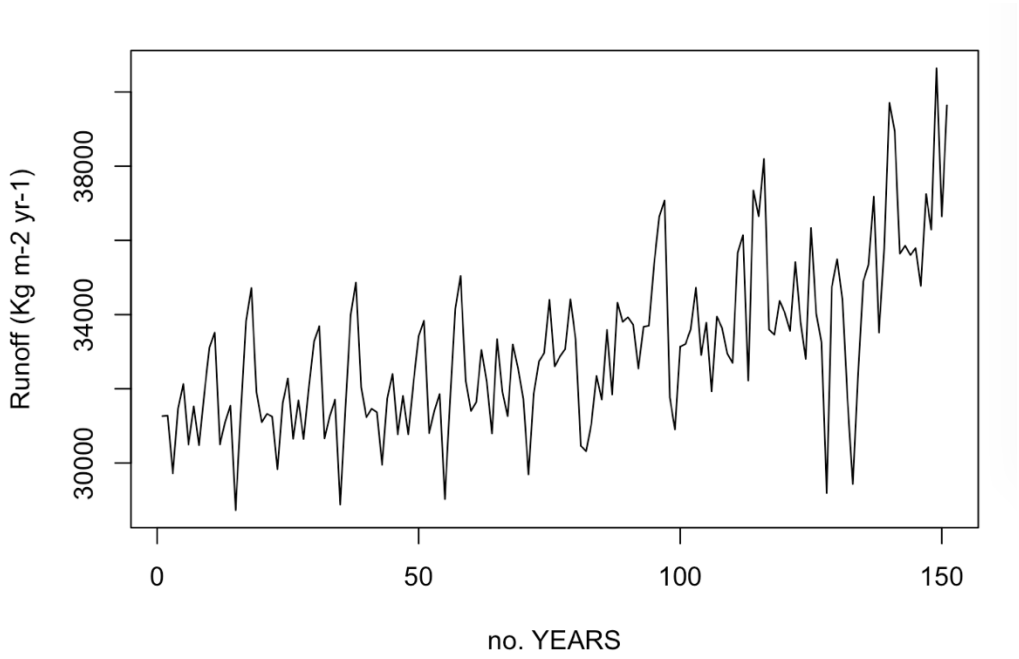


**Fig 6.** Total runoff between 1860-2010

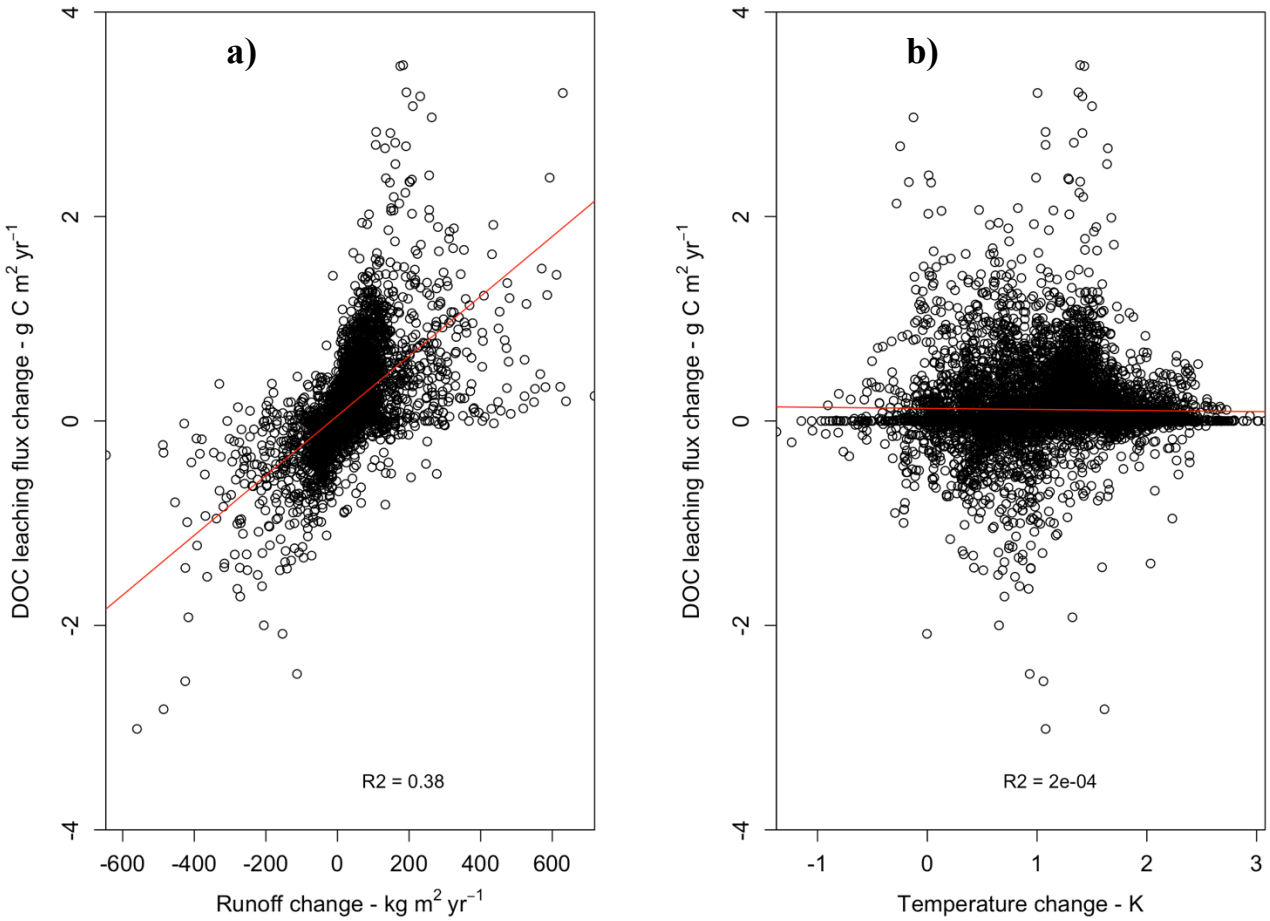


**Fig 7.** DOC leaching flux changes for period 1860 to 2010 due to climate change against a) runoff and b) temperature changes per grid cells.

The soil C dependency on NPP has been already reported (Todd-Brown *et al.*, 2013). Moreover, the DOC loss rate is assumed to be equal to the NPP rate at equilibrium (Kicklighter *et al.*, 2013). We simulated an average present day (2001 – 2010) NPP and soil respiration of 92 Pg C $yr^{-1}$ and 90 Pg C $yr^{-1}$, respectively (Fig. 8), which comparing to the period 1861 – 1870 have increased by 21 Pg C $yr^{-1}$ (+30%) and 19 Pg C $yr^{-1}$ (+26%), respectively. Interestingly, the DOC leaching flux increased by the similar proportion of 17%, and we identified a high spatial and temporal correlation of the DOC leaching flux with NPP ($r^2 = 0.88$) (Fig. 10 and Table 2).

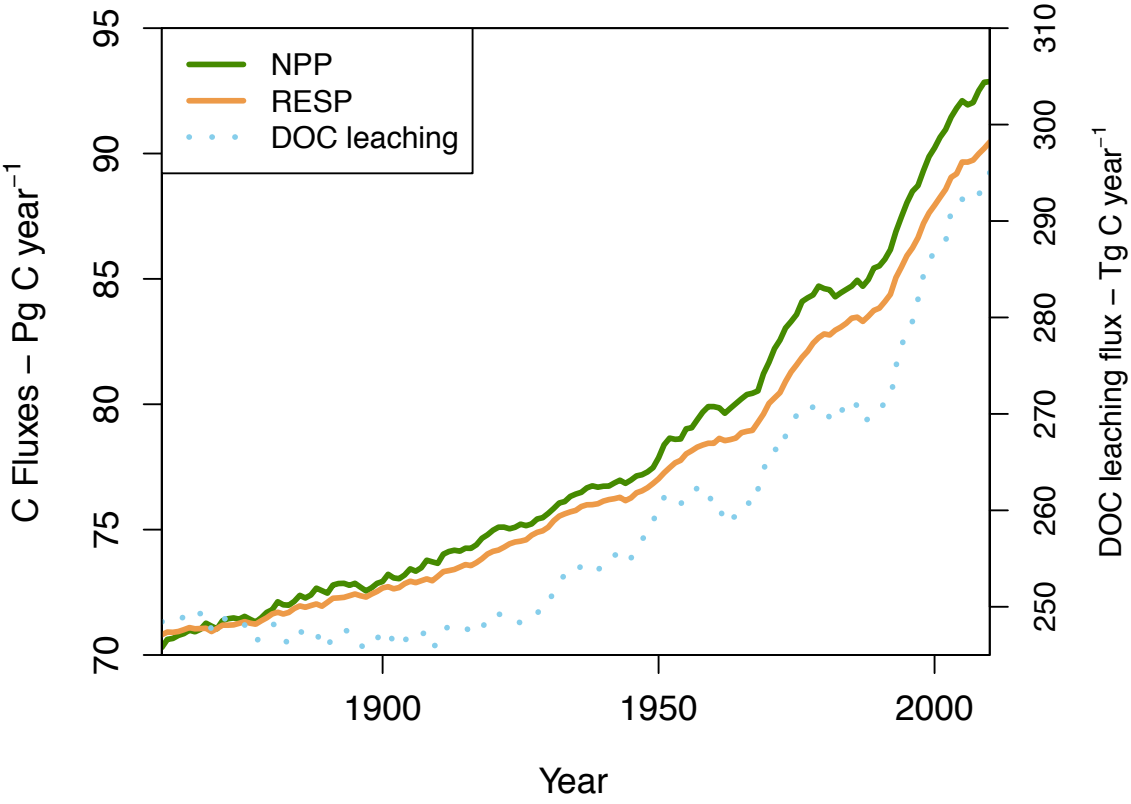


**Fig 8.** C fluxes vs DOC leaching flux

**Table 2.** C fluxes and stocks changes

| | Average 1860s (Pg C yr-1) | Average 2000s (Pg C yr-1) | Difference 1860s:2000s (Pg C yr-1) | % of increase |
|---|---|---|---|---|
| **NPP** | 71 | 91.94 | 20.94 | 29.49 |
| **Resp*** | 71 | 89.65 | 18.65 | 26.26 |
| **DOC LCH*** | 0.24 | 0.29 | 0.042 | 16.82 |
| **SOC stock** | 1014.09 | 1082.32 | 68.229 | 6.72 |
| **DOC stock** | 0.32 | 0.335 | 0.014 | 4.6 |

* resp = soil respiration ; LCH = leaching flux; 1860 – 2010 is calculate by (avg. (2001 to 2010) - avg. (1861 to 1870))

Nevertheless, the percentage of leached NPP from the period 1861-1870 at 0.35% has decreased to 0.31% for the present day (Fig. 9). This is due to the long residence times in biomass and SOC and later effect of decomposition and leaching. Moreover, the increase of DOC leaching is following the same rate as runoff (17%) which indicates the transport limited system of leaching.

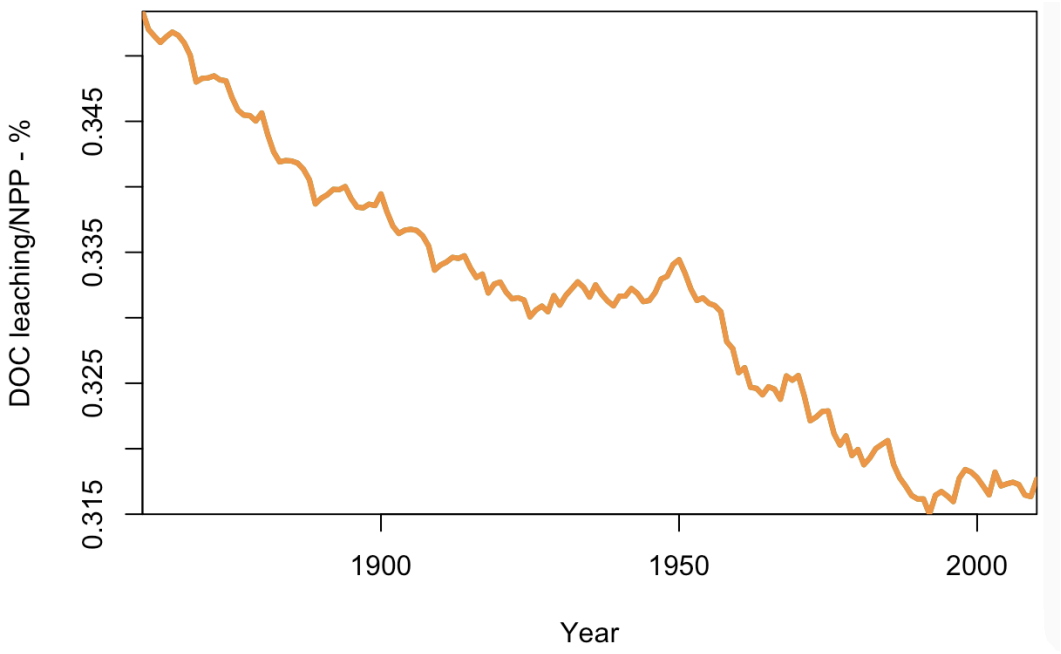


**Fig 9.** Percentage of leached NPP

Moreover, the global SOC and DOC stocks increased by only 7% and 5%, respectively, over the same period. Over the simulation period, top soil (here defined as the upper 35 cm) leaching contributes about 90% to total DOC leaching from soil. However, as it was shown in our previous study (Nakhavali *et al.*, 2019), the top soil layer contains only ~ 40% of total soil DOC stocks. The subsoil DOC stocks receive most of the organic matter through diffusion (Braakhekke *et al.*, 2013). The magnitude of diffusion flux is 0.2 % of DOC leaching flux (averaged total diffusion for period 1860 to 2010 is 0.5 Tg C yr-1). This explains why the change in total DOC stock can be decoupled from the change in DOC leaching: since leaching is mainly related to top soil, total stocks are mainly in the bottom soil, and the exchange between top and bottom soils is slow. NPP increase drives increase in biomass, litterfall, SOC and finally DOC leaching. The increase in NPP entrains a stronger increase in DOC concentrations in the topsoil compared to the subsoil (Guggenberger and Kaiser, 2003), and thus a stronger increase in the DOC leaching flux than in the total soil DOC stock.

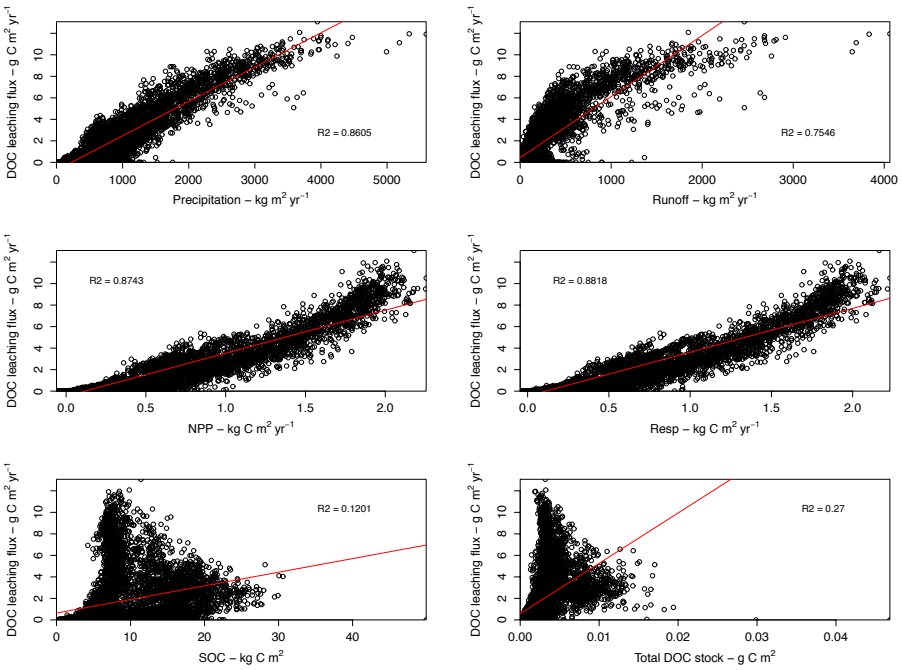


**Fig 10.** Environmental controls on the global spatial pattern of terrestrial DOC export averaged over 2000s.

In addition, we quantified the effect of representing the DOC leaching flux on the simulated SOC and DOC stocks for the periods 1861-70 vs. 2001-10 (Table 3). Results show no significant effect of DOC leaching on the SOC stock for whole period (ca. 0.1 %) but a more significant influence on the DOC stocks (ca. 16%).

**Table 3.** C Stocks changes with DOC leaching flux

| | C stocks | | | |
|---|---|---|---|---|
| | 1861-1870 (Pg C yr-1) | 2001-2010 (Pg C yr-1) | 1860-2010 (Pg C) | % of increase |
| SOC | 1014.0 | 1082.3 | 68.2 | 6.7 |
| DOC | 0.32 | 0.33 | 0.01 | 4.7 |

While we simulate the historical change of DOC exports from soils to the river network, previous studies have simulated the historical change of fluvial DOC transfers at regional scale: for the Arctic rivers (period 1900-2006) with TEM model (Kicklighter *et al.*, 2013), for east coast of the US (period 1901-2008) with DLEM model (Tian *et al.*, 2015) and for Amazon River (period 1861-2005) with ORCHILEAK model (Lauerwald *et al.*, 2017) (Fig. 11).

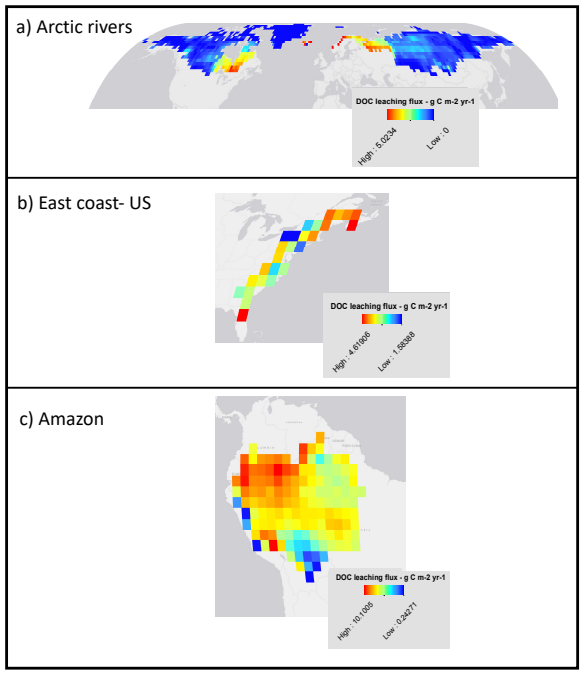


**Fig 11.** Historical DOC leaching flux simulated by JULES at a) Arctic rivers b) East coast US and c) Amazon

Our simulated DOC leaching for the Artic rivers is lower than the simulated riverine flux based on the TEM model (16 Tg C $yr^{-1}$ vs 32 Tg C $yr^{-1}$). This could be due to the missing wetland representation in JULES, hence lower flux from this area (Nakhavali, et al. 2018). Our results for East coast US are slightly higher than that from the DLEM model (4.8 Tg C $yr^{-1}$ vs 2.4 Tg C $yr^{-1}$), which could be due to the negative impact of the land-use on the DOC leaching flux in DLEM model. However, the DOC leaching from soils to rivers will still be higher than the riverine flux simulated by DLEM which indicates that the additional sources of DOC not represented in JULES-DOCM are less important than DOC decomposition in transit. Our result for the Amazon was lower than the ORCHILEAK model (39 Tg C $yr^{-1}$ vs 78 Tg C $yr^{-1}$), which could again be due to the lack of wetlands representation which are of importance in Amazon (Lauerwald *et al.*, 2017), or from different C model formulation, turnover rate, different forcing and hydrology (Table 4).

**Table 4.** Historical DOC leaching flux comparison between JULES-DOC vs other studies

| Model | Period | DOC leaching flux (Tg C $yr^{-1}$) | This study |
|---|---|---|---|
| TEM (Artic Rivers) | 1900-2006 | 32 | 16 |
| DLEM (East Coast US) | 1901-2008 | 2.4 | 4.8 |
| ORCHILEAK (Amazon) | 1861-2005 | 78 | 39 |

# 4. Conclusion

The land C sink is increasing in response to global change, mainly due to the atmospheric $CO_2$ increase. The DOC leaching flux increases as well due to the same reason but at a slightly lower rate. Nevertheless, the C inputs via DOC to inland waters and thus ultimately $CO_2$ emission and C inputs to the ocean have likely increased over that period. Consequently, beside the land C sink of the anthropogenic $CO_2$ emission, an intensification of the global C cycle with increasing fluxes of C from land to ocean and from inland waters to the atmosphere can be expected.

Finally, although we included the well-studied DOC controls such as temperature, precipitation and vegetation in model, still the representations of pH and nutrients are missing. Additionally, current version of model only accounts for vegetation transitions and some processes

representing land use change such as fire and soil erosion following the deforestation are still missing which can have a significant impact on the vegetation and consequently on the C inputs to the soil.

Hence, including these drivers and processes can improve the ability of model to fully represent and predict the temporal and spatial dynamics of soil DOC.

# Chapter 4

# Chapter 4 - Future prediction of global terrestrial transported dissolved organic carbon to the river system

This chapter presents future trend of terrestrial exported DOC to the global river system using three different future scenarios and will be submitted soon to be submitted to Earth System Dynamics.

## Abstract

A fraction of the terrestrial uptake of $CO_2$ is displaced as organic carbon along the terrestrial-aquatic continuum, which represents an important link in the global carbon (C) cycle (Battin *et al.*, 2009; Regnier *et al.*, 2013). These exports are important for the terrestrial C budget, but are hard to assess globally as they are largely only based on empirical methods (Regnier *et al.*, 2013). Leaching of dissolved organic carbon (DOC) from soils to rivers represents an important fraction of this C export, and is assumed to drive a large proportion of the net-heterotrophy of river systems and the related $CO_2$ emissions (Battin et al., 2008). Using our newly developed model JULES-DOCM (Nakhavali *et al.*, 2018), we estimate the present-day DOC leaching flux at 277 Tg C $yr^{-1}$ which is comparable to our previously estimated flux at 292 Tg C $yr^{-1}$ (Nakhavali et al. 2019). In chapter 3, we also estimated that over the historical period, DOC leaching increased by 17%, primarily because of the increase in atmospheric CO2, leading to larger biomass, soil carbon and hence DOC production and leaching. Here we use the same JULES-DOCM model to project future evolution of DOC leaching to the river system at the global scale over the 21$^{st}$ century, following three representative concentration pathways (RCP's), RCP2.6, RCP4.5 and RCP8.5. We simulate the highest increase in DOC leaching under the RCP 8.5 scenario, reaching 395Tg C $yr^{-1}$ by 2100, that is 42% higher than at present-day. In comparison RCP2.6 and RCP4.5 only lead to increase of 10 and 21% respectively. Comparing the results for the boreal, temperate, sub-tropical and the tropical zones, we identify the highest relative increase between present day and end of 21$^{st}$ century in DOC leaching of 50% for the sub-tropical zone using RCP8.5 scenario. For the boreal and tropic zones, we simulate similar increases of 48% and 41%, respectively, but since the tropics have the highest DOC leaching, the magnitude of the increase is actually largest from this zone (+59 Tg C $yr^{-}$

[1]). For the temperate zone, we simulate the lowest relative increase of only 35%, We identified the rising atmospheric $CO_2$ concentration and its fertilizing effect on terrestrial NPP as the main reason for the future increase in DOC leaching.

# 1. Introduction

The lateral transfer of carbon (C) from vegetation and soils to rivers plays a significant role for ecological processes in both the terrestrial and aquatic ecosystem (Aitkenhead and Mcdowell, 2000; Kalbitz *et al.*, 2000). This flux has so far only poorly been estimated based on a budget calculation involving the riverine C exports to the coast and estimates of $CO_2$ emissions from inland waters and C burial in aquatic sediments. Global estimates range between 1.9 to 2.7 Pg C $yr^{-1}$ (J J Cole *et al.*, 2007; Tranvik *et al.*, 2009; Regnier *et al.*, 2013), which is about 2-5% of terrestrial NPP (Regnier *et al.*, 2013). However, ignoring this flux when projecting the response of terrestrial C budgets to anthropogenic $CO_2$ emissions may lead to an overestimation of C accumulation in soils or soil heterotrophic respiration(Jackson, Banner and Jobbágy, 2002; Janssens *et al.*, 2003). The representation of this flux in Earth System Models (ESM) would be an important step towards improved projections of global C cycling and its interaction with climate (Ciais *et al.*, 2013). At the same time, an accordingly upgraded ESM would be the ideal tool to project future changes in lateral C exports from soils in response to global change, and its effect on the terrestrial C budget.

Leaching of dissolved organic carbon (DOC) from soils to rivers represents an important fraction of this C export, and is assumed to drive a large proportion of the net-heterotrophy of river systems and the related $CO_2$ emissions (Battin et al., 2008). As the soil organic carbon (SOC) is the main source of DOC in the soil, drivers that affect SOC are potential controls of the long-term evolution of the DOC leaching flux. These drivers are climate related, such as temperature(Rind *et al.*, 1990; Freeman *et al.*, 2001) and precipitation(Hongve, Riise and Kristiansen, 2004), atmospheric $CO_2$ (Clair et al. 1999) and land-use change(Brye *et al.*, 2001). In addition, the DOC leaching flux is strongly controlled by hydrology, which determines which fraction of the DOC in the soil column is exported with runoff, and which fraction of the DOC is left to be decomposed within the soil column.

Recently, we developed a process-based model, JULES-DOCM (Nakhavali *et al.*, 2018) which simulates C budgets of terrestrial vegetation and soils, explicitly representing the cycling of DOC within the soil column and the leaching of DOC from the soil into the river network. This

model has been successfully applied to obtain an estimate of present-day soil DOC stocks and DOC leaching fluxes at the global scale (Nakhavali et al. 2019a) and to reconstruct the spatio-temporal evolution of the DOC leaching flux over the historical period (Nakhavali et al. 2019b).

In this study, we use the model to project the spatio-temporal evolution of DOC leaching fluxes over the 21st century following the three representative concentration pathways (RCPs), RCP 2.6 (Van Vuuren *et al.*, 2007), RCP 4.5 (Clarke *et al.*, 2007) and RCP 8.5 (Riahi, Grubler and Nakicenovic, 2007). We analyse how DOC leaching will respond to the different aspects of global change, i.e. increasing atmospheric $CO_2$ levels, climate change and land use change, and we localize the expected hotspots of future change in DOC leaching.

# 2. Methodology

In order to study the future evolution of DOC leaching from soils at the global scale we used the newly developed extension of Joint UK Land Environment Simulator (JULES) (Clark *et al.*, 2011) version 4.4, JULES-DOCM (Nakhavali *et al.*, 2018). In JULES-DOCM, vegetation is represented by the TRIFFID model in nine distinct plant functional types (PFT's) (Harper *et al.*, 2016) and soil C processes are defined by the RothC model(Jenkinson *et al.*, 1990) down to three meters, and SOC stocks are distributed over four soil layers (0-10cm, 10-35cm, 35-100cm and 100-300cm) assuming an exponential decay in concentration with depth (Jobbágy and Jackson, 2000). All the C related processes such as production, decomposition, ad/desorption are calculated for each of these layers. The leaching of DOC is calculated based on simulated DOC concentrations and runoff. This export flux is defined for the top soil (0-35cm) by means of surface runoff and for the bottom soil (35-300cm) by means of sub-surface runoff.

The calibrated global version of JULES-DOCM was tested successfully (Nakhavali et al. 2019a) and used for studying the historical trend of DOC leaching for the historical period (1860-2010) (Nakhavali 2019b). Here we study the response of DOC and leaching to future environmental changes, following three RCP scenarios (2.6, 4.5 and 8.5). The number for each RCP represents the increase in radiative forcing level from 1750 to 2100, as 2.6 W $m^{-2}$, 4.5 W $m^{-2}$ and 8.5 W $m^{-2}$. Each of these scenarios were produced by different Integrated Assessment Models (IAMs): RCP 2.6 by Integrated Model to Assess the Global Environment (IMAGE)

(Van Vuuren *et al.*, 2007), RCP 4.5 by MiniClimate Assessment Model (MiniCAM) (Clarke *et al.*, 2007) and RCP 8.5 by Model for Energy Supply Alternative and their General Environmental Impact (MESSAGE) (Riahi, Grubler and Nakicenovic, 2007).

The RCP 2.6 scenario includes the highest level of mitigation. This scenario considers the lowest energy use and dependency on fossil fuels, assumes the highest shift in energy supply to biofuels and high advances in technologies regarding C capture and storage, which result in a $CO_2$ emission reduction. Hence the atmospheric $CO_2$ in 2050 is at 443 ppm and decreases down to 421 ppm in 2100. The RCP 4.5 is the intermediate scenario which relies more on fossil fuels compared to RCP 2.6, but considers some sources of cleaner energy and possibility of C capture and storage. In this scenario, the atmospheric $CO_2$ is at 487 ppm in 2050 and will reach 538 ppm in 2100. The RCP 8.5 scenario represents a lack of mitigation before 2100 and the lowest advances in C capture and storage technologies. It includes the highest dependency on fossil fuels and highest level of $CO_2$ emission resulting in the accelerated increase in atmospheric $CO_2$ from 541 ppm in 2050 to 936ppm in 2100 (Moss *et al.*, 2010).

In terms of forcing for JULES-DOCM, we used the climate forcing for historical (1860-2005) and future (2006-2100) period following three RCP scenarios (2.6, 4.5 and 8.5) produced by the HadGEM2-ES model (Martin *et al.*, 2011) at N96 resolution (1.875◦ longitude×1.25◦ latitude). We also prescribed the land use change, using crop and pasture cover data from HYDE version 3.1 (Klein Goldewijk *et al.*, 2011) for the historical period, and according to each RCP for the future. Last, atmospheric CO2 forcing was taken from historical observations (Dlugokencky and Tans, 2013) and directly from the RCPs for the future (Meinshausen *et al.*, 2011).

In order to start transient simulations from pre-Industrial SOC and DOC pools in a steady state, we used the accelerated spin-up method in JULES (Harper *et al.*, 2016), explained in our historical study (chapter 3, and Nakhavali 2019). The initial condition for the transient simulation over the historical period was defined by the final outputs of the spin-up. For each of the RCP scenarios, we ran the model over the whole simulation period from 1860 to 2100, collating historical and the respective future climate forcing data. All results were analysed for temporal trends based on 10 year running means.

Finally, in order to study the atmospheric $CO_2$ influence and its fertilization effect on terrestrial NPP and DOC leaching flux, we ran the simulation with deactivated atmospheric $CO_2$ change for all three future scenarios, while the other changes were kept activated. Additionally, in

order to study land use change impact on DOC leaching flux, we ran a simulation with deactivated land use change for all three scenarios. The impact of land use change was then calculated as the difference transient run ($S_{ALL}$)- land use deactivated run ($S_{LUC}$), and atmospheric $CO_2$ increase as $S_{ALL}$- deactivated atmospheric CO2 change run ($S_{CO2}$).

# 3. Results and discussion

We estimated the global DOC leaching flux for the present day (1995-2004) at 277 Tg C $yr^{-1}$, with 142 Tg C $yr^{-1}$ being contributed by the tropical, 56 Tg C $yr^{-1}$ by the temperate, 52 Tg C $yr^{1}$ by the sub-tropical and 27 Tg C $yr^{-1}$ by the boreal zone. Note that in this study by using HadGEM2-ES, the present day flux is within 5% of our previous estimate based on CRU-NCEP climate forcing (chapter 3 and Nakhavali 2019). For comparison of present-day finding with this chapter, we reported the chapter 3 and current study present-day flux in Table 1.
However, this present-day flux is already significantly higher than the simulated flux for pre-industrial period (1860s) of 243 Tg C $yr^{-1}$. Until the end of the 21$^{st}$ century (2090-2099), we simulate the highest increase in global DOC leaching of 43% (395 Tg C $yr^{-1}$) when using RCP 8.5. RCP 4.5 and RCP 2.6 lead to lower simulated increase of 22% (335 Tg C $yr^{-1}$) and 10% (306 Tg C $yr^{-1}$), respectively (Fig. 1). A similar effect of the selected RCP on the simulated increase in DOC leaching flux can be seen for each of the four climate zones (Table. 1).

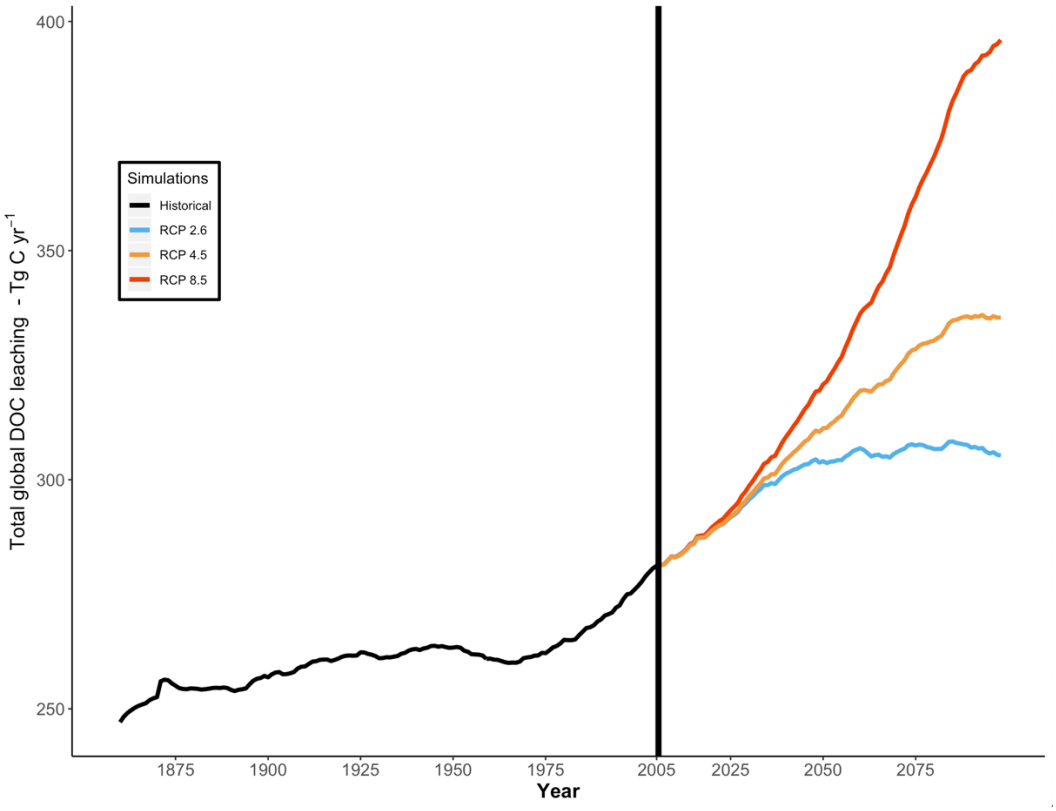


**Fig 1.** Historical and future dissolved organic carbon leaching

The highest increase in DOC leaching was simulated for the sub-tropic zone (50% for RCP 8.5), followed by the boreal zone (48.2% for RCP 8.5) and tropic (41.6% for RCP 8.5), while the temperate zone shows the lowest simulated increase (35.8% for RCP 8.5). The ranking of relative increase per climate zone is the same for all RCPs (Table 1).

**Table 1.** Dissolved organic carbon leaching in each major climate zone

| | **Average 2000s** | | **Average 2090s** | | |
|---|---|---|---|---|---|
| **Averaged DOC leaching ( Tg C yr$^{-1}$)** | Historical *(HadGEM)* | Historical *(CRUNCEP)** | RCP 2.6 | RCP 4.5 | RCP 8.5 |
| **Global** | 277 | 292 | 306 | 335 | 395 |
| **Boreal zone** | 27 | 24 | 36 | 37 | 40 |
| **Temperate zone** | 56 | 49 | 63 | 67 | 76 |
| **Tropic zone** | 142 | 173 | 146 | 164 | 201 |
| **Sub-tropic zone** | 52 | 46 | 61 | 67 | 78 |

*(Nakhavali, 2019)

In our previous study, we showed a strong correlation between the historical increase in DOC leaching and terrestrial NPP(Nakhavali, 2019). Here we simulate an increase in NPP from a pre-industrial value of 69 Pg C $yr^{-1}$ to a present-day flux of 83 Pg C $yr^{-1}$. Projecting the terrestrial NPP for the period 2090-2099, we simulate values of 138 Pg C $yr^{-1}$, 104 Pg C $yr^{1}$ and 89 Pg C $yr^{-1}$ following the RCP scenarios 8.5, 4.5 and 2.6, respectively (Fig. 2). Similar to our historical study, the future DOC leaching flux showed the highest spatial-temporal correlation with the NPP flux in all RCP scenarios ($R^2$ value: 0.8) (Fig 3), which is consistent between historical and different future scenarios. This is to be expected as the studies showed the high dependency of soil carbon stocks on NPP (Todd-Brown *et al.*, 2013). Consistent with our results for the increase in DOC leaching, we simulated the highest relative increase in NPP in the boreal and sub-tropic zones and the lowest in the tropical zone (Fig 4).

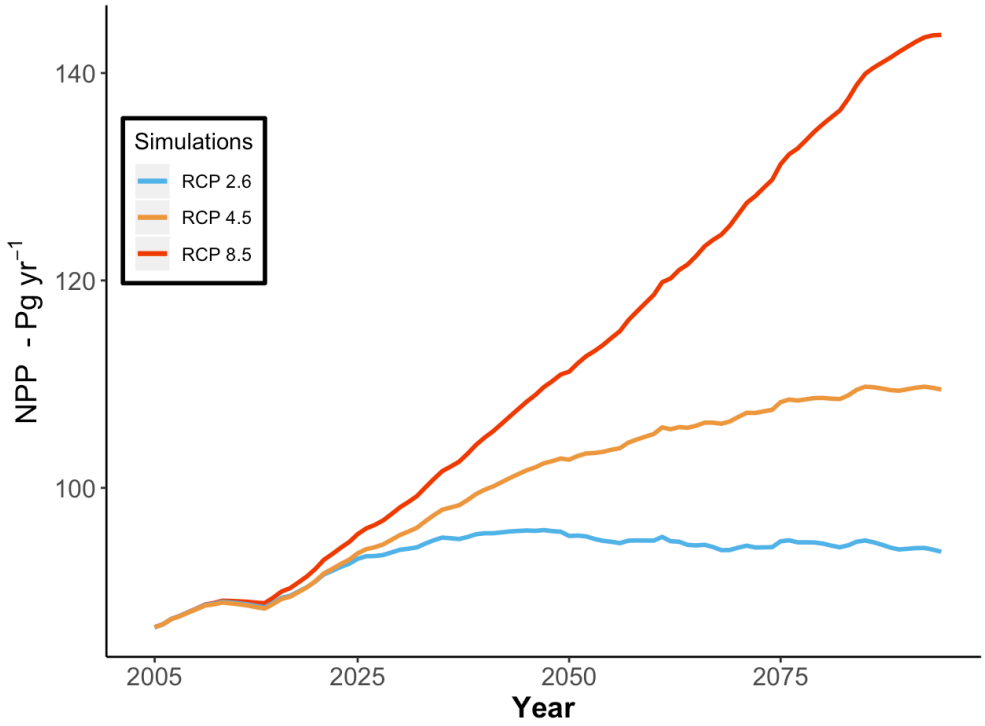


**Fig 2.** Global NPP change based on three RCP scenarios

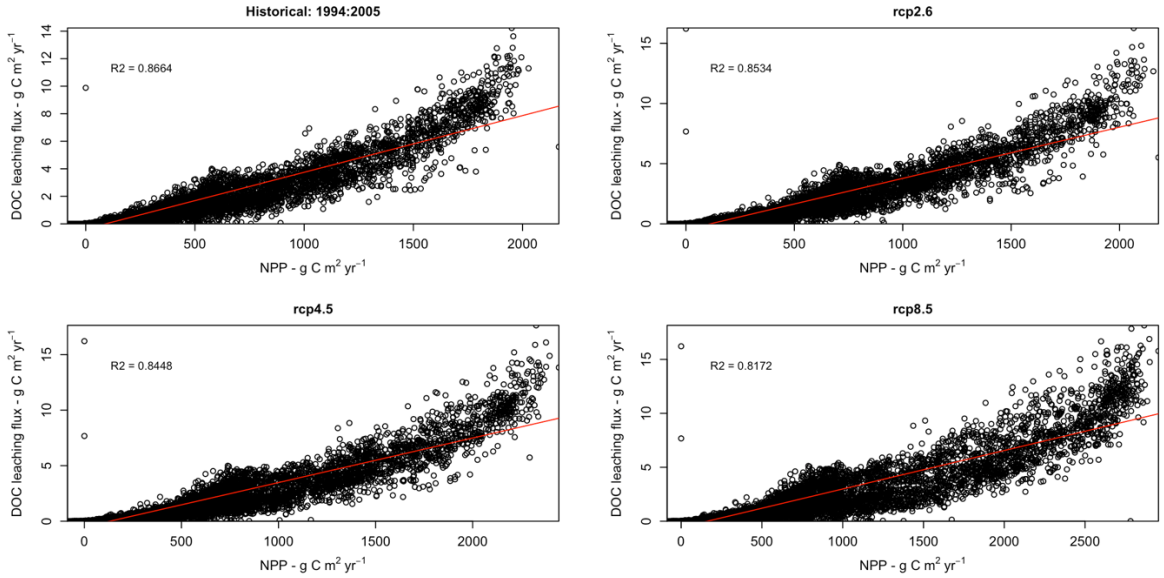


**Fig 3.** NPP vs DOC leaching flux (g c $m^2$ $yr^{-1}$) for historical period (1994:2005) and three RCP scenarios (2090s)

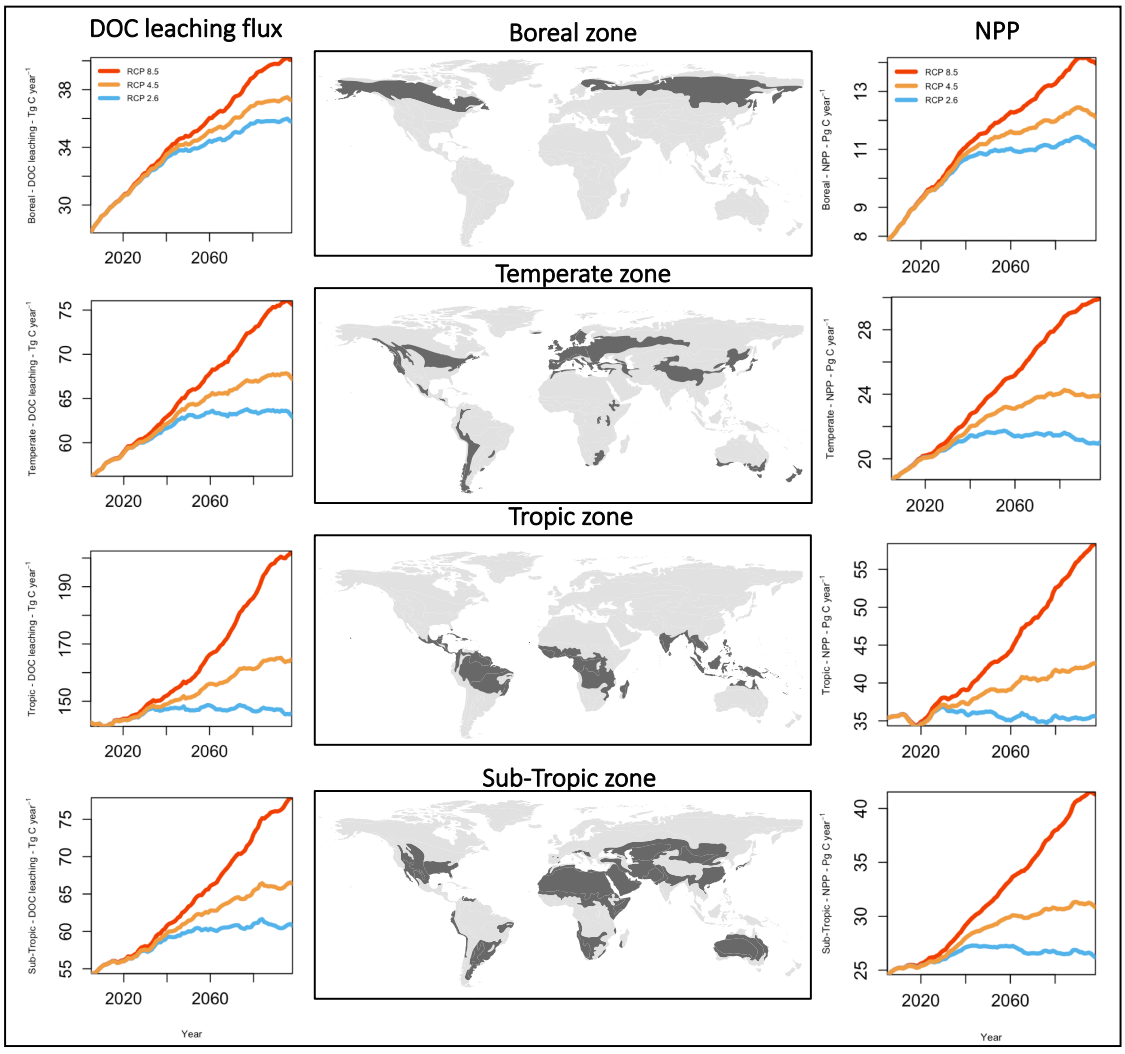


**Fig 4.** Future dissolved organic carbon leaching flux and NPP in each major climate zone.

Moreover, our results show a change in SOC and DOC stocks from present day (1995-2004) to the end of the 21st century (2090-2099) based on three RCP scenarios. The global SOC stock increased by 4%, 11% and 23% using RCP 2.6, 4.5 and 8.5, respectively which is driven by litterfall changes following the NPP changes. Similarly, DOC stocks showed an increase of 6%, 8% and 13% using RCP 2.6, 4.5 and 8.5, respectively (Table 2), driven by the SOC changes.

**Table 2.** Historical and future C fluxes and stocks

| | **Average 1860s** | **Average 2000s** | | **Average 2090s** | |
|---|---|---|---|---|---|
| | Historical | | RCP 2.6 | RCP 4.5 | RCP 8.5 |
| **Avg. NPP** (Pg C/yr) | 69 | 83 | 89 | 104 | 138 |
| **Avg. RESP** (Pg C/yr) | 69 | 81 | 88 | 101 | 130 |
| **Avg.DOC LCH**(Pg C/yr) | 0.24 | 0.27 | 0.31 | 0.34 | 0.4 |
| **Avg. SOC** (Pg C) | 900 | 955 | 993 | 1062 | 1181 |
| **Avg. DOC** (Pg C) | 0.2 | 0.255 | 0.27 | 0.275 | 0.289 |

After NPP, precipitation showed the highest spatial-temporal correlation with DOC leaching flux ($R^2$ value: 0.8) (Fig. 5). This significant correlation is consistent between future scenarios and historical runs. As soil moisture is one of the key DOC production modifiers in our model, water balance in the soil as precipitation and drainage is determining the soil DOC concentration. Additionally, precipitation is the main controller of runoff in our model, and the transport of DOC from soil to the river is controlled by this flux (Nakhavali *et al.*, 2018). This can explain why the correlation between DOC leaching and precipitation higher than runoff (Fig. 6). Nevertheless, the fairly well correlation between runoff and DOC leaching flux is not changing between historical and future scenarios.

At the global scale, the spatial pattern of changes in runoff (Fig. 7b) coincides with those of changes in NPP (Fig. 7a) which leads to strong hotspots of increase in DOC leaching (Fig. 7c).

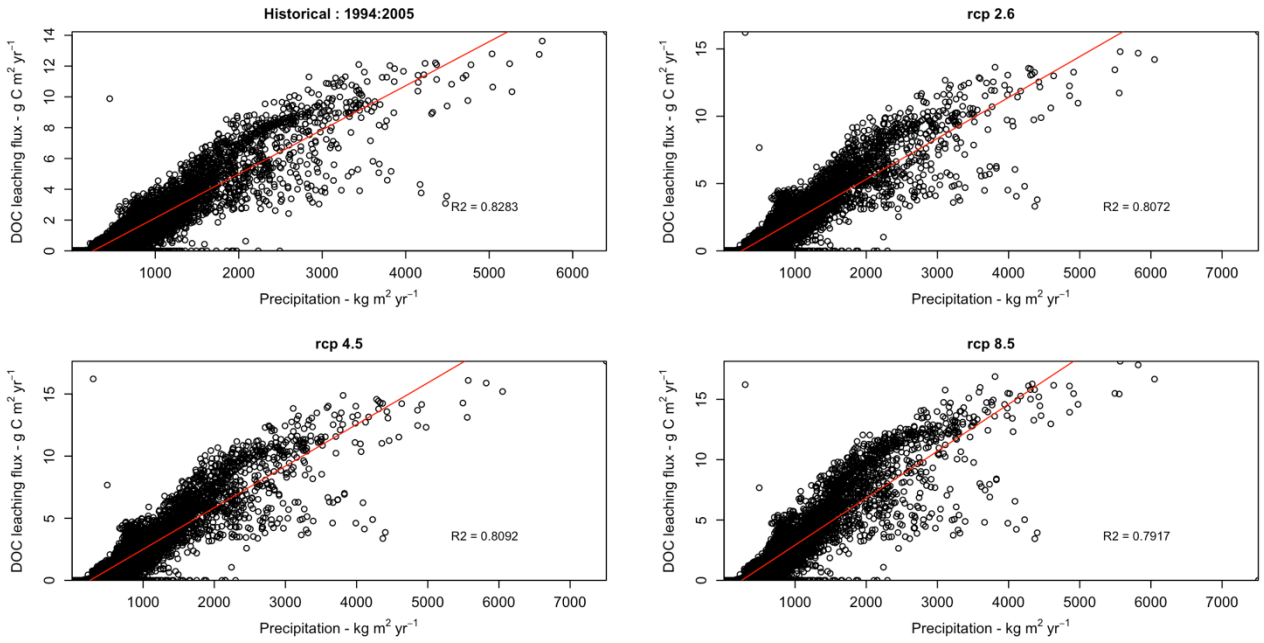


**Fig 5.** Precipitation (Kg $m^2$ $yr^{-1}$) vs DOC leaching flux (g c $m^2$ $yr^{-1}$) for historical period (1994:2005) and three RCP scenarios (2090s)

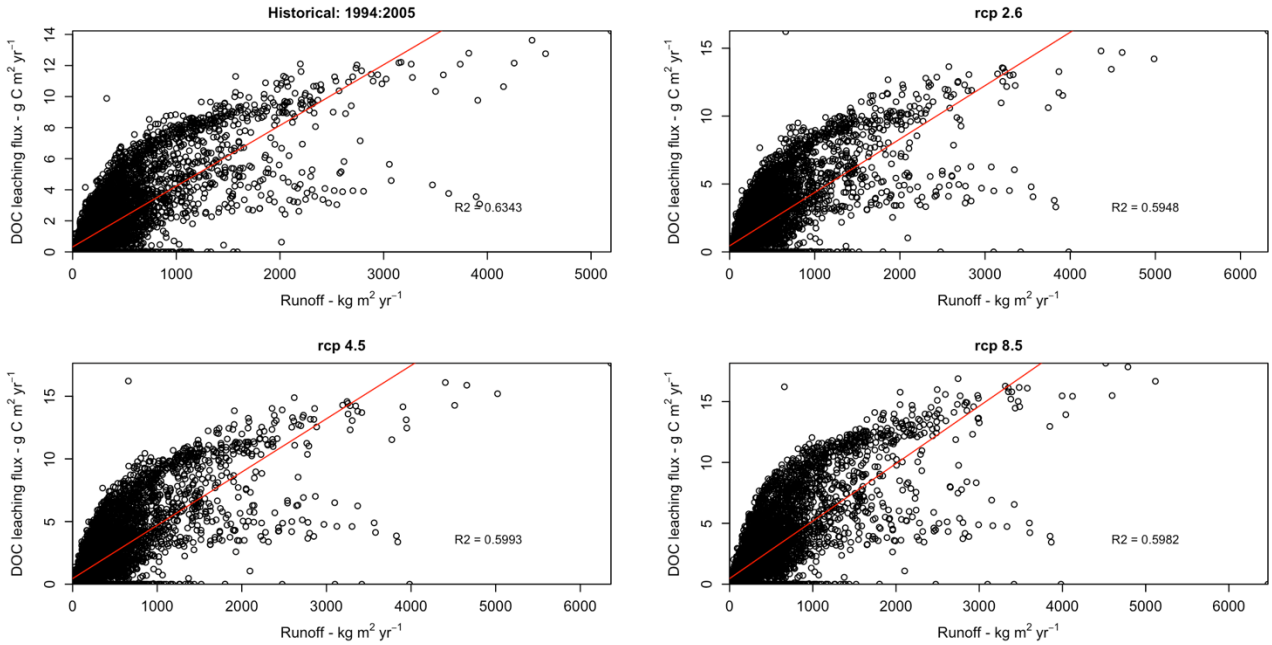


**Fig 6.** Runoff (Kg $m^2$ $yr^{-1}$) vs DOC leaching flux (g c $m^2$ $yr^{-1}$) for historical period (1994:2005) and three RCP scenarios (2090s)

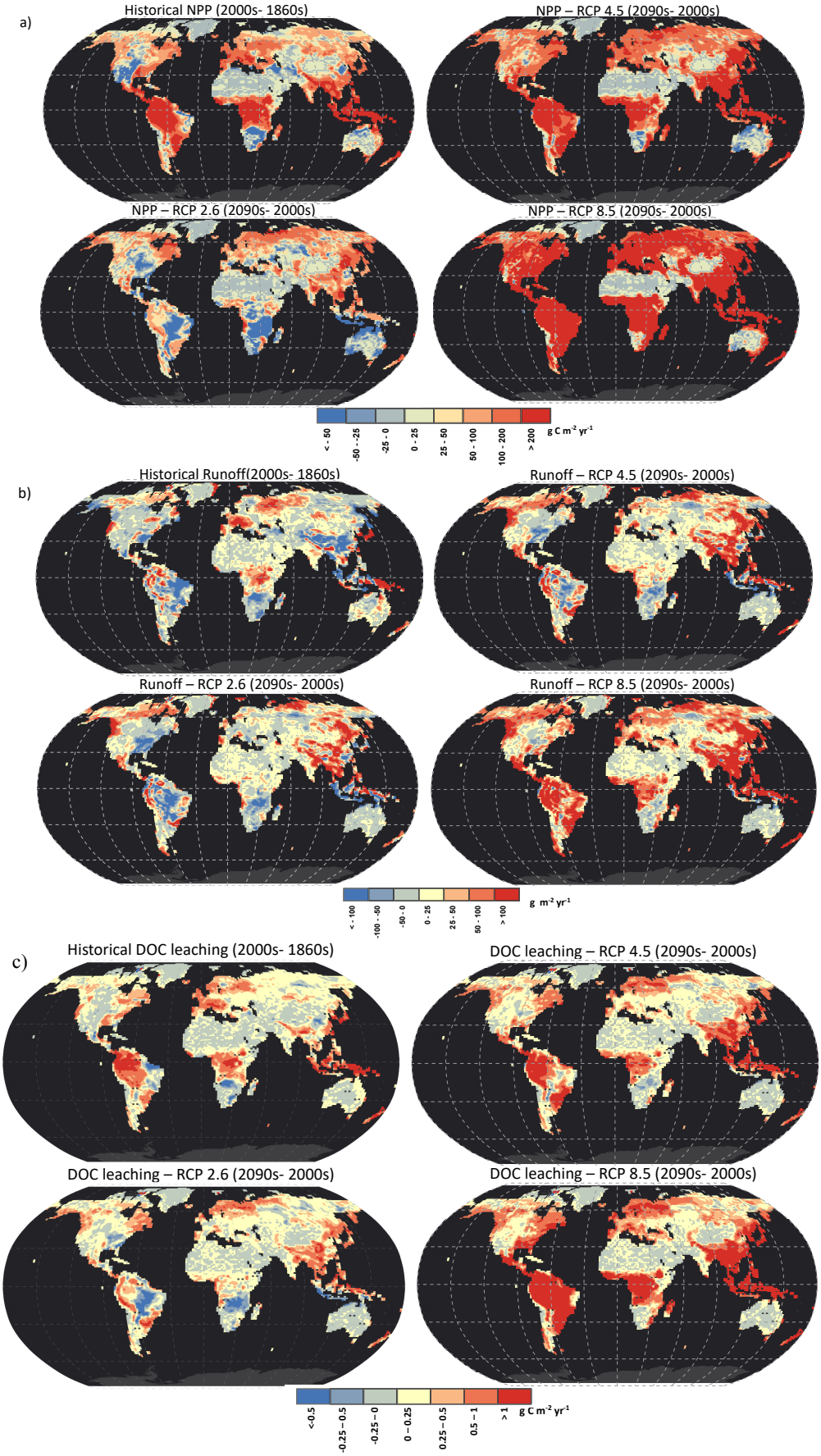


**Fig 7.** Historical and future prediction of changes in a) NPP (g C $m^{-2}$ $yr^{-1}$) b) Runoff (g $m^{-2}yr^{-1}$) c) DOC leaching (g C $m^{-2}$ $yr^{-1}$)

As for the historical result, regions that are hotspots of DOC leaching include SE Asia, the Amazon basin, New-Zealand, Western Europe and large portions of the Eastern part of North America. These patterns are similar between RCP 2.6 and historical with decrease in Africa and amazon basin and increase in China. Nevertheless, RCP 4.5 and 8.5 shows the similar patterns of increase, where the increase in West Russia, amazon basin and East US is more larger in RCP 8.5.

We calculated the ratio of transported NPP through DOC leaching flux. This ratio is not changing significantly for present day to the end of the 21$^{st}$ century by 0.34%, 0.32% and 0.28% following RCPs 2.6, 4.5 and 8.5 respectively. Nevertheless, the percentage of leached NPP for RCP 4.5 and 8.5 has decreased. This is due to the long residence times in biomass and SOC and later effect of decomposition and leaching for these two scenarios.

Finally, we simulated the DOC leaching flux with deactivated land-use change for all three RCP (Fig. 8). Additionally, we also run our model with deactivated atmospheric CO2 change for all future scenarios (Fig. 8-9).

Results from RCP 2.6 scenario runs using fixed land use change showed no major difference from runs with fixed land use setup for period 2090 to 2099. However, CO2 fertilisation has the largest impact on DOC leaching flux (70 Tg C yr$^{-1}$). Similar to RCP 2.6, results from RCP 4.5 showed no significant impact of land use change, but a main controlling impact CO2 increase on DOC leaching (98 Tg C yr$^{-1}$). Results from RCP 8.5 for period 2090 to 2099 showed a positive impact of both CO2 fertilisation and land-use change, with a main controlling impact of $CO_2$ fertilization (171 Tg C yr$^{-1}$) and smaller impact of land use change (4 Tg C yr$^{-1}$). However, the small increase in DOC from land use change is in line with our historical analysis (Nakhavali *et al.*, 2019).

Moreover, results show that atmospheric CO2 change is the main controlling effect on terrestrial NPP on DOC leaching flux in all three RCP scenarios for the period 2005-2100. Nevertheless, it should also be noted that nitrogen limitation is not included in this version of the model, and this could reduce the strength of the $CO_2$ fertilisation effect.

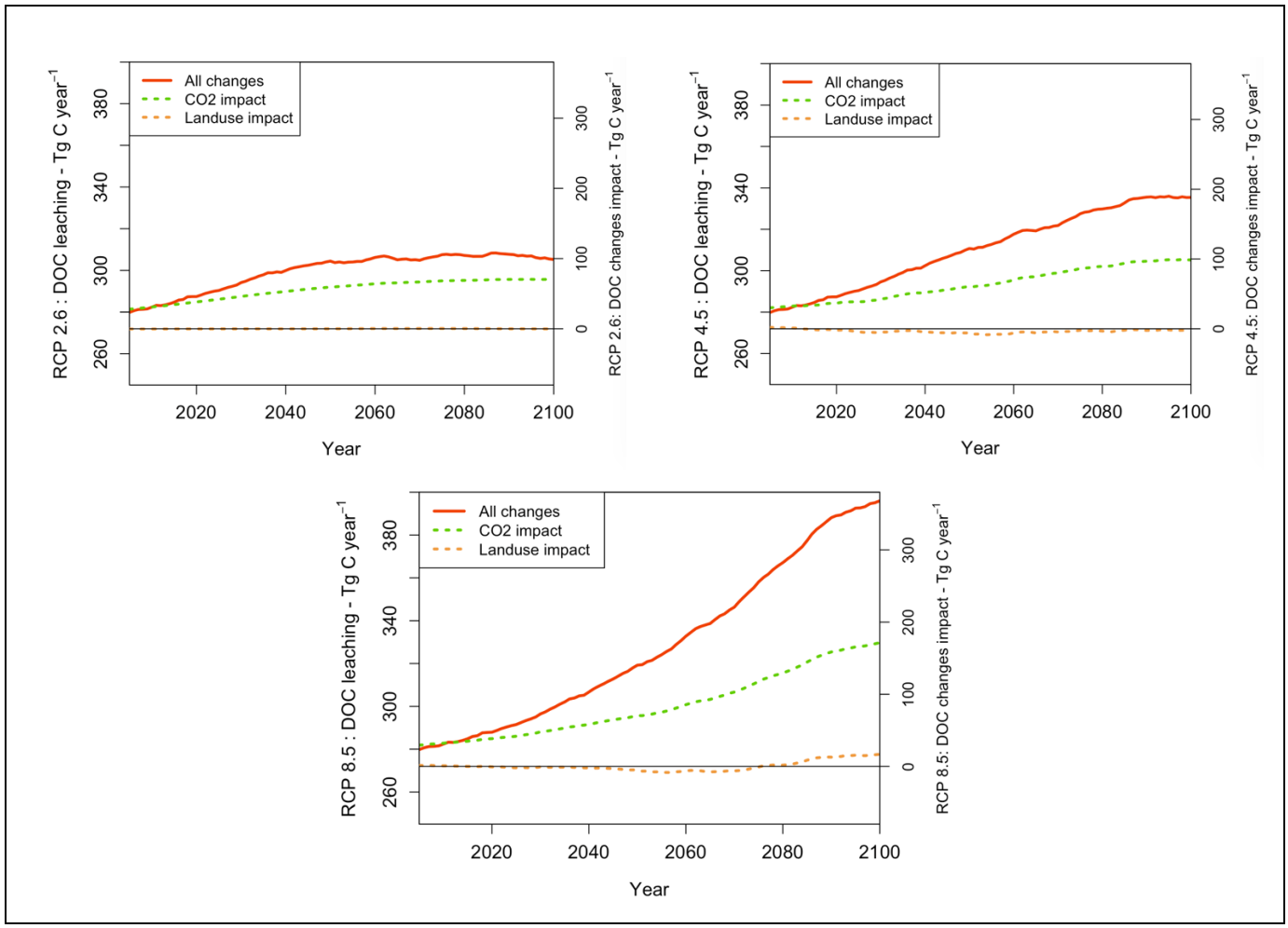


**Fig 8.** Dissolved organic carbon leaching controllers per three future scenarios

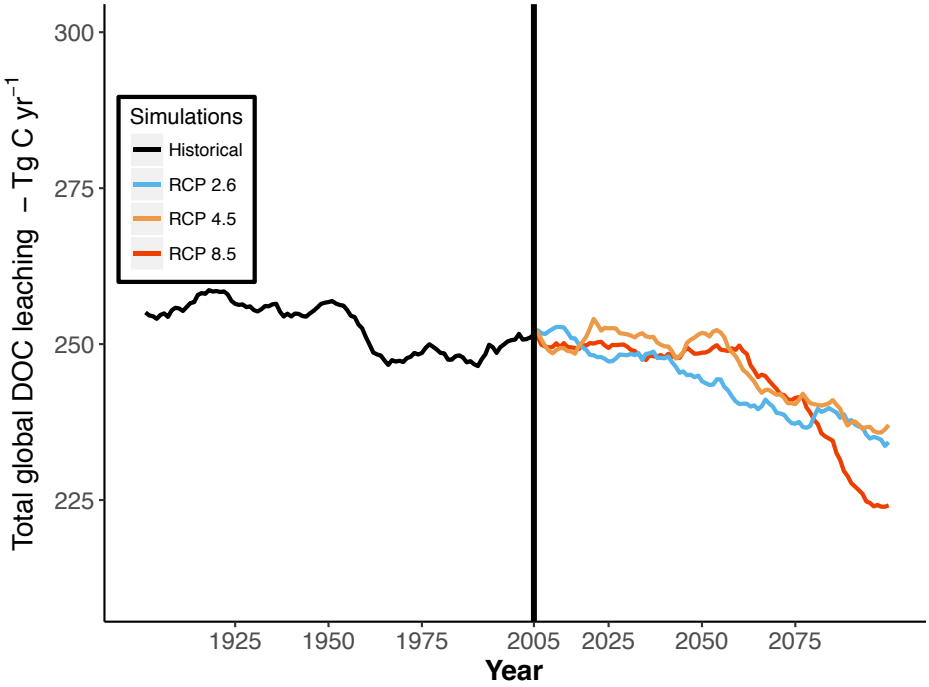


**Fig 9.** Global DOC leaching without atmospheric $CO_2$ change based on three RCP scenarios

# 4. Conclusion

Dissolved organic carbon (DOC) leaching is representing a fraction of terrestrial uptake of $CO_2$ which is displaced along the terrestrial-aquatic continuum and is an important link in the global C cycle. Our results show an increase of leached DOC based on three RCP scenarios (RCP 2.6, 4.5 and 8.5), mainly due to the increase in atmospheric $CO_2$ and its fertilization effect on terrestrial NPP, but also due to increasing runoff in some areas such as West Russia, amazon basin and East US. Hence as a component of the global carbon cycle it becomes more important in future.

However, our model does not include nutrient limitation, which results in overestimation of CO2 fertilization effect in the high latitudes areas. Hence, further development and including the missing processes will improve our estimations.

# Conclusions

# Conclusions

## 1. Summary of the research

My work focused on improving the capabilities of the Joint UK Land Environment Simulator (JULES). Land surface models, such as JULES, are components of Earth System models, which represent the cycles of for energy, water and C. However, JULES did not include a representation of soil DOC cycling and the soil-river export of DOC.
Due to the lack of measurements and adequate upscaling techniques, this transported C flux cannot be estimated with empirical models, leaving processes-based models such as JULES as the most feasible option for this estimation.
Hence in the first part of my thesis, I developed an extension of JULES version 4.4 (JULES-DOCM), representing the key processes which control soil DOC cycling. I tested the model on two types of sites, level 1 sites with more detail and frequent measurements, and level 2 sites with less information.

In the second part of my thesis, I provided a bigger data base from different biomes in order to re-calibrate processes that control the soil DOC concentrations in JULES-DOCM: the rate of DOC production associated with soil organic carbon decomposition and the rate of DOC decomposition. Then, I used JULES-DOCM with calibrated values to produce the first global map of present-day soil DOC stocks, concentration and leaching fluxes.

In the third part of my thesis, I used the global calibrated version of JULES-DOCM to study the historical trend of terrestrial DOC transported to the riverine ecosystem. I ran different experiments to study the impact of atmospheric $CO_2$ concentrations, climate and land-use change on the transported DOC flux, as well as the impact of these in different climate zones.

In the last part of my thesis, I used the global calibrated version of JULES-DOCM with three representative concentration pathways (RCPs), RCP 2.6, RCP 4.5 and RCP 8.5, in order to estimate the future terrestrial DOC flux transported to the river system. I also estimated the changes in DOC flux for each RCP scenario and for each major climate zone, and their correlation with NPP and water fluxes.

## 2. Key findings

In the first chapter, the results show that the new model is able to reproduce the temporal dynamics of soil DOC concentration and controlling processes including leaching to the riverine system at five sites (four forest sites (in Germany, Belgium, United States and Taiwan) and one grassland (in Ireland) ).

In the second chapter, I estimated the global DOC stock in the top-soil (35 cm) and in the total soil column (down to 3 m) as 0.14±0.02 Pg C and 0.33±0.08 Pg C, respectively. The simulated DOC concentration averages 26.01±2.00 mg C $L^{-1}$ in the top-soil and 7.62±3.04 mg C $L^{-1}$ in the bottom-soil (35 cm to 3 m depth) layers. The DOC leaching estimation from soils to rivers is 0.28±0.07 Pg C $yr^{-1}$ which was comparable with previous estimations of exported C from rivers to oceans.

In the third chapter, I estimated a global increase in terrestrial DOC exports of 42 Tg C $yr^{-1}$ from 1860 to 2010, with a present day flux of 292 Tg C $yr^{-1}$. At the global scale, $CO_2$ fertilization was identified as the main controlling factor, followed by climate and land use change. Most of the DOC export originated from tropical ecosystems, which however increased only moderately from 152 to 173 Tg C $yr^{-1}$ over the historical period, also primarily due to the increase in atmospheric $CO_2$, leading to larger biomass, soil carbon and hence DOC. In the temperate and boreal zones, the role of climate change becomes increasingly important. Contrary to general assumptions, land use changes only play a minor role in driving the changes in DOC leaching.

In the last chapter, I estimated the highest change of terrestrial DOC input for period 2090-2099 as 36% increase (376 Tg C yr-1) in RCP 8.5, and the boreal zone showed the highest percentage change with 89% increase (51 Tg C yr-1). The RCP's 4.5 and 2.6 show a 22% (338.5 Tg C yr-1) and 10% (306 Tg C yr-1) increase respectively. The increase of the atmospheric $CO_2$ concentration is the main reason for the future increase of transported terrestrial DOC.

# 3. Limitations and future direction

## 3.1 Data availability

As argued in Chapter 1, DOC leaching is controlled significantly by catchment hydrology. Although model parameters that control the DOC concentration in the soil could be optimised, based on the extensive measured soil DOC data that I collected (Chapter 2), besides some available global runoff data (Fekete, Vörösmarty and Grabs, 2000; Dai, 2017), yet the hydrological data are still very limited. Hence, calibration of the drainage and runoff for the calibration sites was limited or not possible.

Furthermore, I argue that in general, insufficient measurements of soil and in-stream DOC concentration and runoff make a proper calibration a challenging issue. Moreover, the available data is not distributed geographically even, as the most of the available data belongs to the US and parts of the Europe (Hartmann, Lauerwald and Moosdorf, 2014), where data from tropical zone is very limited. Nevertheless, the accessibility of the available measurements is another issue, as there are often some restrictions in sharing by the data providers. Hence, one of the future steps should be collecting more measurements, making them easily accessible and calibrating the model with this bigger data-base.

However, the definition of DOC in different literature might be different. For instance, in some studies the dissolved organic matter (DOM) term is used as the DOC, where in other studies DOM refers not only to DOC but also includes dissolved organic N (DON). Moreover, the sample extraction method differs between the studies, which can have a significant impact on the final reported DOC (Zsolnay, 2003). Hence, due to the above-mentioned reasons, the available information on DOC are often not comparable.

Finally, modelling and experimentalist communities should work more closely together to develop a better integration between models and data (Bahn, M., 2010). At the moment, the modelling and field/laboratory studies have different approaches and definitions. Hence, a better communication between these two communities will improve both experiments and modelling quality through adopting the most suitable sampling method and providing a more detailed and compatible data for models.

### 3.2 Process understanding and Modelling

In JULES-DOCM, although we included the well-studied DOC controls such as temperature, precipitation and vegetation type, still representations of pH and nutrient controls are missing. These are known to impact DOC dynamics, although their influence is not well-constrained (Kalbitz *et al.*, 2000). For example, DOC degradability depends significantly on C:N ratio of plant material and SOM (Sanderman *et al.*, 2009; Van den berg, Shotbolt and Ashmore, 2012). Hence, including these drivers could improve the ability of the model to better represent and predict the temporal and spatial dynamics of soil DOC.

Additionally, we are still missing the representation of peatlands in the JULES-DOCM model. Although peatlands cover a small fraction of the total land area, they are a significant store of terrestrial C (Blodau, 2002). Moreover, recent studies show a high DOC concentration in peatlands (Billett *et al.*, 2010), indicating the importance of representing peatlands in the model. Hence, another aspect of future development should focus on peatland representation and contribution to DOC export.

Furthermore, DOC is only a small fraction of the total terrestrial transported C flux. Previous estimations such as Cole *et al.*(2007), Tranvik *et al.* (2009), Battin *et al.*, (2009) and Regnier *et al.*, (2013) were generally based on closing the riverine carbon budget at the global scale, accounting for all forms of carbon, DOC, but also TOC and DIC. Also, these estimates contain a large uncertainty as carbon export from soils to rivers is only deduced from carbon export from rivers to ocean plus carbon sequestered and carbon outgassed to the atmosphere along the aquatic continuum. Hence, future modelling work should include the representation of soil dissolved inorganic carbon and particulate organic carbon flux, and the fate of these exported fluxes in the river system, in order to be more comparable to global aquatic carbon budgets.

Finally, to gain a better understanding of the fate of transported DOC in aquatic systems, we need to connect the terrestrial DOC export to the river routing scheme and include the DOC processes within the river system such as sedimentation and outgassing. Currently, there is a version of JULES that is representing the river system (Walters *et al.*, 2014) which can be connected to the terrestrial part from JULES-DOCM for further validation.

# References


Aguilar, L. and Thibodeaux, L. J. (2005) 'Kinetics of peat soil dissolved organic carbon release from bed sediment to water. Part 1. Laboratory simulation', *Chemosphere*, 58(10), pp. 1309–1318. doi: 10.1016/j.chemosphere.2004.10.011.

Aitkenhead, J. A. and Mcdowell, W. H. (2000) 'Aitkenhead JA, McDowell WH. 2000. Soil C:N ratio as a predictor of annual riverine DOC flux at local and global scales. Global Biogeochem Cycles', *Global Biogeochemical Cycles*, 14(1), pp. 127–138.

Augustoa, L. and , Jacques Rangera,*, D. B. and A. R. (2002) 'Karyotypic studies in ecotypes of hippophaë rhamnoides l. from romania', *Annals of Forest Science*, 59, pp. 233–253. doi: 10.1051/forest.

Bahn, M., W. L. K. and A. H. (2010) 'Synthesis: emerging issues and challenges for an integrated understanding of soil carbon fluxes. Kutsch, W.L., M. Bahn and A. Heinemeyer (eds.)', *Soil Carbon Dynamics: An Integrated Methodology. Cambridge, UK: Cambridge University Press*, pp. 257–271.

Battin, T. J. *et al.* (2008) 'Biophysical controls on organic carbon fluxes in fluvial networks', *Nature Geoscience*, 1(8), pp. 95–100. doi: 10.1038/ngeo602.

Battin, T. J. *et al.* (2009) 'The boundless carbon cycle', *Nature Geoscience*. Nature Publishing Group, 2(9), pp. 598–600. doi: 10.1038/ngeo618.

Van den berg, L. J. L., Shotbolt, L. and Ashmore, M. R. (2012) 'Dissolved organic carbon (DOC) concentrations in UK soils and the influence of soil, vegetation type and seasonality', *Science of the Total Environment*. Elsevier B.V., 427–428, pp. 269–276. doi: 10.1016/j.scitotenv.2012.03.069.

Best, M. J. *et al.* (2011) 'The Joint UK Land Environment Simulator (JULES), model description – Part 1: Carbon fluxes and vegetation dynamics', *Geoscientific Model Development*, 4(3), pp. 701–722. doi: 10.5194/gmd-4-701-2011.

Billett, M. F. *et al.* (2010) 'Carbon balance of UK peatlands : current state of knowledge and future research challenges', *CLIMATE RESEARCH*, 45(December), pp. 13–29. doi: 10.3354/cr00903.

Blodau, C. (2002) 'Carbon cycling in peatlands - A review of processes and controls', *Environmental Reviews*. NRC Research Press, 10(2), pp. 111–134. doi: 10.1139/a02-004.

Borken, W. *et al.* (2011) 'Site-to-site variability and temporal trends of DOC concentrations

and fluxes in temperate forest soils', *Global Change Biology*, 17(7), pp. 2428–2443. doi: 10.1111/j.1365-2486.2011.02390.x.

Botch, M. S. *et al.* (1995) 'Carbon pools and accumulation in peatlands of the former Soviet Union', *Global Biogeochemical Cycles*, 9(1), pp. 37–46.

Bouchard, A. (1997) 'RECENT LAKE ACIDIFICATION AND RECOVERY TRENDS IN SOUTHERN QUEBEC, CANADA', 5, pp. 225–245.

Boyer, J. N. and Groffman, P. M. (1996) 'Bioavailability of water extractable organic carbon fractions in forest and agricultural soil profiles', *Soil Biology and Biochemistry*, 28(6), pp. 783–790. doi: 10.1016/0038-0717(96)00015-6.

Braakhekke, M. C. *et al.* (2013) 'Modeling the vertical soil organic matter profile using Bayesian parameter estimation', *Biogeosciences*, 10(1), pp. 399–420. doi: 10.5194/bg-10-399-2013.

Brye, K. R. *et al.* (2001) 'Nitrogen and Carbon Leaching in Agroecosystems and Their Role in Denitrification Potential', *Journal of Environment Quality*, 30(1), p. 58. doi: 10.2134/jeq2001.30158x.

Burke, E. J., Chadburn, S. E. and Ekici, A. (2017) 'A vertical representation of soil carbon in the JULES land surface scheme (vn4.3-permafrost) with a focus on permafrost regions', *Geoscientific Model Development*, 10(2), pp. 959–975. doi: 10.5194/gmd-10-959-2017.

Cai, W.-J. (2011) 'Estuarine and Coastal Ocean Carbon Paradox: $CO_2$ Sinks or Sites of Terrestrial Carbon Incineration?', *Annual Review of Marine Science*, 3(1), pp. 123–145. doi: 10.1146/annurev-marine-120709-142723.

Camino-Serrano, M. *et al.* (2014) 'Linking variability in soil solution dissolved organic carbon to climate, soil type, and vegetation type', *Global Biogeochemical Cycles*, (September 2015), pp. 497–509. doi: 10.1002/2013GB004726.Received.

Cauwet, G. (2002) 'DOM in the coastal zone', in Hansell, D. and Carlson, C. (eds) *Biogeochemistry of Marine Dissolved Organic Matter*. San Diego: Academic Press; 2002:579-609.

Ciais, P. *et al.* (2013) 'Carbon and Other Biogeochemical Cycles. In: Cli- mate Change 2013: The Physical Science Basis. Contribution of Working Group I to the Fifth Assessment Report of the Intergovernmental Panel on Climate Change', *Cambridge University Press, Cambridge, United Kingdom and New York, NY, USA*, pp. 465–570.

Clair, T. A., Ehrman, J. M. and Higuchi, K. (1999) 'Changes in freshwater carbon exports from

Canadian terrestrial basins to lakes and estuaries under a 2xCO2 atmospheric scenario', *Global Biogeochemical Cycles*, 13(4), pp. 1091–1097. doi: 10.1029/1999GB900055.
Clark, D. B. *et al.* (2011) 'The Joint UK Land Environment Simulator (JULES), model description – Part 2: Carbon fluxes and vegetation dynamics', *Geoscientific Model Development*, 4(3), pp. 701–722. doi: 10.5194/gmd-4-701-2011.
Clark, D. B. and Gedney, N. (2008) 'Representing the effects of subgrid variability of soil moisture on runoff generation in a land surface model', 113(May 2007), pp. 1–13. doi: 10.1029/2007JD008940.
Clark, J. M. *et al.* (2010) 'The importance of the relationship between scale and process in understanding long-term DOC dynamics', *Science of the Total Environment*. Elsevier B.V., 408(13), pp. 2768–2775. doi: 10.1016/j.scitotenv.2010.02.046.
Clarke, L. E. *et al.* (2007) 'Scenarios of Greenhouse Gas Emissions and Atmospheric Concentrations', *Program*, 2011(July), p. 164. doi: 10.1002/yd.424.
Clutterbuck, B. and Yallop, A. R. (2010) 'Land management as a factor controlling dissolved organic carbon release from upland peat soils 2: Changes in DOC productivity over four decades', *Science of the Total Environment*. Elsevier B.V., 408(24), pp. 6179–6191. doi: 10.1016/j.scitotenv.2010.08.038.
Cole, J. J. *et al.* (2007) 'Plumbing the global carbon cycle: Integrating inland waters into the terrestrial carbon budget', *Ecosystems*, 10(1), pp. 171–184. doi: 10.1007/s10021-006-9013-8.
Cole, J J *et al.* (2007) 'Plumbing the Global Carbon Cycle: Integrating Inland Waters into the Terrestrial Carbon Budget', *Ecosystems*, 10(1), pp. 172–185. doi: 10.1007/s10021-006-9013-8.
Coleman, K. and Jenkinson, D. . (2014) 'RothC - A Model for the Turnover of Carbon in Soil. Model description and windows user guide.', *Evaluation of Soil Organic Matter Models: Using Existing Long-Term Datasets*, I(June), pp. 237–246. doi: 10.1007/978-3-642-61094-3_17.
Cotrufo, M. F. *et al.* (2013) 'The Microbial Efficiency-Matrix Stabilization (MEMS) framework integrates plant litter decomposition with soil organic matter stabilization: Do labile plant inputs form stable soil organic matter?', *Global Change Biology*, 19(4), pp. 988–995. doi: 10.1111/gcb.12113.
Dai, A. (2017) 'Dai and Trenberth Global River Flow and Continental Discharge Dataset'.

Boulder, CO: Research Data Archive at the National Center for Atmospheric Research, Computational and Information Systems Laboratory. doi: 10.5065/D6V69H1T.
Dai, M. *et al.* (2012) 'Spatial distribution of riverine DOC inputs to the ocean : an updated global synthesis', *Current Opinion in Environmental {…}*. Available at: http://www.sciencedirect.com/science/article/pii/S1877343512000358.
Davidson, E. A. *et al.* (2006) 'Temperature sensitivity of soil carbon decomposition and feedbacks to climate change.', *Nature*, 440(7081), pp. 165–73. doi: 10.1038/nature04514.
Davis, C. (2015) 'ihs: Inverse Hyperbolic Sine Distribution'. Available at: https://cran.r-project.org/package=ihs.
DeLuca, T. H., Keeney, D. R. and McCarty, G. W. (1992) 'Effect of freeze-thaw-events on mineralization of soil nitrogen', *Biol. Fertil. Soils*, 14, pp. 116–120. doi: 10.1007/BF00336260.
Dlugokencky, E. and Tans, P. (2013) *No Title*.
Donnell, J. A. O. *et al.* (no date) *DOM composition and transformation in boreal forest soils : the effects of temperature and organic-horizon decomposition state*. doi: 10.1002/2016JG003431.
Drake, T. W., Raymond, P. A. and Spencer, R. G. M. (2017) 'Terrestrial carbon inputs to inland waters: A current synthesis of estimates and uncertainty', *Limnology and Oceanography Letters*, pp. 132–142. doi: 10.1002/lol2.10055.
Drake, T. W., Raymond, P. A. and Spencer, R. G. M. (2018) 'Terrestrial carbon inputs to inland waters : A current synthesis of estimates and uncertainty', *Limnology and Oceanography Letters*, pp. 132–142. doi: 10.1002/lol2.10055.
Eimers, M. C. *et al.* (2008) 'Examination of the potential relationship between droughts, sulphate and dissolved organic carbon at a wetland-draining stream', *Global Change Biology*, 14(4), pp. 938–948. doi: 10.1111/j.1365-2486.2007.01530.x.
Evans, C. D., Monteith, D. T. and Cooper, D. M. (2005) 'Long-term increases in surface water dissolved organic carbon: Observations, possible causes and environmental impacts', *Environmental Pollution*, 137(1), pp. 55–71. doi: 10.1016/j.envpol.2004.12.031.
Fang, Y. *et al.* (2009) 'Large loss of dissolved organic nitrogen from nitrogen-saturated forests in subtropical China', *Ecosystems*, 12(1), pp. 33–45. doi: 10.1007/s10021-008-9203-7.
Fekete, B. M., Vörösmarty, C. J. and Grabs, W. (2000) *UNH/GRDC Composite Runoff Fields V 1.0*.

Freeman, C. *et al.* (2001) 'Export of organic carbon from peat soils', *Nature*, 412(6849), pp. 785–785. doi: 10.1038/35090628.

Fröberg, M. *et al.* (2011) 'Dissolved organic carbon and nitrogen leaching from Scots pine, Norway spruce and silver birch stands in southern Sweden', *Forest Ecology and Management*, 262(9), pp. 1742–1747. doi: 10.1016/j.foreco.2011.07.033.

Fujii, K. *et al.* (2009) 'Fluxes of dissolved organic carbon in two tropical forest ecosystems of East Kalimantan, Indonesia', *Geoderma*. Elsevier B.V., 152(1–2), pp. 127–136. doi: 10.1016/j.geoderma.2009.05.028.

Fujii, K., Funakawa, S., *et al.* (2011) 'Fluxes of dissolved organic carbon and nitrogen throughout Andisol, Spodosol and Inceptisol profiles under forest in Japan', *Soil Science and Plant Nutrition*, 57(6), pp. 855–866. doi: 10.1080/00380768.2011.637304.

Fujii, K., Hartono, A., *et al.* (2011) 'Fluxes of dissolved organic carbon in three tropical secondary forests developed on serpentine and mudstone', *Geoderma*. Elsevier B.V., 163(1–2), pp. 119–126. doi: 10.1016/j.geoderma.2011.04.012.

Futter, M. N. *et al.* (2007) 'Modeling the mechanisms that control in-stream dissolved organic carbon dynamics in upland and forested catchments', *Water Resources Research*, 43(2), pp. 1–16. doi: 10.1029/2006WR004960.

Gedney, N. , Cox, P. M. (2003) 'The Sensitivity of Global Climate Model Simulations to the Representation of Soil Moisture Heterogeneity', (2000), pp. 1265–1275.

Gielen, B. *et al.* (2010) 'Decadal water balance of a temperate Scots pine forest (Pinus sylvestris L.) based on measurements and modelling', *Biogeosciences*, 7(October), pp. 1247–1261. doi: 10.5194/bg-7-1247-2010.

Gielen, B. *et al.* (2011) 'The importance of dissolved organic carbon fluxes for the carbon balance of a temperate Scots pine forest', *Agricultural and Forest Meteorology*, 151(3), pp. 270–278. doi: 10.1016/j.agrformet.2010.10.012.

Gödde, M. *et al.* (1996) 'Carbon mineralization from the forest floor under red spruce in the northeatern {USA}', *Soil Biol. Biochem.*, 28(9), pp. 1181–1189.

Guenet, B. *et al.* (2010) 'Priming effect: Bridging the gap between terrestrial and aquatic ecology', *Ecology*, 91(10), pp. 2850–2861. doi: 10.1890/09-1968.1.

Guggenberger, G. and Kaiser, K. (2003) 'Dissolved organic matter in soil : challenging the paradigm of sorptive preservation', *Geoderma*, 113, pp. 293–310. doi: 10.1016/S0016-7061(02)00366-X.

Haaland, S. *et al.* (2010) 'Quantifying the drivers of the increasing colored organic matter in boreal surface waters', *Environmental Science and Technology*, 44(8), pp. 2975–2980. doi: 10.1021/es903179j.

Harper, A. B. *et al.* (2016) 'Improved representation of plant functional types and physiology in the Joint UK Land Environment Simulator (JULES v4.2) using plant trait information', *Geoscientific Model Development*, 9(7), pp. 2415–2440. doi: 10.5194/gmd-9-2415-2016.

Harris, I. *et al.* (2014) 'Updated high-resolution grids of monthly climatic observations - the CRU TS3.10 Dataset', *International Journal of Climatology*, 34(3), pp. 623–642. doi: 10.1002/joc.3711.

Harrison, J. A., Caraco, N. and Seitzinger, S. P. (2005) 'Global patterns and sources of dissolved organic matter export to the coastal zone: Results from a spatially explicit, global model', *Global Biogeochemical Cycles*, 19(4). doi: 10.1029/2005gb002480.

Hartmann, J., Lauerwald, R. and Moosdorf, N. (2014) 'A Brief Overview of the GLObal RIver Chemistry Database, GLORICH', *Procedia Earth and Planetary Science*, 10, pp. 23–27. doi: 10.1016/j.proeps.2014.08.005.

Hastie, A. *et al.* (2020) 'Aquatic carbon fluxes dampen the overall variation of net ecosystem productivity in the Amazon basin : An analysis of the interannual variability in the boundless carbon cycle', (February 2019), pp. 1–18. doi: 10.1111/gcb.14620.

Hejzlar, J. *et al.* (2003) 'The apparent and potential effects of climate change on the inferred concentration of dissolved organic matter in a temperate stream (the Malše River, South Bohemia)', *Science of the Total Environment*, 310(1–3), pp. 143–152. doi: 10.1016/S0048-9697(02)00634-4.

Hirano, T. *et al.* (2009) 'Controls on the carbon balance of tropical peatlands', *Ecosystems*, 12(6), pp. 873–887. doi: 10.1007/s10021-008-9209-1.

Hongve, D., Riise, G. and Kristiansen, J. F. (2004) 'Increased colour and organic acid concentrations in Norwegian forest lakes and drinking water - A result of increased precipitation?', *Aquatic Sciences*, 66(2), pp. 231–238. doi: 10.1007/s00027-004-0708-7.

Hoogsteen, M. J. J. *et al.* (2015) 'Estimating soil organic carbon through loss on ignition: Effects of ignition conditions and structural water loss', *European Journal of Soil Science*, 66(2), pp. 320–328. doi: 10.1111/ejss.12224.

Jackson, R., Banner, J. and Jobbágy, E. (2002) 'Ecosystem carbon loss with woody plant invasion of grasslands', *Nature*, 277(July), pp. 623–627. doi: 10.1038/nature00952.

Janssens, I. A. *et al.* (1999) 'Above- and belowground phytomass and carbon storage in a Belgian Scots pine stand', *Annals of Forest Science*, 56(2), pp. 81–90. doi: 10.1051/forest:19990201.

Janssens, I. A. *et al.* (2003) 'Europe ' s Terrestrial Biosphere Anthropogenic CO 2 Emissions', *Science*, 300(June), pp. 1538–1542. doi: 10.1126/science.1083592.

Jenkinson, D. S. *et al.* (1990) 'The turnover of organic carbon and nitrogen in soil', *The Royal Society*, 329(1255). doi: https://doi.org/10.1098/rstb.1990.0177.

Jenkinson, D. S. and Coleman, K. (2008) 'The turnover of organic carbon in subsoils. Part 2. Modelling carbon turnover', *European Journal of Soil Science*, 59(2), pp. 400–413. doi: 10.1111/j.1365-2389.2008.01026.x.

Jobbágy, E. G. and Jackson, R. B. (2000) 'The vertical distribution of soil organic carbon and its relation to climate and vegetation', *Ecological Applications*, 10(2), pp. 423–436. doi: 10.1890/1051-0761(2000)010[0423:TVDOSO]2.0.CO;2.

Johnson, C. E. *et al.* (2000) 'Position and Landscape in a Northern Hardwood Watershed Ecosystem', *Gene*, 3(2), pp. 159–184.

Kalbitz, K. *et al.* (2000) 'Controls on the Dynamics of Dissolved Organic Matter in Soils A Review', *Soil Science*, pp. 277–304.

Kalbitz, K. *et al.* (2003) 'Biodegradation of soil-derived dissolved organic matter as related to its properties', *Geoderma*, 113, pp. 273–291.

Khomutova, T. E. *et al.* (2000) 'Mobilization of DOC from sandy loamy soils under different land use (Lower Saxony, Germany)', *Plant and Soil*, pp. 13–19.

Kicklighter, D. W. *et al.* (2013) 'Insights and issues with simulating terrestrial DOC loading of Arctic river networks', *Ecological Applications*, 23(8), pp. 1817–1836. doi: 10.1890/11-1050.1.

Kindler, R. *et al.* (2011) 'Dissolved carbon leaching from soil is a crucial component of the net ecosystem carbon balance', *Global Change Biology*, 17(2), pp. 1167–1185. doi: 10.1111/j.1365-2486.2010.02282.x.

Kindler, R. and Siemens, J. (2010) 'Dissolved carbon leaching from soil is a crucial component of the net ecosystem carbon balance', *Global Change …*, pp. 1167–1185. doi: 10.1111/j.1365-2486.2010.02282.x.

Klein Goldewijk, K. *et al.* (2011) 'The HYDE 3.1 spatially explicit database of human-induced global land-use change over the past 12,000 years', *Global Ecology and Biogeography*, 20(1),

pp. 73–86. doi: 10.1111/j.1466-8238.2010.00587.x.
Koven, C. D. *et al.* (2013) 'The effect of vertically resolved soil biogeochemistry and alternate soil C and N models on C dynamics of CLM4', *Biogeosciences*, 10(11), pp. 7109–7131. doi: 10.5194/bg-10-7109-2013.
Kuiters, A. T. (1993) 'Dissolved Organic Matter in Forest Soils: Sources, Complexing Properties and Action On Herbaceous Plants', *Chemistry and Ecology*. Taylor & Francis, 8(3), pp. 171–184. doi: 10.1080/02757549308035307.
Kutsch, W. L. *et al.* (2010) 'Heterotrophic soil respiration and soil carbon dynamics in the deciduous Hainich forest obtained by three approaches', *Biogeochemistry*, 100(1–3), pp. 167–183. doi: 10.1007/s10533-010-9414-9.
Langerwisch, F. *et al.* (2015) 'Deforestation in Amazonia impacts riverine carbon dynamics', *Earth System Dynamics Discussions*, 6(2), pp. 2101–2136. doi: 10.5194/esdd-6-2101-2015.
Langerwisch, F. *et al.* (2016) 'Climate change increases riverine carbon outgassing, while export to the ocean remains uncertain', *Earth System Dynamics*, 7(3), pp. 559–582. doi: 10.5194/esd-7-559-2016.
Lauerwald, R. *et al.* (2012) 'Assessing the nonconservative fluvial fluxes of dissolved organic carbon in North America', *Journal of Geophysical Research*, 117(G1). doi: 10.1029/2011jg001820.
Lauerwald, R. *et al.* (2015) 'Spatial patterns in CO2 evasion from the global river network', *Global Biogeochemical Cycles*, 29(5), pp. 534–554. doi: 10.1002/2014GB004941.Received.
Lauerwald, R. *et al.* (2017) 'ORCHILEAK: A new model branch to simulate carbon transfers along the terrestrial-aquatic continuum of the Amazon basin', *Geoscientific Model Development*, (April), pp. 1–58. doi: 10.5194/gmd-2017-79.
Ledesma, J. L. J., Köhler, S. J. and Futter, M. N. (2012) 'Long-term dynamics of dissolved organic carbon: Implications for drinking water supply', *Science of the Total Environment*. Elsevier B.V., 432, pp. 1–11. doi: 10.1016/j.scitotenv.2012.05.071.
LeQuéré, C. *et al.* (2015) 'Global Carbon Budget 2015', *Earth System Science Data*, 7(2), pp. 349–396. doi: 10.5194/essd-7-349-2015.
Liechty, H. O., Kuuseoks, E. and Mroz, G. D. (1995) 'Dissolved Organic-Carbon in Northern Hardwood Stands with Differing Acidic Inputs and Temperature Regimes', *Journal of Environmental Quality*, 24(July 1994), pp. 927–933. doi: 10.2134/jeq1995.00472425002400050021x.

Liu, C. P. and Sheu, B. H. (2003) 'Dissolved organic carbon in precipitation, throughfall, stemflow, soil solution, and stream water at the Guandaushi subtropical forest in Taiwan', *Forest Ecology and Management*, 172(2–3), pp. 315–325. doi: 10.1016/S0378-1127(01)00793-9.

Ludwig, W. and Probst, J. L. (1996) 'Predicting the oceanic input of organic carbon by continental erosion', *Global Biogeochemical Cycles*, 10(1), pp. 23–41. doi: 10.1029/95GB02925.

Ludwig, W., Probst, J. L. and Kempe, S. (1996) 'Predicting the oceanic input of organic carbon by continental erosion', *Global Biogeochemical Cycles*, 10(1), pp. 23–41. doi: 10.1029/95GB02925.

Lundquist, E. J., Jackson, L. E. and Scow, K. M. (1999) 'Wet-dry cycles affect dissolved organic carbon in two California agricultural soils', *Soil Biology and Biochemistry*, 31(7), pp. 1031–1038. doi: 10.1016/S0038-0717(99)00017-6.

Manzoni, S. *et al.* (2012) 'Environmental and stoichiometric controls on microbial carbon-use efficiency in soils', *New Phytologist*, 196(1), pp. 79–91. doi: 10.1111/j.1469-8137.2012.04225.x.

Markewitz, D. and Richter, D. D. (1998) 'The bio in Aluminum and Silicon Geochemistry', *Biogeochemistry*, pp. 235–252. doi: 10.1023/A.

Marschner, B. and Bredow, A. (2002) 'Temperature effects on release and ecologically relevant properties of dissolved organic carbon in sterilised and biologically active soil samples', *Soil Biology and Biochemistry*, 34(4), pp. 459–466. doi: 10.1016/S0038-0717(01)00203-6.

Marschner, H. (1995) *Mineral Nutrition of Higher Plants*. Academic Press (Special Publications of the Society for General Microbiology). Available at: https://books.google.co.uk/books?id=phnp-H1XeBkC.

Martin, G. M. *et al.* (2011) 'Model Development The HadGEM2 family of Met Office Unified Model climate configurations', *Geoscientific Model Development*, pp. 723–757. doi: 10.5194/gmd-4-723-2011.

Mayorga, E. *et al.* (2010) 'Environmental Modelling & Software Global Nutrient Export from WaterSheds 2 ( NEWS 2 ): Model development and implementation', *Environmental Modelling and Software*. Elsevier Ltd, 25(7), pp. 837–853. doi: 10.1016/j.envsoft.2010.01.007.

Mcdowell, W. H. and Oulehle, F. (2009) 'Increased Dissolved Organic Carbon ( DOC ) in Central European Streams is Driven by Reductions in Ionic Strength Rather than Climate Change or Decreasing Acidity', 43(12), pp. 4320–4326.

Meinshausen, M. *et al.* (2011) 'The RCP greenhouse gas concentrations and their extensions from 1765 to 2300', *CLIMATE change*, pp. 213–241. doi: 10.1007/s10584-011-0156-z.

Melillo, J. M. *et al.* (1989) 'Carbon and nitrogen dynamics along the decay continuum: Plant litter to soil organic matter', *Plant and Soil*, 115(2), pp. 189–198. doi: 10.1007/BF02202587.

Meybeck, M. (1982) 'Carbon, nitrogen, and phosphorus transport by world rivers', *American Journal of Science*, pp. 401–450. doi: 10.2475/ajs.282.4.401.

Meybeck, M. (1993) 'Riverine transport of atmospheric carbon: Sources, global typology and budget', *Water, Air, & Soil Pollution*, 70(1–4), pp. 443–463. doi: 10.1007/BF01105015.

Meybeck, M., Dürr, H. H. and Vörösmarty, C. J. (2006) 'Global coastal segmentation and its river catchment contributors: A new look at land-ocean linkage', *Global Biogeochemical Cycles*, 20(1), pp. 1–15. doi: 10.1029/2005GB002540.

Michalzik, B. *et al.* (1999) 'Dynamics of dissolved organic nitrogen and carbon in a Central European Norway spruce …', *European Journal of Soil Science*, (December), pp. 579–590. doi: 10.1046/j.1365-2389.1999.00267.x.

Michalzik, B. *et al.* (2001) 'Fluxes and concentrations of dissolved organic carbon and nitrogen–a synthesis for temperate forests', *Biogeochemistry*, 52, pp. 173–205. Available at: http://link.springer.com/article/10.1023/A:1006441620810.

Michalzik, B. *et al.* (2003) 'Modelling the production and transport of Dissolved Organic Carbon in forest soils', *Biogeochemistry*, 66, pp. 241–264. doi: 10.1023/B:BIOG.0000005329.68861.27.

Moore, T. R. and Clarkson, B. R. (2007) 'Dissolved organic carbon in New Zealand peatlands', *New Zealand Journal of Marine and Freshwater Research*, 41(1), pp. 137–141. doi: 10.1080/00288330709509902.

Moore, T. R. and Dalva, M. (2001) 'Organic Carbon By Plant Tissues and Soils', *Soil Science*, 166(1), pp. 38–47.

Moore, T. R., Paré, D. and Boutin, R. (2008) 'Production of dissolved organic carbon in Canadian forest soils', *Ecosystems*, 11(5), pp. 740–751. doi: 10.1007/s10021-008-9156-x.

Moore, T. R., De Souza, W. and Koprivnjak, J.-F. (1992) 'Controls on the sorption of dissolved organic carbon by soils', *Soil Science*, 154(2). Available at:

http://journals.lww.com/soilsci/Fulltext/1992/08000/CONTROLS_ON_THE_SORPTION_OF_DISSOLVED_ORGANIC.5.aspx.
Moss, R. H. *et al.* (2010) 'The next generation of scenarios for climate change research and assessment', *Nature*. Nature Publishing Group, 463(7282), pp. 747–756. doi: 10.1038/nature08823.
Mulder, J. *et al.* (2000) *Effects of natural climatic variations on production and transport of dissolved organic matter in European forest ecosystems*.
Mund, M. *et al.* (2010) 'The influence of climate and fructification on the inter-annual variability of stem growth and net primary productivity in an old-growth, mixed beech forest', *Tree Physiology*, 30(6), pp. 689–704. doi: 10.1093/treephys/tpq027.
Nachtergaele, F. *et al.* (2010) 'The Harmonized World Soil Database', *Proceedings of the 19th World Congress of Soil Science, Soil Solutions for a Changing World, Brisbane, Australia, 1-6 August 2010*, pp. 34–37. doi: 3123.
Naipal, V. *et al.* (2018) 'Global soil organic carbon removal by water erosion under climate change and land use change during 1850–2005 AD', *Biogeosciences Discussions*, (January), pp. 1–33. doi: 10.5194/bg-2017-527.
Nakhavali, M. *et al.* (2018) 'Representation of dissolved organic carbon in the JULES land surface model (vn4.4_JULES-DOCM)', *Geoscientific Model Development*, 11(2), pp. 593–609. doi: 10.5194/gmd-11-593-2018.
Nakhavali, M. *et al.* (2019) 'Soil leaching as minor source to inland water carbon budget', *under revision*.
Nakhavali, M. et al (2019) 'Historical trend of lateral transported dissolved organic carbon from soil to river system'.
Neff, J. C. and Asner, G. P. (2001) 'Dissolved organic carbon in terrestrial ecosystems: Synthesis and a model', *Ecosystems*, 4(1), pp. 29–48. doi: 10.1007/s100210000058.
Neff, J. C. and Hooper, D. U. (2002) 'Vegetation and climate controls on potential CO2, DOC and DON production in northern latitude soils', *Global Change Biology*, 8(9), pp. 872–884. doi: 10.1046/j.1365-2486.2002.00517.x.
Nydahl, A. C., Wallin, M. B. and Weyhenmeyer, G. A. (2017) 'No long-term trends in $p\,CO_2$ despite increasing organic carbon concentrations in boreal lakes, streams, and rivers', *Global Biogeochemical Cycles*, 31(6), pp. 985–995. doi: 10.1002/2016GB005539.
Olson, J. S. (1963) 'Energy Storage and the Balance of Producers and Decomposers in

Ecological Systems', 44(2), pp. 322–331.
Ota, M., Nagai, H. and Koarashi, J. (2013) 'Root and dissolved organic carbon controls on subsurface soil carbon dynamics: A model approach', *Journal of Geophysical Research: Biogeosciences*, 118(4), pp. 1646–1659. doi: 10.1002/2013JG002379.
Parton, W, J., Schimel, D. S. and Ojima, C. V. C. D. S. (1987) 'Analysis of Factors Controlling Soil Organic Matter Levels in Great Plains Grasslands', *Soil Science Society of America Journal*, 51(i), pp. 1173–1179. doi: 10.2136/sssaj1987.03615995005100050015x.
Peichl, M. *et al.* (2007) 'Concentrations and fluxes of dissolved organic carbon in an age-sequence of white pine forests in Southern Ontario, Canada', *Biogeochemistry*, 86(1), pp. 1–17. doi: 10.1007/s10533-007-9138-7.
Peichl, M. *et al.* (2010) 'Biometric and eddy-covariance based estimates of carbon fluxes in an age-sequence of temperate pine forests', *Agricultural and Forest Meteorology*. Elsevier B.V., 150(7–8), pp. 952–965. doi: 10.1016/j.agrformet.2010.03.002.
Peichl, M. and Arain, M. A. (2006) 'Above- and belowground ecosystem biomass and carbon pools in an age-sequence of temperate pine plantation forests', *Agricultural and Forest Meteorology*, 140(1–4), pp. 51–63. doi: 10.1016/j.agrformet.2006.08.004.
Peichl, M., Arain, M. A. and Brodeur, J. J. (2010) 'Age effects on carbon fluxes in temperate pine forests', *Agricultural and Forest Meteorology*. Elsevier B.V., 150(7–8), pp. 1090–1101. doi: 10.1016/j.agrformet.2010.04.008.
Piirainen, S. *et al.* (2004) 'Effects of forest clear-cutting on the sulphur, phosphorus and base cations fluxes through podzolic soil horizons', *Biogeochemistry*, 69(3), pp. 405–424. doi: 10.1023/B:BIOG.0000031061.80421.1b.
Pregitzer, K. S. *et al.* (2004) 'Chronic nitrate additions dramatically increase the export of carbon and nitrogen from northern hardwood ecosystems', *Biogeochemistry*, 68(2), pp. 179–197. doi: 10.1023/B:BIOG.0000025737.29546.fd.
Presant, E.W., Acton, C. J. (1984) 'The soils of the regional municipality of Haldimand-Norfolk', *Agricul- ture Canada, Ministry of Agriculture and Food*, Volume 1(Report No. 57), p. 100.
Le Quéré, C. *et al.* (2014) 'Global carbon budget 2014', *Earth System Science Data*, 7(2), pp. 521–610. doi: 10.5194/essdd-7-521-2014.
Le Quéré, C. *et al.* (2018) 'Global Carbon Budget 2017', *Earth Syst. Sci. Data Etsushi Kato Markus Kautz Ralph F. Keeling Kees Klein Goldewijk Nathalie Lefèvre Andrew Lenton Danica*

*Lombardozzi Nicolas Metzl Yukihiro Nojiri Antonio Padin Janet Reimer*, 1010333739(10), pp. 405–448. doi: 10.5194/essd-10-405-2018.
R-Documentation (2016) *Random Samples And Permutations*. Available at: https://www.rdocumentation.org/packages/base/versions/3.4.3/topics/sample (Accessed: 12 December 2017).
Ravichandran, M. (2004) 'Interactions between mercury and dissolved organic matter - A review', *Chemosphere*, 55(3), pp. 319–331. doi: 10.1016/j.chemosphere.2003.11.011.
Raymond, P. A. and Saiers, J. E. (2010) 'Event controlled DOC export from forested watersheds', *Biogeochemistry*, 100(1), pp. 197–209. doi: 10.1007/s10533-010-9416-7.
Refaeilzadeh, P., Tang, L. and Liu, H. (2009) 'Cross-Validation', in LIU, L. and ÖZSU, M. T. (eds) *Encyclopedia of Database Systems*. Boston, MA: Springer US, pp. 532–538. doi: 10.1007/978-0-387-39940-9_565.
Regnier, P. *et al.* (2013) 'Anthropogenic perturbation of the carbon fluxes from land to ocean', *Nature Geoscience*, 6(8), pp. 597–607. doi: 10.1038/ngeo1830.
Riahi, K., Grubler, A. and Nakicenovic, N. (2007) 'Scenarios of long-term socio-economic and environmental development under climate stabilization', *Technological Forecasting and Social Change*. Elsevier, 74(7), pp. 887–935. doi: 10.1016/j.techfore.2006.05.026.
Rind, D. *et al.* (1990) 'Potential evapotranspiration and the likelihood of future drought', *Journal of Geophysical Research*, 95(D7), pp. 9983–10004. doi: 10.1029/JD095iD07p09983.
Rumpel, C. and Kögel-Knabner, I. (2011) 'Deep soil organic matter-a key but poorly understood component of terrestrial C cycle', *Plant and Soil*, 338(1), pp. 143–158. doi: 10.1007/s11104-010-0391-5.
Sanderman, J. *et al.* (2009) 'Linking soils and streams: Sources and chemistry of dissolved organic matter in a small coastal watershed', *Water Resources Research*, 45(3), pp. 1–13. doi: 10.1029/2008WR006977.
Sanderman, J. and Amundson, R. (2008) 'A comparative study of dissolved organic carbon transport and stabilization in California forest and grassland soils', *Biogeochemistry*, 89(3), pp. 309–327. doi: 10.1007/s10533-008-9221-8.
Scheel, T. *et al.* (2008) 'Stabilization of dissolved organic matter by aluminium: A toxic effect or stabilization through precipitation?', *European Journal of Soil Science*, 59(6), pp. 1122–1132. doi: 10.1111/j.1365-2389.2008.01074.x.
Schelker, J. *et al.* (2013) 'Drivers of increased organic carbon concentrations in stream water

following forest disturbance: Separating effects of changes in flow pathways and soil warming', *Journal of Geophysical Research: Biogeosciences*, 118(4), pp. 1814–1827. doi: 10.1002/2013JG002309.

Schrumpf, M. *et al.* (2011) 'How accurately can soil organic carbon stocks and stock changes be quantified by soil inventories?', *Biogeosciences*, 8(5), pp. 1193–1212. doi: 10.5194/bg-8-1193-2011.

Schwendenmann, L. and Veldkamp, E. (2005) 'The role of dissolved organic carbon, dissolved organic nitrogen, and dissolved inorganic nitrogen in a tropical wet forest ecosystem', *Ecosystems*, 8(4), pp. 339–351. doi: 10.1007/s10021-003-0088-1.

Seitzinger, S. P. *et al.* (2005) 'Sources and delivery of carbon, nitrogen, and phosphorus to the coastal zone: An overview of Global Nutrient Export from Watersheds (NEWS) models and their application', *Global Biogeochemical Cycles*, 19(4), pp. 1–11. doi: 10.1029/2005GB002606.

Siemens, J. (2003) 'The European Carbon Budget: A Gap', *Science (New York, N.Y.)*, 302(5651), p. 1681. doi: 10.1126/science.302.5651.1677b.

Sitch, S. *et al.* (2003) 'Evaluation of ecosystem dynamics, plant geography and terrestrial carbon cycling in the LPJ dynamic global vegetation model', *Global Change Biology*, 9, pp. 161–185. doi: 10.1046/j.1365-2486.2003.00569.x.

Sitch, S. *et al.* (2015) 'Recent trends and drivers of regional sources and sinks of carbon dioxide', *Biogeosciences*, 12(3), pp. 653–679. doi: 10.5194/bg-12-653-2015.

Smith, J *et al.* (2010) 'Estimating changes in national soil carbon stocks using ECOSSE - a new model that includes upland organic soils. Part II. Application in Scotland', (February 2016), pp. 1–35. doi: 10.3354/cr00899.

Smith, Jo *et al.* (2010) 'Model to Estimate Carbon in Organic Soils – Sequestration and Emissions ( ECOSSE ).', *Carbon*, 44(August), pp. 1–73.

Smith, S. V and Hollibaugh, J. T. (1993) 'Coastal Metabolism an D the Ocean Ic Organ', *Reviews of Geophysics*, 31(1), pp. 75–89.

Soil Classification Working Group (1998) 'The Canadian System of Soil Classification', *The Canadian System of Soil Classification, 3rd ed. Agriculture and Agri-Food Canada Publication 1646*, p. 187.

Solinger, S., Kalbitz, K. and Matzner, E. (2001) 'Controls on the dynamics of dissolved organic carbon and nitrogen in a Central European deciduous forest', *Biogeochemistry*, 55(3), pp.

327–349. doi: 10.1023/A:1011848326013.
Sollins, P., Homann, P. and Caldwell, B. a. (1996) 'Stabilization and destabilization of soil organic matter1.pdf', *Geoderma*, 74(1–2), pp. 65–105. doi: 10.1016/S0016-7061(96)00036-5.
Stein, M. (1987) 'Large Sample Properties of Simulations Using Latin Hypercube Sampling', *Technometrics*, 29(2), pp. 132–151. doi: https://doi.org/10.1080/00401706.1987.10488205.
Stoddard, J. L. *et al.* (2003) *Responses of Maine surface waters to the Clean Air Act Amendments of 1990*. U.S. Environmental Protection Agency.
Stotzky, G. (1967) 'DIVISION OF ENVIRONMENTAL SCIENCES: CLAY MINERALS AND MICROBIAL ECOLOGY*,†', *Transactions of the New York Academy of Sciences*, 30(1 Series II), pp. 11–21. doi: 10.1111/j.2164-0947.1967.tb02449.x.
Thibodeaux, L. J. and Aguilar, L. (2005) 'Kinetics of peat soil dissolved organic carbon release to surface water. Part 2. A chemodynamic process model', *Chemosphere*, 60(9), pp. 1190–1196. doi: 10.1016/j.chemosphere.2005.02.047.
Tian, H. *et al.* (2015) 'Anthropogenic and climatic influences on carbon fluxes from eastern North America to the Atlantic Ocean: A process-based modeling study', *Journal of Geophysical Research: Biogeosciences*, 120(4), pp. 752–772. doi: 10.1002/2014JG002760.
Todd-Brown, K. E. O. *et al.* (2013) 'Causes of variation in soil carbon simulations from CMIP5 Earth system models and comparison with observations Earth System', *Biogeosciences*, pp. 1717–1736. doi: 10.5194/bg-10-1717-2013.
Tranvik, L. J. *et al.* (2009) 'Lakes and reservoirs as regulators of carbon cycling and climate', *Limnology and Oceanography*, 54(1), pp. 2298–2314. doi: 10.4319/lo.2009.54.6_part_2.2298.
Vanguelova, E. I. *et al.* (2010) 'Chemical fluxes in time through forest ecosystems in the UK - Soil response to pollution recovery', *Environmental Pollution*. Elsevier Ltd, 158(5), pp. 1857–1869. doi: 10.1016/j.envpol.2009.10.044.
Vogel, C. *et al.* (2015) 'Clay mineral composition modifies decomposition and sequestration of organic carbon and nitrogen in fine soil fractions', *Biology and Fertility of Soils*, 51(4), pp. 427–442. doi: 10.1007/s00374-014-0987-7.
Van Vuuren, D. P. *et al.* (2007) 'Stabilizing greenhouse gas concentrations at low levels: An assessment of reduction strategies and costs', *Climatic Change*, 81(2), pp. 119–159. doi: 10.1007/s10584-006-9172-9.

Waldner, P. *et al.* (2014) 'Detection of temporal trends in atmospheric deposition of inorganic nitrogen and sulphate to forests in Europe', *Atmospheric Environment*, 95, pp. 363–374. doi: 10.1016/j.atmosenv.2014.06.054.

Walmsley, D. C. (2009) *Quantifying Dissolved Carbon and Nitrogen Losses from Soils Subjected to Different Land-use and Management Practices*. University College Dublin (Ph. D. Thesis). Available at: https://books.google.fr/books?id=HCz2ZwEACAAJ.

Walmsley, D. C. *et al.* (2011) 'Dissolved carbon leaching from an Irish cropland soil is increased by reduced tillage and cover cropping', *Agriculture, Ecosystems and Environment*. Elsevier B.V., 142(3–4), pp. 393–402. doi: 10.1016/j.agee.2011.06.011.

Walters, D. N. *et al.* (2014) 'The Met Office Unified Model Global Atmosphere 4 . 0 and JULES Global Land 4 . 0 configurations', (2011), pp. 361–386. doi: 10.5194/gmd-7-361-2014.

Weedon, G. P. *et al.* (2010) 'The Watch Forcing Data 1958-2001: a Meteorological Forcing Dataset for Land Surface-and Hydrological-Models', *WATCH Tech. Rep. 22*, (22), p. 41p.

Worrall, F. *et al.* (2012) 'The flux of DOC from the UK - Predicting the role of soils, land use and net watershed losses', *Journal of Hydrology*, 448–449, pp. 149–160. doi: 10.1016/j.jhydrol.2012.04.053.

Worrall, F. and Burt, T. P. (2007) 'Trends in DOC concentration in Great Britain', *Journal of Hydrology*, 346(3–4), pp. 81–92. doi: 10.1016/j.jhydrol.2007.08.021.

Wu, Y., Clarke, N. and Mulder, J. (2010) 'Dissolved organic carbon concentrations in throughfall and soil waters at level II monitoring plots in norway: Short- and long-term variations', *Water, Air, and Soil Pollution*, 205(1–4), pp. 273–288. doi: 10.1007/s11270-009-0073-1.

Yano, Y. *et al.* (2004) 'Chemical and seasonal controls on the dynamics of dissolved organic matter in a coniferous old-growth stand in the Pacific Northwest, USA', *Biogeochemistry*, 71(2), pp. 197–223. doi: 10.1007/s10533-004-8130-8.

Yule, C. M. and Gomez, L. N. (2009) 'Leaf litter decomposition in a tropical peat swamp forest in Peninsular Malaysia', *Wetlands Ecology and Management*, 17(3), pp. 231–241. doi: 10.1007/s11273-008-9103-9.

Yurova, A. *et al.* (2008) 'Modeling the dissolved organic carbon output from a boreal mire using the convection-dispersion equation: Importance of representing sorption', *Water Resources Research*, 44(7), pp. 1–15. doi: 10.1029/2007WR006523.

Zhao, M. *et al.* (2005) 'Improvements of the MODIS terrestrial gross and net primary

production global data set', *Remote Sensing of Environment*, 95(2), pp. 164–176. doi: 10.1016/j.rse.2004.12.011.
Zhao, M. and Running, S. W. (2010) 'Drought-Induced Reduction in Global Terrestrial Net Primary Production from 2000 Through 2009', *Science*, 329(5994), pp. 940–943. doi: 10.1126/science.1192666.
Zhou, W. J. *et al.* (2016) 'Hydrologically transported dissolved organic carbon influences soil respiration in a tropical rainforest', *Biogeosciences*, 13(19), pp. 5487–5497. doi: 10.5194/bg-13-5487-2016.
Zsolnay, A. (2003) 'Dissolved organic matter : artefacts , definitions , and functions', *Geoderma*, 113, pp. 187–209. doi: 10.1016/S0016-7061(02)00361-0.